Design of Functionalized Peptide Nucleic Acids and the Applications to Gene Detection and Photochemistry

Kazuhito TANABE

2003

Design of Functionalized Peptide Nucleic Acids and the Applications to Gene Detection and Photochemistry

Kazuhito TANABE

2003

Preface

The study presented in this thesis has been carried out under the direction of Professor Isao Saito at the Department of Synthetic Chemistry and Biological Chemistry of Kyoto University during April 1994 to March 1997 and during October 1999 to March 2002. The study is concerned with the design of functionalized peptide nucleic acids and the applications to gene detection and photochemistry.

The author wishes to express his sincere gratitude to Professor Isao Saito for his kind guidance, valuable suggestions, and encouragement through this work. The author is deeply grateful to Associate Professor Kazuhiko Nakatani and Dr. Akimitsu Okamoto for their valuable suggestions, and encouragement throughout this work. The author is also indebted to Professor Hiroshi Sugiyama and Associate Professor Kenzo Fujimoto for their helpful suggestions. The author is also indebted to Dr. Hisafumi Ikeda, Dr. Kiyohiko Kawai, Dr. Takashi Nakamura, Dr. Shuji Ikeda, Dr. Shinsuke Sando, Dr. Shigeo Matsuda, Dr. Chikara Dohno, and Dr. Heike Heckroth for their helpful discussions.

The author is grateful to Supercomputer Laboratory, Institute for Chemical Research, Kyoto University for providing computation time. The author is also grateful to Kyoto University Radioisotope Research Center for providing the space for ^{32}P-end-labeled DNA cleavage experiment. The author wishes to express his gratitude to Mr. Haruo Fujita, Mr. Tadao Kobatake, and Ms. Hiromi Ushitora for the measurements of NMR spectra and mass spectra. The author wishes to thank Messrs. Satoshi Maekawa, Hiroshi Miyazaki, Yusuke Nomura, Kazuki Tainaka, and Takeshi Inasaki for their active collaboration. The

author is thankful to Messrs. Junya Shirai, Yasuki Komeda, Nobuhiro Higashida, Kazuhiko Fujisawa, Takahiro Matsuno, Kaoru Adachi, Shinya Hagihara, Kohzo Yoshida, Toshiji Taiji, Takashi Yoshida, Yutaka Ikeda, Kazuo Tanaka, Hiroyuki Kumasawa, Hideaki Yoshino, Masayuki Hayashi, Keiichiro Kanatani, Souta Horie, Akio Nakazawa, Tetsuo Fukuta, Takashi Murase, Motoya Nishida, and Yohei Miyauchi for their helpful suggestions and warm encouragement. The author is also grateful to all members of Prof. Saito's research group for their kind considerations.

The author deeply thanks Professor Sei-ichi Nishimoto and Mr. Hiroshi Hatta at Department of Energy and Hydrocarbon Chemistry, Kyoto University for their kind advice and encouragement. The author also thanks all members of Prof. Nishimoto's research group for their hearty encouragement.

Finally, the author expresses his deep appreciation to his parents, Dr. Tada-aki Tanabe and Dr. Kazuko Tanabe, for their affectionate encouragement throughout the work.

Kazuhito Tanabe
October, 2002

Contents

General Introduction

The most important molecular recognition event in nature is the base-pairing of nucleic acids, which guarantees the stroge, transfer, and expression of genetic information in living systems. The highly specific recognition through the natural pairing of the nucleobases has become increasingly important for the gene diagnostics and for gene therapeutics.[1] In this decade, oligonucleotide analogs with modification to the phosphate group, the ribose or the nucleobase have attracted much attention in due to their potential as antisense and antigene therapeutic agents.[2] The vast majority of these compounds are very close analogs to DNA because of the almost dogmatic notion that the slighter the modification the better. Although a major effort has been put into developing the chemistry of these close DNA analogs, they remain relatively difficult to prepare in large scale and the introduction of modified moieties presents even bigger challenges.

The most radical change to the natural structure was made by the Danish group of Buchardt, Nielsen, and Berg[3] who replaced the entire suger-phosphate backbone by an *N*-(2-aminoethyl)glycine-based polyamide structure. This DNA analog containing polyamide backbone, peptide nucleic acids (PNA, Figure 1), retain the nucleic acid recognizing property of the nucleic acids while overcoming the relatively poor biostability of both nucleic acids and peptides. One of the most remarkable properties of PNA is very high affinity to complementary nucleic acids because of the lack of repulsive phosphate-phosphate interactions. Targeting of homopyrimidine PNA to double-stranded DNA results in strand-displacement complexes which is formed in the sequence specific manner rather than the traditional and expected triple helix structure (Figure 1B).[3a,4]

This very favorable DNA hybridization property of PNA led to the development of a large variety of biomolecular and potential medical

application of PNA[5-7] as well as antisense and antigene drug approach. We attempted to use this strand-displacement complex of PNA and duplex DNA as a base for the transmission of the genetic information.

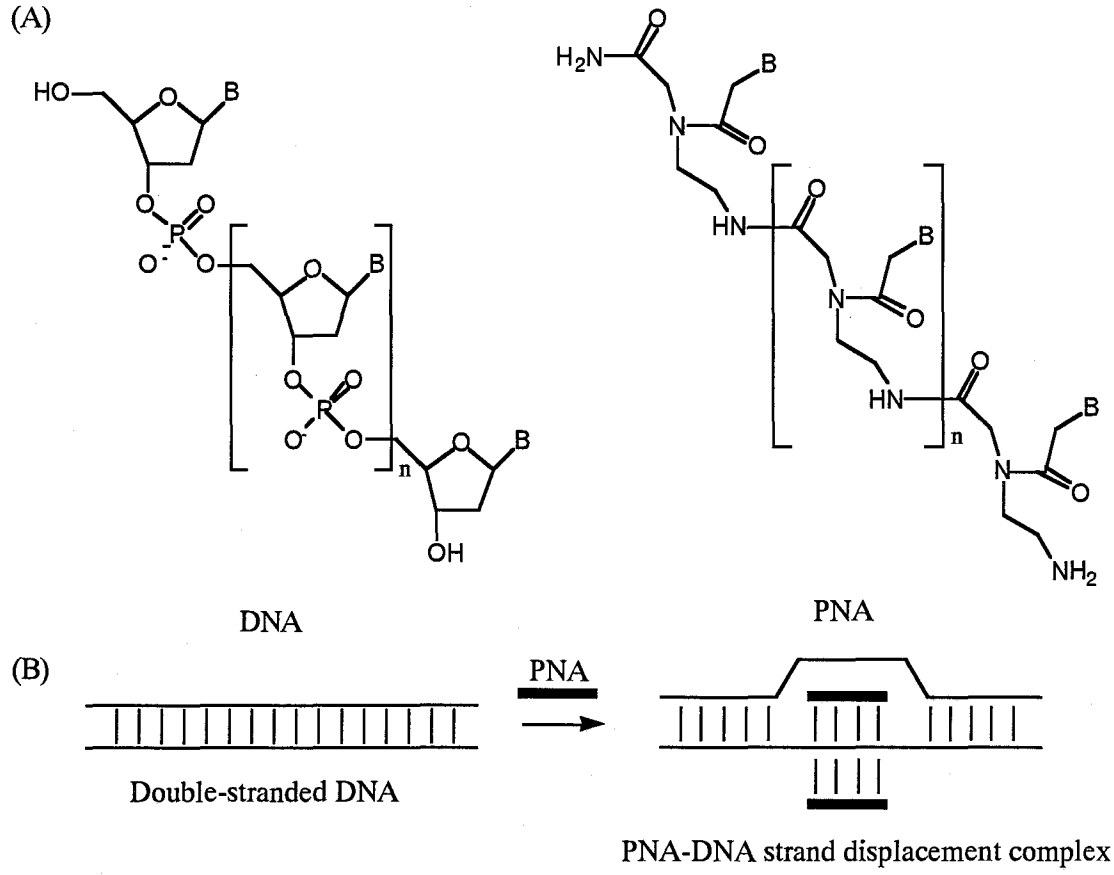

Figure 1. (A) Schematic comparison of DNA and PNA. (B) Binding of PNA to targeting double-stranded DNA. Thick structures signify PNA.

Significance of difference in DNA sequence.

Inherited differences in DNA sequence contribute to phenotypic variation, influencing an individual's anthropometric characteristics, risk of disease and response to the environment. Single-nucleotide polymorphism (SNP) is the most abundant type of DNA sequence variation in the human genome.[8] A SNP is a site on the DNA in which a single base-pair varies from person to person. If a SNP is found within a small, unique segment of DNA, it serves both as a physical landmark and a genetic marker that one can follow its transmission from parent to child. SNPs have gained popularity in recent years, and touted as the genetic markers[2] of choice for the study of complex genetic traits.[9,10] According to the theoretical models, if one studies the genetic make-up (the genotype) of a group of individuals with a common disease and that of a group without the disease, one may see certain genotypes consistently associated with those individuals who have the disease.[10] From these viewpoint, development of methods for the discovery and genotyping of SNPs have been attracted considerable attention for many scientists.

Methods for discovery of SNPs dependent on polymerase chain reaction (PCR).

The detecting methods of SNPs that are suitable for high-throughput screening rely on fluorescence to generate a target-specific signal. One of the most useful methods is single base sequencing on oligomicroarray developed by Drmanac and coworkers.[11] This protocol is based on the use of oligonucleotide hybridization to determine the set of constituent subsequences present in a DNA fragment. Unknown DNA samples can be attached to a support and sequentially hybridized with labeled oligonucleotides; alternatively, the DNA can be labeled and sequentially hybridized to an array of support-bound oligonucleotides (Figure 2).

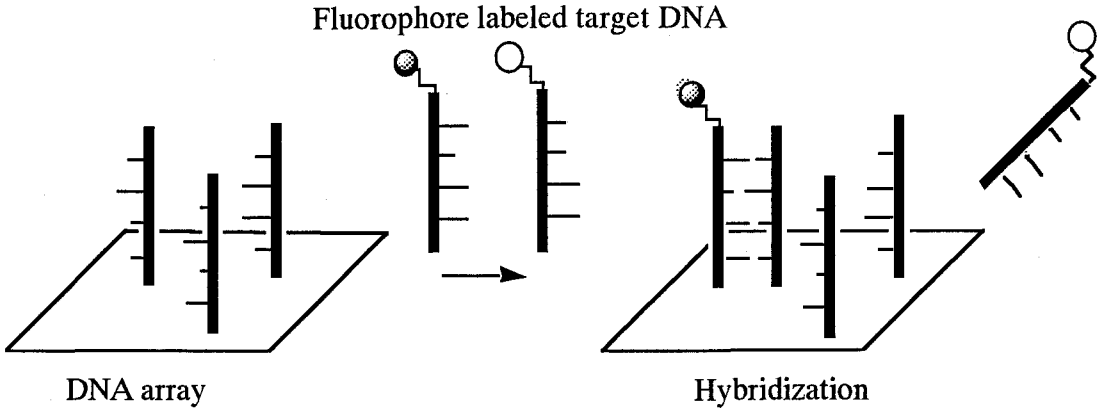

Figure 2. Schematic outline of DNA array to discriminate between samples containing duplexes with a perfect match and hybrids with the mismatiched base pair.

Since DNAs containing mismatched base pair cannot form stable duplex, hybridization can discriminate between samples containing duplexes with a prefect match and hybrids with the mismatched base pairs. This concept makes use of an array of all possible n-nucleotide oligomers to identify n-mers present in an unknown DNA sequence.

Another successive method for the detection of SNP is the molecular beacon developed by Tyagi and coworkers.[12] This method can be used to indicate the presence of specific nucleic acids in homogenous solutions.[12b] This probe can monitor nucleic acids synthesis in real-time, without interrupting the reactions. The molecular beacon undergoes a fluorogenic conformational change when it hybridizes to their target. It possesses a stem-and-loop structure (Figure 3), where the loop portion of the molecule is a probe sequence that is complementary to a target sequence in the nucleic acid to be detected. A fluorescent moiety is covalently linked to the end of one arm and a quenching moiety is covalently linked to the end of the other arm. The stem keeps these two moieties in close proximity to each other, causing the fluorescence of the fluorophore to be quenched by energy transfer. When the probe encounters a target molecule, it forms a probe-target hybrid that is longer and more stable than the stem hybrid. Consequently, the molecular beacon undergoes a spontaneous

conformational reorganization that forces the stem hybrid to dissociate and the fluorophore and the quencher to move away from each other, restoring fluorescence. Thus, the molecular beacon is able to distinguish targets that differ from one another by as little as a single nucleotide by the use of the conformational change of DNA.

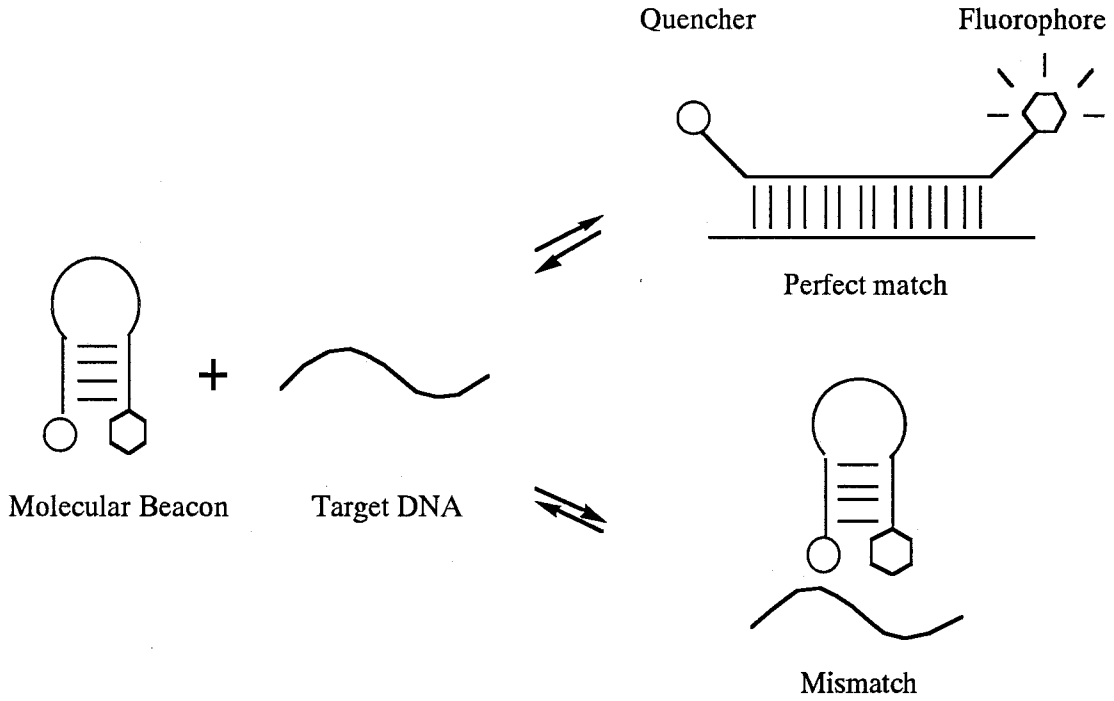

Figure 3. Operation of the molecular beacons. On their own, these molecules are non-fluorescent, because the stem hybrid keeps the fluorophore close to the quencher. When the probe sequence in the loop hybridizes to its target, forming a rigid double helix, a conformational reorganization occurs that separates the quencher from the fluorophore, restoring fluorescence.

Nearly all of the numerous methods that presently exist for fast and accurate detection of SNPs in DNA require the target DNA which was amplified by the polymerase chain reaction (PCR).[13] Most cannot directly detect SNPs within complex mixtures of genomic DNA because they lack sufficient specificity and sensitivity. The PCR has become the accepted "gold standard" for genetic testing. Although this technique can amplify its target a million-fold to generate sufficient copies for analysis, it is not

perfect. Carryover contamination and differential amplification efficiency arising from allele-specific bias for some sequences can produce incorrect results.[14]

Methods for discovery of SNPs independent of PCR.

In order to resolve SNPs, some detecting methods independent of PCR amplification technology were developed. One of the most successful methods is the invador technology[15] developed by Brow and coworkers (Figure 4). Invador technology detects the target of interest in amplified, genomic DNA and amplifies a target-specific signal, but not the target itself. The accuracy of the invador technology arises from the combination of two components: sequence-specific oligonucleotides hybridization and structure-specific enzymatic cleavage. Cleavage enzymes, member of a class of structure-specific flap endonucleases (FENs), recognize and cleave a structure formed when two overlapping oligonucleotides hybridize to a target DNA strand. Thermostable FENs allows the reaction to be performed at temperatures that promote probe turnover without the need for temperature cycling. The resulting amplification of the cleavage signal enables the detection of specific DNA targets at sub-attomole levels within complex mixture. This technology offers a simple diagnostic platform that detects the target with high specificity and sensitivity from genomic DNA and RNA.

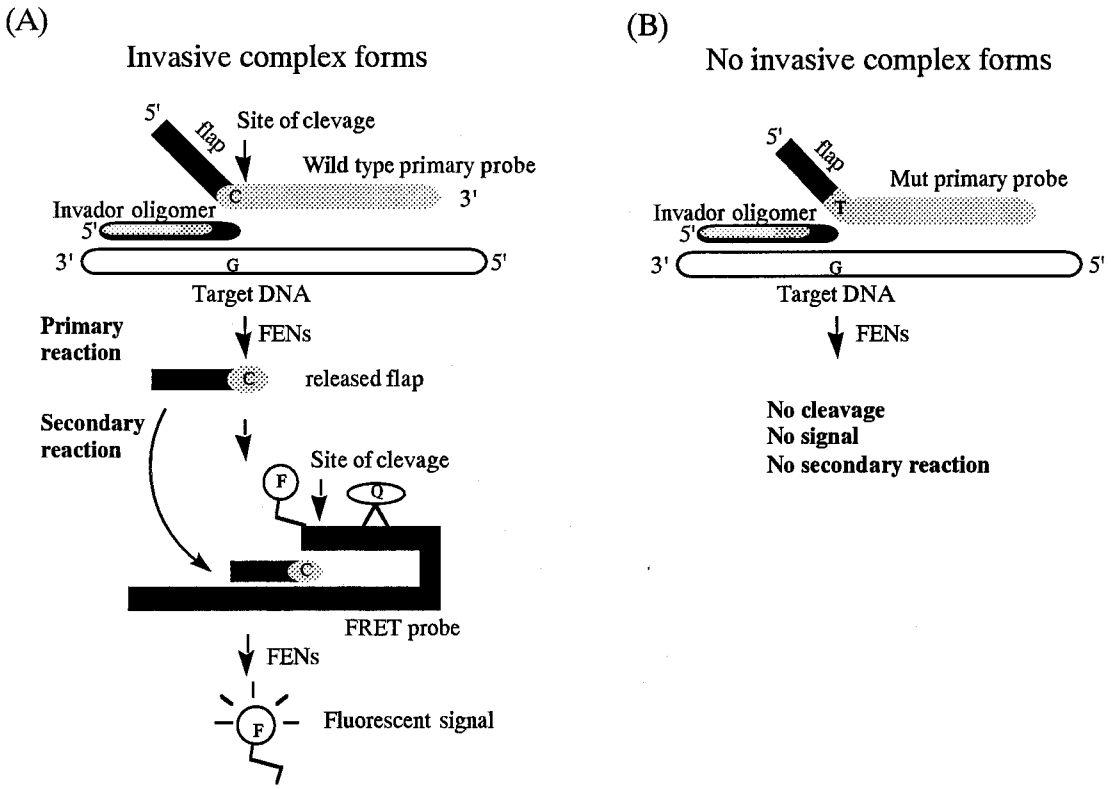

Figure 4. Schematic representation of Invador technology. The cleavase enzyme (FENs) recognizes the invasive structure and cleaves the 5' flap off the primary oligomer (A). If the primary oligomer and the target DNA sequence do not match perfectly at the cleavage site (B), the invasive structure will not form and cleavage will be suppressed. The flaps released from the cleaved primary probe oligomer continue the reaction sequence by acting as Invader oligomer in a second invasive cleavage reaction that uses fluorescence resonance energy transfer (FRET) probes as the target. When a released flap hybridizes to a FRET probe, it produces the invasive complex recognized by cleavase enzyme. Cleavage of the FRET probe separates the two dyes and produces a detectable florescent signal.

These protocols described above are useful for the detection of SNPs, but have some drawbacks. First, although DNA form double strand helix, all protocols required single-stranded DNA as targets. Second, they can not be available for a detection of methylated gene (methylated cytosine or methylated adenine) which are known to be correlated with the silencing of the gene,[16,17] because these modified bases can hybridize with guanine and thymine as same as cytosine and adenine. Therefore, new protocols for detection of SNPs and modified bases in double stranded DNA have been required. In this study, high affinity of PNA to double-stranded DNA and

the loop portion in the strand-displacement complex was used for the resolution of these problems.

Design of intelligent drug that is selectively toxic to disease-causing organism.

In addition to the detection of SNPs, the design of tailor chemotherapeutic agents for individual patients based on genetic information has become crucial. The goal of the chemotherapy is to discover drugs that are selectively toxic to the diseased cell or the disease causing organism.[18] This is a quite difficult challenge for cancer chemotherapy, however, because there is often little, biochemically, to distinguish a normal cell from a cancerous cell.[19] There have been a number of approaches to increasing the selectivity of anticancer agents through the use of antibody, gene- and bacterial-directed enzymatic activation of prodrugs and by capitalizing an elevated levels of certain enzymes and receptors within the cancer cells.[20] Recently, Taylor and coworker reported the chemotherapeutic agents that make use of a disease-specific nucleic acid sequence to template the association of a prodrug with a catalyst which catalyzed the release of the drug (Figure 5).[21] In this system, the prodrug consists of a drug that is attached to a molecule that binds reversibly to DNA sequence that is specific to the disease. The corresponding catalytic component consists of a catalyst attached to another molecule that binds to the site on the triggering sequence that is adjacent to the prodrug binding site. They demonstrated the release of a drug in a sequence specific manner, however, the system required two modified oligonucleotides to accomplish the drug release. This prodrug consist of two component cannot serve realistic uses because of an immense complexity of the organism. Therefore, the simple drug release system in a sequence specific manner has been imperative.

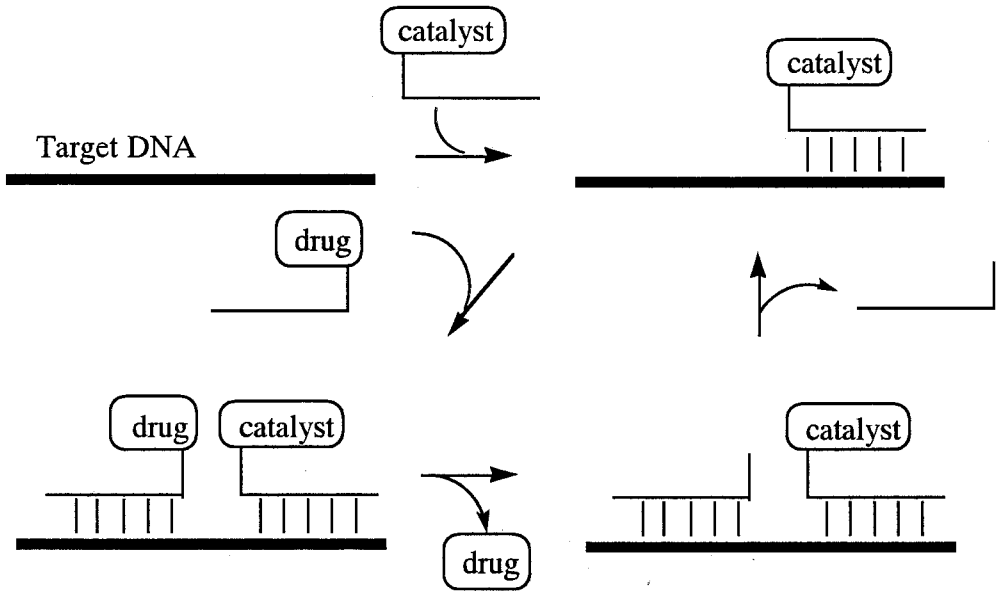

Figure 5. Nucleic acids triggered catalytic drug release reported by Taylor. The catalyst and drug was attached to single-stranded DNA. The drug-releasing catalytic component bound tightly to the target DNA to form an enzyme-like catalyst, whereas the prodrug bound reversibly, so that it could be exchanged for another prodrug after release of drug.

Survey of this thesis.

This thesis consists of six chapters on the design of functionalized peptide nucleic acids and the application to gene detection and photochemistry. Former four chapters describe the development of the method for the discovery of single nucleotide variation in DNA by the use of peptide nucleic acids (PNA) and the photochemistry of PNA-DNA hybrid. The fifth chapter describes development of an intelligent drug release system by the use of modified oligodeoxynucleotide. In addition, the novel photocyclization of 1,2-diketone was described in the last chapter.

Chapter 1 concerns the synthesis and properties of peptide nucleic acids containing a psoralen unit. The fluorescence of the full-matched PNA containing psoralen unit and DNA duplex is distinguishable from that of

the mismatched duplex.

Chapter 2 concerns the modulation of remote DNA oxidation by hybridization with peptide nucleic acids. Remote oxidation of oxidant-tethered DNA/PNA hybrid was considerably suppressed.

Chapter 3 concerns the discrimination of cytosine and 5-methylcytosine in duplex DNA by PNA. Through the enzymatic digestion of PNA –DNA complex containing fluorophore and quencher, the site-specific detection of methylation status of DNA was accomplished.

Chapter 4 concerns the detailed study of enzymatic digestion of PNA-DNA complex. The strand-displacement complex (P-loop) acts as a catalytic template for the enzymatic digestion of complementary DNA.

Chapter 5 concerns the photo-induced drug release from functionalized oligonucleotide modulated by molecular beacon strategy. The photoirradiation resulted in a rapid release of drug from functionalized oligonucleotide in the presence of complementary DNA. In contrast, the release of drug was strongly suppressed by triplet quenching in the absence of complementary DNA.

Chapter 6 concerns the novel furan-forming photocyclization of 1,2-diketone conjugated with ene-yne. Photoinduced generation of (2-furyl)carbene from 1,2-diketone conjugated with ene-yne and an efficient trap of the carbene was investigated.

References

(1) (a) Uhlmann, A.; Peyman, A. *Chem. Rev.* **1990**, *90*, 543–584. (b) Englisch, U, Gauss, D. H. *Angew. Chem. Int. Ed. Engl.* **1991**, *30*, 613–630. (c) Tuong, N. T.; Helene, C. *Angew. Chem. Int. Ed. Engl.* **1993**, *32*, 666–690. (d) Crooke, S. T.; Bennett, C. F. *Annu. Rev. Pharmacol. Toxicol.* **1996**, *36*, 107–127.

(2) (a) Uhlmann, E.; Peyman, A.; Will, D. W. *Encyclopedia of Cancer, Vol. 1* (Ed.: Bertino, J. R.), Academic Press, San Diego, CA, **1997**, pp. 64–81. (b) Stein, C. A.; Cheng, Y. -C. *Science* **1993**, *261*, 1004–1012.

(3) (a) Nielsen, P. E.; Egholm, M.; Berg, R. H.; Buchardt, O. *Science* **1991**, *254*, 1497–1500. (b) Egholm, M.; Buchardt, O.; Nielsen, P. E.; Berg, R. H. *J. Am. Chem. Soc.* **1992**, *114*, 1895–1897. (c) Nielsen, P. E. *Acc. Chem. Res.* **1999**, *32*, 624–630.

(4) (a) Bukanov, N. O.; Demidov, V. V.; Nielsen, P. E.; Frank-Kamenetskii, M. D. *Proc. Natl. Acad. Sci. USA* **1998**, *95*, 5516–5520. (b) Smulevitch, S. V.; Simmons, C. G.; Norton, J. C.; Corey, D. R. *Nat. Biotechnol.* **1996**, *14*, 566–568.

(5) (a) Hanvey, J. C.; Peffer, N. C.; Bisi, J. E.; Thomson, S. A.; Cadilla, R.; Josey, J. A.; Ricca, D. J.; Hassman, C. F.; Bonham, M. A.; Au, K. G.; Carter, S. G.; Bruckenstein, D. A.; Boyd, A.; Noble, S. A.; Babiss, L. E. *Science* **1992**, *258*, 1481–1485. (b) Knudsen, H.; Nielsen, P. E. *Nucleic Acids Res.* **1996**, *24*, 494–500. (c) Bonham, M. A.; Brown, S.; Boyd, A. L.; Brown, P. H.; Bruckenstein, D. A.; Hanvey, J. C.; Thomson, S. A.; Pipe, A.; Hassman, F.; Bisi, H. E.; Froehler, B. C.; Matteucci, M. D.; Wagner, R. W.; Noble, S. A.; Babiss, L. E. *Nucleic Acids Res.* **1995**, *23*, 1197–1203. (d) Gambacorti-Passerini, C.; Mologni, L.; Bertazzoli, C.; Marchesi, E.; Grignani, F.; Nielsen, P. E. *Blood* **1996**, *88*, 1411–1417.

(6) (a) Nielsen, P. E.; Egholm, M.; Buchadt, O. *Gene* **1994**, *149*, 139–145. (b) Vickers, T. A.; Griffith, M. C.; Ramasamy, K.; Risen, L.

M.; Freier, S. M. *Nucleic Acids Res.* **1995**, *23*, 3003–3008.

(7) (a) Lansdorp, P. M.; Verwoerd, N. P.; Rijke van de, F. M.; Dragowska, V.; Little, M. -T.; Dirks, R. W.; Raap, A. K.; Tanke, H. *J. Hum. Mol. Genet.* **1996**, *5*, 685–691. (b) Perry-O'Keefe, H.; Yao, X. –W.; Coull, J.; Fuchs, M.; Egholm, M. *Proc. Natl. Acad. Sci. USA* **1996**, *93*, 14670–14675. (c) Weiler, J.; Gausepohl, H.; Hauser, N.; Jensen, O. N.; Hoheisel, J. D. *Nucleic Acids Res.* **1997**, *25*, 2792–2799. (d) Griffin, T.; Tang, W.; Smith, L. M. *Nat. Biotechnol.* **1997**, *15*, 1368–1370. (e) Wang, J.; Palecek, E.; Nielsen, P. E.; Rivas, G.; Cai, X.; Shiraishi, H.; Dontha, N.; Luo, D.; Farias, M. A. *J. Am. Chem. Soc.* **1996**, *118*, 7667–7670. (f) Ørum, H.; Nielsen, P. E.; Egholm, M.; Berg, R. H.; Buchardt, O.; Stanley, C. *Nucleic Acids Res.* **1993**, *21*, 5332–5336. (g) Veselkov, A. G.; Demidov, V. V.; Nielsen, P. E.; Frank-Kamenetskii, M. D. *Nucleic Acids Res.* **1996**, *24*, 2483–2487.

(8) (a) Cooper, D. N.; Smith, B. A. Cooke, H. J,; Niemann, S.; Schumidtke, J. *Hum. Genet.* **1985**, *69*, 201–205. (b) Kwok, P. -Y.; Deng, Q.; Zakeri, H.; Taylor, S. L.; Nickerson, D. A. *Genomics* **1996**, *31*, 123–126.

(9) Collins, F. S.; Guyer, M. S. Charkravarti, A. *Science* **1997**, *278*, 1580–1581.

(10) Risch, N.; Merikangas, K. *Science* **1997**, *278*, 1580–1581.

(11) (a) Drmanac, R.; Labat, I.; Brukner, I.; Crkvenjakov, R. *Genomics* **1989**, *2*, 114–128. (b) Chee, M.; Yang, R.; Hubbell, E.; Berno, A.; Huang, X. C.; Sfern, D.; Winkler, J.; Lockhart, D. J.; Morris, H. S.; Fodor, S. P. *Science* **1996**, *274*, 610–614. (c) Wang, D. G.; Fan, J. B.; Siao, C. J.; Berno, A.; Young, P.; Sapolsky, R.; Ghandour, G.; Perkin, S. N.; Winchester, E.; Spencer, J.; Kruglyak, L.; Stein, L.; Hsie, L.; Topaloglou, T.; Hubbell, E.; Robinson, E.; Mittmann, M.; Morris, M. S.; Shen, N.; Kilburn, D.; Rioux, J.; Nusbaum, C.; Rozen, S.; Hudson, T. J.; Lander, E. S. *Science* **1998**, *280*, 1077–1082. (d)

Cargill, M.; Altshuler, D.; Ireland, J.; Sklar, P.; Ardlie, K.; Patil, N.; Shaw, N.; Lane, C. R.; Lim, E. P.; Kalyanaraman, N.; nemish, J.; Ziaugra, L.; Freidland, L.; Rolfe, A.; Warrington, J.; Lipshutz, R.; Daley, G. Q.; Lander, E. S. *Nat. Genet.* **1999**, *3*, 231–238. (e) Halushka, M. K.; Fan, J. B.; Bentley, K.; Hsie, L.; Shen, N.; Weder, A.; Cooper, R.; Lipshutz, R. *Nat. Genet.* **1999**, *3*, 239–247.

(12) (a) Tyagi, S.; Kramer, F. R. *Nat. Biotechnol.* **1996**, *14*, 303–308. (b) Tyagi, S.; Btaru, D. P.; Kramer, F. R. *Nat. Biotechnol.* **1998**, *16*, 49–53. (c) Piatek, A. S.; Tyagi, S.; Pol, A. C.; Telenti, A.; Miller, L. P.; Kramer, F. R.; Alland, D. *Nat. Biotechnol.* **1998**, *16*, 359–363.

(13) Saiki, R. K.; Scharf, S. J.; Faloona, F.; Mullis, K. B.; Horu, G. T.; Erlich, H. A.; Arnheim, N. *Science* **1985**, *230*, 1350–1354.

(14) Barnard, R.; Futo, V.; Pecheniuk, N.; Slattery, M.; Walsh, T. *Biotechniques* **1998**, *25*, 684–691.

(15) (a) Lyamichev, V.; Brow, M. A.; Dahlberg, J. E. *Science* **1993**, *260*, 778–783. (b) Kaiser, M. W.; Lyamicheva, N. Ma, W.; Miller, C.; Neri, B.; Fors, L.; Lyamichev, V. I. *J Biol. Chem.* **1999**, *30*, 21387–21394. (c) Lyamichev, V.; Mast, A. L.; Hall, J. G.; Prudent, J. R.; Kaiser, M. W.; Takova, T.; Kwiatkowski, R. W.; Sander, T. J.; de Arruda, M.; Arco, D. A.; Neri, B. P.; Brow, M. A. *Nat. Biotechnol.* **1999**, *3*, 292–296.

(16) (a) Jones, P. A.; Takai, D. *Science* **2001**, *293*, 1068–1070. (b) Martienssen, R. A.; Colot, V. *Science* **2001**, *293*, 1070–1074. (c) Cogoni, C. *Annu. Rev. Microbiol.* **2001**, *55*, 381–406. (d) Paszkowski, J.; Whitham, S. *Curr. Opin. Plant Biol.* **2001**, *4*, 123–129.

(17) (a) Church, G. M.; Gilbert, W. *Proc. Natl. Acad. Sci. USA* **1984**, *81*, 1991–1995. (b) Frammer, M.; McDonald, L. E.; Millar, D. S.; Collis, C. M.; Watt, F.; Grigg, G. W.; Molloy, P. L.; Paul, C. L. *Proc. Natl. Acad. Sci. USA* **1992**, *89*, 1827–1831. (c) Herman, H. G.; Graff, J.

R.; Myöhänen, S.; Nelkin, B. D.; Baylin, S. B. *Proc. Natl. Acad. Sci. USA* **1996**, *93*, 9821–9826

(18) (a) Albert, A. *Selective Toxicity: The Physico-chemical Basis of Therapy,* Chapman and Hall, London, **1979**. (b) Drews, J. *Science* **2000**, *287*, 1960–1964. (c) Sykes, R. *Int. J. Antimicrob. Agents* **2000**, *14*, 1–12.

(19) Hardman, J. G.; Limbird, L. E.; Molinoff, R. W.; Ruddon, R. W.; Gilman, A. D. eds. *Goodman and Gilman's the Pharmacological Basis of Therapeutics*, McGraw-Hill, New York, **1996**.

(20) (a) Duncan, R.; Connors, T. A.; Meada, H. *J. Drug. Target.* **1996**, *3*, 317–319. (b) Dubowchik, G. M.; Walker, M. A. *Pharmacol. Ther.* **1999**, *83*, 67-123.

(21) (a) Ma, Z.; Taylor, J. -S. *Proc. Natl. Acad. Sci. USA* **2000**, *97*, 11159–11163. (b) Ma, Z.; Taylor, J. S. *Bioorg. Med. Chem.* **2001**, *9*, 2501-2510.

Chapter 1

Synthesis and Properties of Peptide Nucleic Acids Containing Psoralen Unit

Abstract

We prepared psoralen PNA unit from 8-methoxypsoralen and synthesized various PNAs containing psoralen by a typical ᵗBoc method. PNAs containing psoralen (P-PNA) at strand end formed a stable duplex with complementary DNA. The hybridization of P-PNA with complementary DNA resulted in a considerable decrease of the psoralen fluorescence.

Introduction

The studies on the molecular basis for photosensitization induced by psoralen derivatives have attracted considerable attention in recent years.[1] These include investigations of the luminescence properties of their excited states,[2] the formation of psoralen–pyrimidine base crosslink via [2+2]photocycloaddition,[3] cell killing,[4] and the cure of skin diseases such as psoriasis.[5] Psoralens exhibit strong fluorescence by UVA irradiation, and the labelling of DNA and RNA by psoralen has been a promising tool for monitoring interactions with other biomolecules.[6]

Peptide nucleic acids (PNA) is a completely artificial nucleic acid consisting of peptide backbone and can recognize a complementary DNA sequence in a highly sequence-specific manner.[7] The PNA–DNA hybrid is thermodynamically more stable than DNA duplex,[8] and it is fairly independent of ionic strength in solutions.[9] Moreover, the incorporation of modified nucleobases into PNA is relatively easy. Therefore, incorporation of a psoralen unit into PNA seems to be very attractive. The sequence-specific DNA recognition by psoralen-containing PNA would potentially be used for the readout of DNA sequence by monitoring characteristic psoralen fluorescence.

Herein we report the synthesis and properties of PNAs containing psoralen (P-PNA). We synthesized psoralen PNA unit and then incorporated it into PNA by ^{t}BOC method. The fluorescence of P-PNA considerably decreased by forming PNA-DNA hybrid.

Results and Discussion

The synthetic route of psoralen PNA unit is shown in Scheme 1. Methyl group of 8-methoxypsoralen (**1**) was removed (71%), and then the

hydroxy group of **2** was coupled with ethyl bromoacetate to obtain **3** (81%). Ester **3** was hydrolyzed to **4** (99%), which was coupled with *N*-[2-(*tert*-butoxycarbonylamino)ethyl]glycine ethyl ester (**5**) (87%). Ester **6** was converted to free carboxylic acid to give a psoralen PNA unit **7** (86%). PNA oligomers were synthesized according to a typical ^{t}Boc solid phase peptide synthesis using psoralen PNA unit **7**.[10] The crude P-PNA was purified by reversed phase HPLC. A typical example of HPLC profile is shown in Figure 1. The composition of purified P-PNA oligomers was confirmed by MALDI-TOF mass spectrometry as shown in Table 1.

Scheme 1. Synthesis of Psoralen PNA Unit

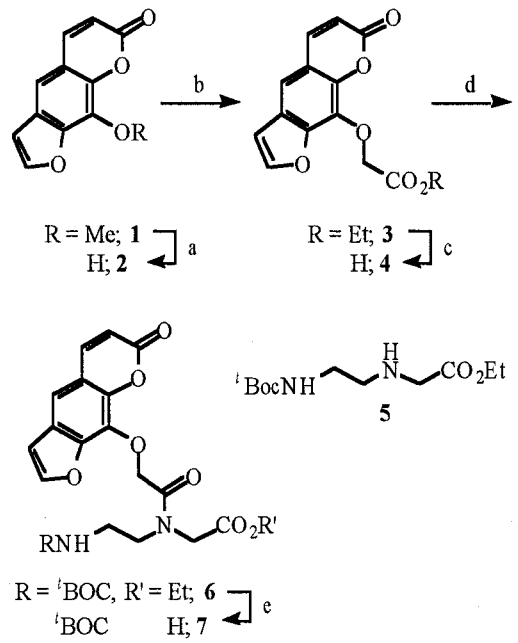

Reagents and conditions: (a) boron tribromide, dichloromethane, 0 °C, 2 h, 71%; (b) ethyl bromoacetate, potassium carbonate, DMF, r.t., 4 h, 81%; (c) lithium hydroxide, ethanol–water (2:1), 0 °C, 10 min, 99%; (d) EDCI, HOBt, DMF, r.t., 1 h, and then **5**, r.t., 4 h, 87%; (e) lithium hydroxide, ethanol–water (4:3), r.t., 4 h, 86%.

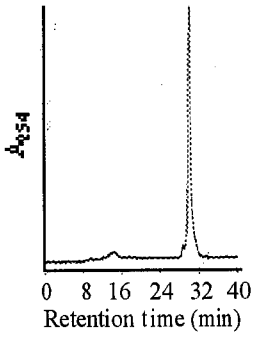

Figure 1. C_{18} reverse-phase HPLC profile of the crude reaction mixture of **P-PNA 5** obtained by solid phase peptide synthesis (29.9 min; 0.05% TFA–water, 0–20% acetonitrile over 40min).

Table 1. Mass Spectral Data of PNAs and T_m of their Hybrids with Complementary DNA Strand

	PNA [a]		
	MALDI-TOF $(M+H)^+$		T_m(°C) [b]
	calcd	found	
PNA 1	H–GTTCCGC–NH_2		38.0
	1886.83	1886.18	
P-PNA 2	H–**P**GTTCCGC–NH_2		46.0
	2229.13	2229.62	
P-PNA 3	H–GTT**P**CGC–NH_2		— [c]
	1977.89	1977.91	
P-PNA 4	H–GTTCC**P**C–NH_2		27.5
	1937.87	1938.69	
P-PNA 5	H–GTTCCGC**P**–NH_2		45.0
	2229.13	2229.61	(20.7)[d]

[a] "H" denotes a free amine end, "NH_2" denotes carboxamide end, and "P" denotes psoralen unit.
[b] T_m value of hybrid with complementary DNA 5'–d(CGCGGAACC)–3'.
[c] The sigmoidal melting curve was not observed.
[d] T_m value of hybrid with 5'–d(CGCCGAACC)–3' which forms a mismatched base pair.

P-PNA was hybridized with corresponding complementary DNA strand, and the stability of P-PNA–DNA hybrid (2.5 μM duplex concentration) was examined by monitoring melting temperature in 10 mM sodium cacodylate buffer (pH 7.0). The results are shown in Table 1. P-PNA containing psoralen unit at the strand end (**P-PNA 2** and **P-PNA 5**) showed 7–8 °C higher T_m values than that of the corresponding psoralen-free PNA oligomer (**PNA 1**). Stabilization of the duplex by psoralen at the strand end is probably due to the π-stacking of the hydrophobic aromatic ring of psoralen with the flanking base. However, T_m of the P-PNA–DNA hybrids containing psoralen unit in the interior of the PNA strand (**P-PNA 3** and **P-PNA 4**) significantly decreased. It was known that a single mismatched base pair considerably destabilizes the PNA–DNA hybrid.[11] Actually, **P-PNA 5**–DNA duplex containing a single-mismatched base pair showed *ca.* 24 °C T_m decrease. The reason for the destabilzation of the duplexes of **P-PNA 3** and **P-PNA 4** would be that psoralen in the interior of the PNA strand is unfeasible to form base-pairing.

The fluorescence spectra of P-PNAs were measured before and after addition of an equimolar amount of the complementary or mismatched DNA strand. The emission maximum of P-PNAs was 485 nm at 330 nm excitation. Single stranded **P-PNA 4** and **P-PNA 5** exhibited strong fluorescence, but the fluorescence of **P-PNA 2** was very weak. The hybridization of **P-PNA 4** and **P-PNA 5** with complementary DNA strand remarkably decreased their fluorescence intensities as compared with that of single-stranded P-PNA without shift of the emission maximum. It is noteworthy that the fluorescence intensity of **P-PNA 5** decreased 43% by hybridization with complementary DNA (Figure 2). On the other hand, the fluorescence intensity of **P-PNA 5**–DNA hybrid containing a single-mismatched base pair decreased only 7% as compared with that of single-stranded **P-PNA 5**. Thus the full-matched P-PNA–DNA duplex is clearly

distinguishable from the mismatched duplex or single-stranded P-PNA by monitoring their fluorescence intensities.

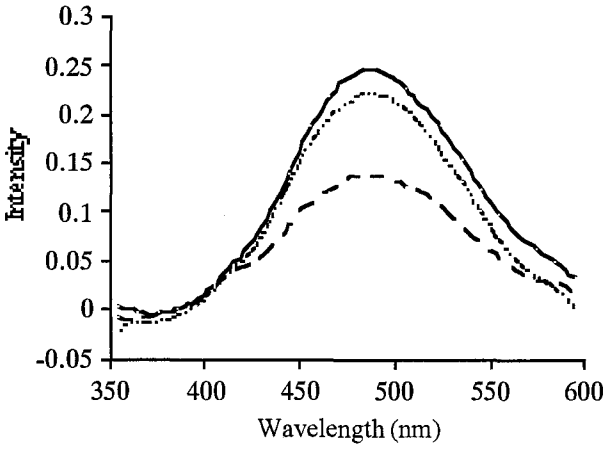

Figure 2. Fluorescence spectral changes caused by **P-PNA 5**–DNA hyblid formation. A solution of 20 *m*M **P-PNA 5** or **P-PNA 5**–DNA duplex in 10 mM sodium cacodylate (pH 7.0) was used. The fluorescence spectra were measured at 330 nm excitation at 21 °C. Solid line, single stranded **P-PNA 5**; dashed line, **P-PNA 5**–5'-d(CGCGGAACC)-3' (matched duplex); dotted line, **P-PNA 5**–5'-d(CGCCGAACC)-3' (mismatched duplex).

In order to understand the effect of P-PNA sequence on the fluorescence intensity of P-PNA, we measured the fluorescence intensities of P-PNAs H–**P**T–NH_2, H–**P**C–NH_2, H–**P**A–NH_2 and H–**P**G–NH_2. The fluorescence intensities of H–**P**T–NH_2, H–**P**C–NH_2 and H–**P**A–NH_2 were close to that of H–**P**–NH_2, whereas the fluorescence of H–**P**G–NH_2 was little observed (Figure 3). This result suggests that the low fluorescence intensity of **P-PNA 2** and the remarkable decrease of the fluorescence intensity by the hybridization of **P-PNA 5** and the complementary DNA are due to the quenching of the fluorescence by the flanking G base.

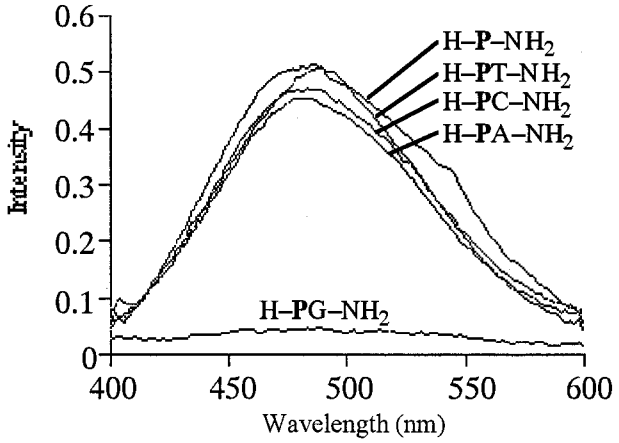

Figure 3. Fluorescence spectra of P-PNAs H–P*N*–NH_2 (*N* = T, C, A or G) and H–P–NH_2. A solution of 20 μM P-PNA in 10 mM sodium cacodylate (pH 7.0) was used. The fluorescence spectra were measured at 330 nm excitation at 19 °C.

Conclusion

In summary, we have disclosed a facile synthetic route of P-PNA from 8-methoxypsoralen. PNA containing a psoralen unit at strand end forms a stable duplex with complementary DNA. The fluorescence intensity of P-PNA considerably decreased by P-PNA–DNA hybrid formation because of the quenching of the fluorescence by a flanking G base. The fluorescence intensity change of P-PNA on hybridization makes it possible to use for monitoring PNA-DNA hybrid formation. P-PNA would also be useful as a tool for molecular biology and as a potent phototherapeutic drug for PUVA (psoralen plus UVA irradiation) therapy.[5b]

Experimental Section

General Techniques. ^{1}H NMR spectra were measured with Varian Mercury (400 MHz) spectrometers and JNM a-400 (400 MHz) spectrometers. Coupling constants (J values) are reported in Hz. The chemical shifts are expressed in ppm downfield from tetramethylsilane, using residual chloroform (δ = 7.24 in ^{1}H NMR) and residual dimethylsulfoxide (δ = 2.49 in ^{1}H NMR) as internal standards. The following abbreviations were used to explain the multiplicities: s, singlet; d, doublet; t, triplet; q, quartet; m, multiplet; br, broad. Melting points were obtained on a Yanaco MP-500D micro melting point apparatus and are uncorrected. Electron impact mass spectra, fast atom bombardment mass spectra and high-resolution mass spectra were recorded on JEOL JMS-DX 300 or JEOL JMS-SX 102A. All reactions were monitored by thin layer chromatography carried out on 0.25-mm E. Merck silica gel plates (60F-254) using UV light, 5% ethanolic phosphomolybdic acid, or *p*-anisaldehyde solution and heat as developing agent. Wako gel (C-200, particle size 75–150 μm, Wako) was used for column chromatography. All reagents were purchased at highest commercial quality and used without further purification unless otherwise stated.

9-Hydroxyfurano[3,2-*g*]2*H*-chromen-2-one (8-Hydroxypsoralen, 2). To a solution of boron tribromide (2.78 mL, 1 M in dichloromethane, 2.78 mmol) in dichloromethane was added 8-methoxypsoralen (**1**) at 0 °C, and the mixture was stirred for 2 h. After diluted with 2M *aq.* NaOH the reaction mixture was warmed to ambient temperature and extracted with chloroform. The organic layer was washed with brine, dried over anhydrous $MgSO_4$, filtered, and concentrated *in vacuo*. The crude product was purified by flash chromatography (SiO_2, 50 % ethyl acetate/hexane)

to give **2** (133 mg, 71 %) as colorless solid: mp 244–246 °C; ^{1}H NMR (400 MHz, $CDCl_3$) δ 7.79 (d, J = 9.7 Hz, 1H), 7.70 (d, J = 2.2 Hz, 1H), 7.25 (s, 1H), 6.80 (d, J = 2.2 Hz, 1H), 6.35 (d, J = 9.7 Hz, 1H); MS (EI) *m/e* (%) 202 (M^+, 100), 174 (57); HRMS (EI) calcd for $C_{11}H_6O_4$ (M^+), 202.0266; found, 202.0262.

Ethyl 2-(2-Oxofurano[3,2-*g*]2*H*-chromen-9-yloxy)acetate (3). To a solution of **2** (280 mg, 1.39 mmol) in DMF (6 mL) was added ethyl bromoacetate (694 mg, 4.16 mmol) and potassium carbonate (574 mg, 4.16 mmol) at 0 °C, and the mixture was stirred for 4 h at ambient temperature. After diluted with water, the reaction mixture was extracted with ethyl acetate. The organic layer was washed with brine, dried over anhydrous $MgSO_4$, filtered, and concentrated *in vacuo*. The crude product was purified by washing with ethylether to give **3** (323 mg, 81 %) as pale yellow solid: mp 107–110 °C; ^{1}H NMR (400 MHz, $CDCl_3$) δ 7.74 (d, J = 9.7 Hz, 1H), 7.66 (d, J = 2.2 Hz, 1H), 7.36 (s, 1H), 6.80 (d, J = 2.2 Hz, 1H), 6.35 (d, J = 9.7 Hz, 1H), 5.12 (s, 2H), 4.23 (q, J = 7.1 Hz, 2H), 1.24 (t, J = 7.1 Hz, 3H); MS (EI) *m/e* (%) 288 (M^+, 100), 215 (36), 201 (43); HRMS (EI) calcd for $C_{15}H_{12}O_6$ (M^+), 288.0633; found, 288.0645.

2-(2-Oxofurano[3,2-*g*]2*H*-chromen-9-yloxy)acetic Acid (4). To a solution of **3** (320 mg, 1.11 mmol) in EtOH–H_2O (2:1, 9 mL) was added $LiOH•H_2O$ (155 mg, 3.69 mmol) and the mixture was stirred for 10 min at 0 °C. After acidification with 2M *aq*. HCl, the mixture was extracted with ethyl acetate. The organic layer was washed with brine, dried over anhydrous $MgSO_4$, and filtered. Removal of the solvent under reduced pressure gave **4** (285 mg, 99 %) as ivory solid: mp 207–210 °C; ^{1}H NMR (400 MHz, DMSO-d_6) δ 8.13 (d, J = 9.6 Hz, 1H), 8.09 (d, J = 2.4 Hz, 1H), 7.63 (s, 1H), 7.07 (d, J = 2.4 Hz, 2H), 6.43 (d, J = 9.6 Hz, 1H), 5.11 (s,

2H); MS (EI) *m/e* (%) 260 (M^+, 100), 215 (20), 201 (51); HRMS (EI) calcd for $C_{13}H_8O_6$ (M^+), 260.0320; found, 260.0309.

Ethyl Ester of PNA Monomer Containing Psoralen (6). To a solution of **4** (280 mg, 1.08 mmol) in DMF (8 mL) was added 1-ethyl-3-(3-dimethylaminopropyl)-carbodiimide monohydro-chloride (619 mg, 3.23 mmol) and 1-hydroxybenzotriazole (436 mg, 3.23 mmol) at 0 °C, and the mixture was stirred for 1 h. To the reaction mixture added ethyl *N*-[2-(*tert*-butoxycarbonylamino)ethyl]amino-acetate (**5**) (399 mg, 1.62 mmol), and the mixture was stirred for 3 h at ambient temperature. After diluted with water, the reaction mixture was extracted with ethyl acetate. The organic layer was washed with brine, dried over anhydrous $MgSO_4$, filtered, and concentrated *in vacuo*. The crude product was purified by flash chromatography (SiO_2, 9 % methanol/chloroform) to give **6** (461 mg, 87 %) as colorless solid: mp 162–166 °C; ^1H NMR (400 MHz, $CDCl_3$): due to restricted rotation around secondary amide bond, several sets of the signals were doubled; δ 7.76 and 7.74 (d, J = 9.5 Hz, 1H), 7.71–7.66 (m, 1H), 7.38 and 7.36 (s, 1H), 6.79 (d, J = 2.2 Hz, 1H), 6.35 and 6.34 (d, J = 9.7 Hz, 1H), 6.05–5.91 (m, 1H), 5.08 and 5.22 (s, 2H), 4.23 and 4.16 (q, J = 7.1 Hz, 2H), 4.41 and 4.07 (s, 2H), 3.74–3.67 and 3.57–3.51 (m, 2H), 3.46–3.39 and 3.30–3.27 (m, 2H), 1.40 and 1.38 (s, 9H), 1.27 and 1.24 (t, J = 7.1 Hz, 3H); MS (FAB) *m/e* 489 [$(M+H)^+$]; HRMS (FAB) calcd for $C_{24}H_{29}N_2O_9$ [$(M+H)^+$], 489.1871; found, 489.1883.

PNA Monomer Containing Psoralen (7). To a solution of **6** (76 mg, 156 μmol) in EtOH–H_2O (2:1, 2.25 mL) was added $LiOH{\bullet}H_2O$ (30 mg, 842 μmol) and the mixture was stirred for 4 h at ambient temperature. The reaction mixture was poured into water and organic impurities were removed by extraction with ethyl acetate. After acidification of the

alkaline aqueous layer with 2M *aq*. HCl, the mixture was extracted with ethyl acetate. The organic layer was washed with brine, dried over anhydrous $MgSO_4$, and filtered. Removal of the solvent under reduced pressure gave **7** (62 mg, 86 %) as ivory solid: mp 104–105 °C; ^{1}H NMR (400 MHz; DMSO-d_6): due to restricted rotation around secondary amide bond, several sets of the signals were doubled; δ 8.14 and 8.13 (d, J = 9.7 Hz, 1H), 8.03 and 8.02 (d, J = 2.2 Hz, 1H), 7.64 and 7.63 (s, 1H), 7.06 (d, J = 2.4 Hz, 1H), 6.94–6.86 and 6.76–6.68 (m, 1H), 6.43 (d, J = 9.7 Hz, 1H), 5.28 and 5.14 (s, 2H), 4.17 and 3.93 (s, 2H), 3.47–3.21 (2H), 3.20–3.11 and 3.03–2.94 (m, 2H), 1.34 and 1.29 (s, 9H); MS (FAB) *m/e* 461 [(M+H)$^+$], 361 [(M–Bu+H)$^+$]; HRMS (FAB) calcd for $C_{22}H_{25}N_2O_9$ [(M+H)$^+$], 461.1558; found, 461.1559; UV (methanol) λ_{max} (nm) 299 (ε = 7.33), 248 (ε = 14.56), 216 (ε = 16.32).

Synthesis of PNA oligomer. PNA oligomers were synthesized by solid phase ^{t}Boc chemistry on a MBHA resin as described by Koch *et al.*[12] After the completion of PNA oligomer synthesis, the resin was treated with a solution of trifluoroacetic acid, trifluoromethanesulfonic acid, thioanisole, and *p*-cresol (6:2:1:1 v/v/v/v) for the cleavage of PNA oligomer from the resin and for the deprotection. The solution was filtered and precipitated in ethyl ether, centrifuged, and decanted. The residue was redissolved in a slight of trifluoroacetic acid, reprecipitated in ethyl ether, centrifuged, and then decanted to give the crude product. The crude oligomer was purified by reversed phase HPLC on a Wakosil II 5-C18-AR using a linear gradient of 0–20% acetonitrile in aqueous 0.05% trifluoroacetic acid.

Melting Temperature (T_m) Measurement. All T_ms of the PNA–DNA duplexes (2.5 μM, duplex concentration) were taken in a buffer containing 10 mM sodium cacodylate, pH 7.0. Absorbance *vs* temperature profiles

were measured at 260 nm using a JASCO TPU-550 UV/VIS spectrometer connected with a JASCO TPU-436 temperature controller. The absorbance of the samples was monitored at 260 nm from 2 °C to 80 °C with a heating rate of 1 °C/min. From these profiles, first derivatives were calculated to determine T_m values.

Fluorescence Measurement. All fluorescence spectra of single-stranded PNAs (20 μM, strand concentration) and PNA–DNA duplexes (20 μM, duplex concentration) were taken in a buffer containing 10 mM sodium cacodylate, pH 7.0. Fluorescence spectra were obtained at 330 nm excitation using a SHIMADZU RF-5300PC spectrofluorophotometer.

References

(1) Cimino, G. D.; Gamper, H. B.; Issacs, S. T.; Hearest, J. E. *Annu. Rev. Biochem.* **1985**, *54*, 1151–1193.

(2) Seret, A.; Piette, J.; Jakobs, A.; Vandevorst, A. *Photochem. Photobiol.* **1992**, *56*, 409–412.

(3) For a review, see: Thuong, N. T.; Héléne, C. *Angew. Chem., Int. Ed. Engl.* **1993**, *32*, 666–690.

(4) Csik, G.; Ronto, G.; Nocentini, S. *J Photochem. Photobiol. B* **1994**, *24*, 129–139.

(5) (a) Johnson, R.; Staiano-Coico, L.; Austin, L.; Cardinale, I.; Nabeya-Tsukifuji, R.; Krueger, J. G. *Photochem. Photobiol.* **1996**, *63*, 566–571. (b) Dall'Acqua, F.; Veldaldi, D. In *Handbook of Organic Photochemistry and Photobiology*; Horspool, W. M.; Song, P.-S., Eds.; CRC Press: Boca Raton, FL, 1995; pp 1357–1366.

(6) Lai, T.; Lim, B. T.; Lim, E. C. *J. Am. Chem. Soc.* **1982**, *104*, 7631–7635.

(7) Nielsen, P. *Acc. Chem. Res.* **1999**, *32*, 624–630.

(8) (a) Schwarz, F. P.; Robinson, S.; Butler, J. M. *Nucleic Acids Res.* **1999**, *27*, 4792–4800. (b) Chakrabarti, M. C.; Schwarz, F. P. *Nucleic Acids Res.* **1999**, *27*, 4801–4806.

(9) Tomac, S.; Sarkar, M.; Ratilainen, T.; Wittung, P.; Nielsen, P. E.; Nordén, B.; Gräslund, A *J. Am. Chem. Soc.* **1996**, *118*, 5544–5552.

(10) Egholm, M. E.; Buchardt, O.; Nielsen, P. E.; Berg, R. H. *J. Am. Chem. Soc.* **1992**, *114*, 1895–1897.

(11) Ratilainen, T.; Holmén, A.; Tuite, E.; Nielsen, P. E.; Nordén, B. Biochemistry 2000, 39, 7781–7791.

(12) Koch, T.; Larsen, T.; Batz, H. G.; Ottesen, K.; Ørum, H. *J. Peptide Res.* **1997**, *49*, 80–88.

Chapter 2

Modulation of Remote DNA Oxidation by Hybridization with Peptide Nucleic Acids

Abstract

We have examined the efficiency of DNA photooxidation in DNA/PNA duplex and DNA/$(PNA)_2$ triplex for the first time. DNA/PNA duplex was cleaved at GG steps by external riboflavin with high efficiency like specific GG cleavage in DNA/DNA duplex. However, the 5'G selectivity of the GG oxidation in DNA/PNA duplex was much lower than that observed in DNA/DNA duplex. Remote DNA oxidation of oxidant-tethered DNA/PNA duplex was considerably suppressed. In contrast, the formation of DNA/$(PNA)_2$ triplex by hybridization with two PNA strands completely inhibited the remote GG oxidation, indicating that PNA acts as an inhibition for remote oxidative DNA damage.

Introduction

Stacked bases in DNA duplex provide an effective media for long-range charge transport through DNA.[1–6] Oxidative DNA damage caused by metabolism,[7] UV irradiation,[8] gamma-ray,[9] and pulse radiolysis[10] is accumulated at guanine base (G) which has the lowest oxidative potential among nucleobases.[11] Particularly, GG doublet is more easily oxidized than single G, since oxidation potentials of GN sequences are in the order of GG > GA >> GC and GT.[12,13] Recently, it has been suggested that the long-range hole migration proceeds via a multistep hole-hopping mechanism and the efficiency of long-range hole migration is strongly affected by the sequence intervening between hole donor and acceptor.[5,6,14–17] The long-range hole migration through DNA triplex has also been reported.[18,19]

Peptide nucleic acid (PNA) is a nucleic acid analog possessing peptide backbone instead of sugar-phosphate backbone.[20] PNA oligomer is known to tightly bind to complementary DNA and RNA, forming right-handed duplex.[21] While DNA/PNA duplex has been intensively studied with regard to the hybridized structures and thermodynamics, little is known on the chemical reactivity of DNA/PNA duplex and DNA/$(PNA)_2$ triplex. Schuster *et al* reported long-range hole migration through DNA/PNA duplex containing anthraquinone unit.[22,23]

As a general problem for the hybridization of DNA with PNA, elucidation of how the chemical reactivity of DNA is altered as a result of hybridization with PNA is very important. Particularly, we are very much interested in the potential use of PNA as an inhibitor for remote oxidative DNA lesion. Herein, we report how the efficiency of GG oxidation is altered by hybridization with PNA. In this study, two types of guanine oxidation were examined; one is the photooxidation with an external one-

electron photosensitizer such as riboflavin and the other is the remote oxidation with oxidant-tethered DNA. It was found that DNA/PNA duplex was cleaved at GG step of DNA strand by external riboflavin with high efficiency like GG cleavage in DNA/DNA duplex. However, the 5'G selectivity of the GG oxidation in DNA/PNA duplex was lower than that observed in DNA duplex. On the other hand, in the photooxidation of DNA/PNA duplex using an oxidant-tethered DNA strand, the efficiency of the remote GG oxidation in DNA/PNA duplex was considerably suppressed. Remote oxidation through DNA/$(PNA)_2$ triplex containing GG step in the DNA strand was also investigated. It was demonstrated for the first time that the triplex formation with two PNA strands result in an almost completely inhibition of the remote GG oxidation. The present results suggest a possibility for the use of PNA as an inhibitor for long-range oxidative DNA lesion.

Results and Discussion

DNA and PNA strands used in this study are shown in Table 1. 13 mer **DNA 2a** and **2b** were complementary to 5' side part of 21 mer **DNA 1**, and 8 mer **DNA 3** and **PNA 3a** and **3b** were complementary to 3' side part of **DNA 1**. **X** in **DNA 2b** denotes cyanobenzophenone-substituted 2'-deoxyuridine.[24] **DNA 4a** contains a polypurine region, which forms a triplex with 8 mer polypyrimidine strands **DNA 5a**, **5b** and **PNA 5**. PNA strands were synthesized according to a conventional ^{t}Boc solid phase peptide synthesis,[25] and their compositions were confirmed by MALDI-TOF mass spectrometry. The melting temperatures (T_m) of duplexes and triplexes measured by absorption at 260 nm were shown in Table 2. The circular dichromism (CD) spectra of the duplexes and triplexes were all consistent with those reported previously.[26]

Table 1. DNA and PNA strands used in this study.

	Sequences[a]
DNA 1	5'-(^{32}P)-ATTTATAG$_8$TA**G$_{11}$G$_{12}$**TCT**G$_{16}$G$_{17}$**ACAC-3'
DNA 2a	3'-TAAATATCATCCA-5'
DNA 2b	3'-TAAATA**X**CATCCA-5'
DNA 3	3'-GACCTGTG-5'
PNA 3a	H_2N-GACCTGTG-H
PNA 3b	H-GACCTGTG-NH_2
DNA 4a	5'-(^{32}P)-ATTTATAG$_8$TA**G$_{11}$G$_{12}$**TAG$_{15}$AA**G$_{18}$G$_{19}$**AA-3'
DNA 4b	5'-AGAAGGAA-3'
DNA 5a	5'-TCTTCCTT-3'
DNA 5b	3'-TCTTCCTT-5'
PNA 5	H_2N-TCTTCCTT-H

[a] **X** is cyanobenzophenone-substituted 2'-deoxyuridine; NH_2 is carboxyamide end of PNA; H is amino end of PNA.

Table 2. Melting temperatures (T_m) of duplexes and triplexes.

	T_m (°C)
Duplex[a]	
DNA 1/DNA 2a	19
DNA 1/(DNA 2a+DNA 3)	23[b]
DNA 1/(DNA 2a+PNA 3a)	25, 44
DNA 1/(DNA 2a+PNA 3b)	19, 42
Triplex[c]	
DNA 4b/DNA 5a/DNA 5b	8, 31
DNA 4b/(PNA 5)$_2$	64[b]

[a] Conditions: 2.5 μM duplex, 10 mM sodium cacodylate, pH 7.0
[b] Only one sigmoidal curve was observed.
[c] Conditions: 2.5 μM triplex, 10 mM sodium cacodylate, pH 6.2

We first examined the photooxidation of DNA strand in DNA/PNA duplex by an external oxidant and compared the oxidation efficiency and selectivity with those for DNA/DNA duplex. The duplexes containing ^{32}P-5'-end labeled DNA were irradiated at 366 nm in the presence of riboflavin as a photosensitizer at 0 °C for 1 h. The reaction was analyzed by polyacrylamide gel electrophoresis after hot piperidine treatment. The result was shown in Figure 1a. The strong cleavage bands were observed at GG steps in DNA/DNA duplex (lane 3), antiparallel DNA/PNA duplex (lane 6) and parallel DNA/PNA duplex (lane 10) as a result of photoirradiation with riboflavin and hot piperidine treatment. The intensities of cleavage bands at $\mathbf{G_{16}G_{17}}$ steps in DNA/PNA duplexes were nearly equal to the band intensity at $\mathbf{G_{16}G_{17}}$ step in DNA/DNA duplex. However, the 5'G ($\mathbf{G_{16}}$) selectivity for the DNA cleavage of both antiparallel and parallel DNA/PNA duplexes was lower than that observed in DNA/DNA duplex. The results of Figure 1a indicated that the hybridization of PNA to DNA did not suppress the GG oxidation by riboflavin but a considerable loss of the 5'G selectivity was observed.

DNA oxidation initiated by a photosensitizer covalently linked to DNA was next investigated. Through these experiments we obtained an interesting result on the efficiency and selectivity of the long-range oxidative DNA lesion. **DNA 2b**, which contains cyanobenzophenone-substituted 2'-deoxyuridine (**X**) as an electron-accepting photosensitizer, was annealed with ^{32}P-labeled **DNA 1** containing GG site. The duplexes were irradiated at 312 nm at 0 °C for 1 h. The result of autoradiography was shown in Figure 1b. The ratio of cleavage band intensities at GG step in DNA/DNA duplex was very similar to that observed for riboflavin-sensitized photooxidation (lane 3 in Figure 1b *vs* Figure 1a). In contrast, the cleavage bands at $\mathbf{G_{16}G_{17}}$ step in antiparallel (lane 6) and parallel DNA/PNA duplex (lane 10) were smaller as compared with the $\mathbf{G_{16}G_{17}}$

bands in lane 3.

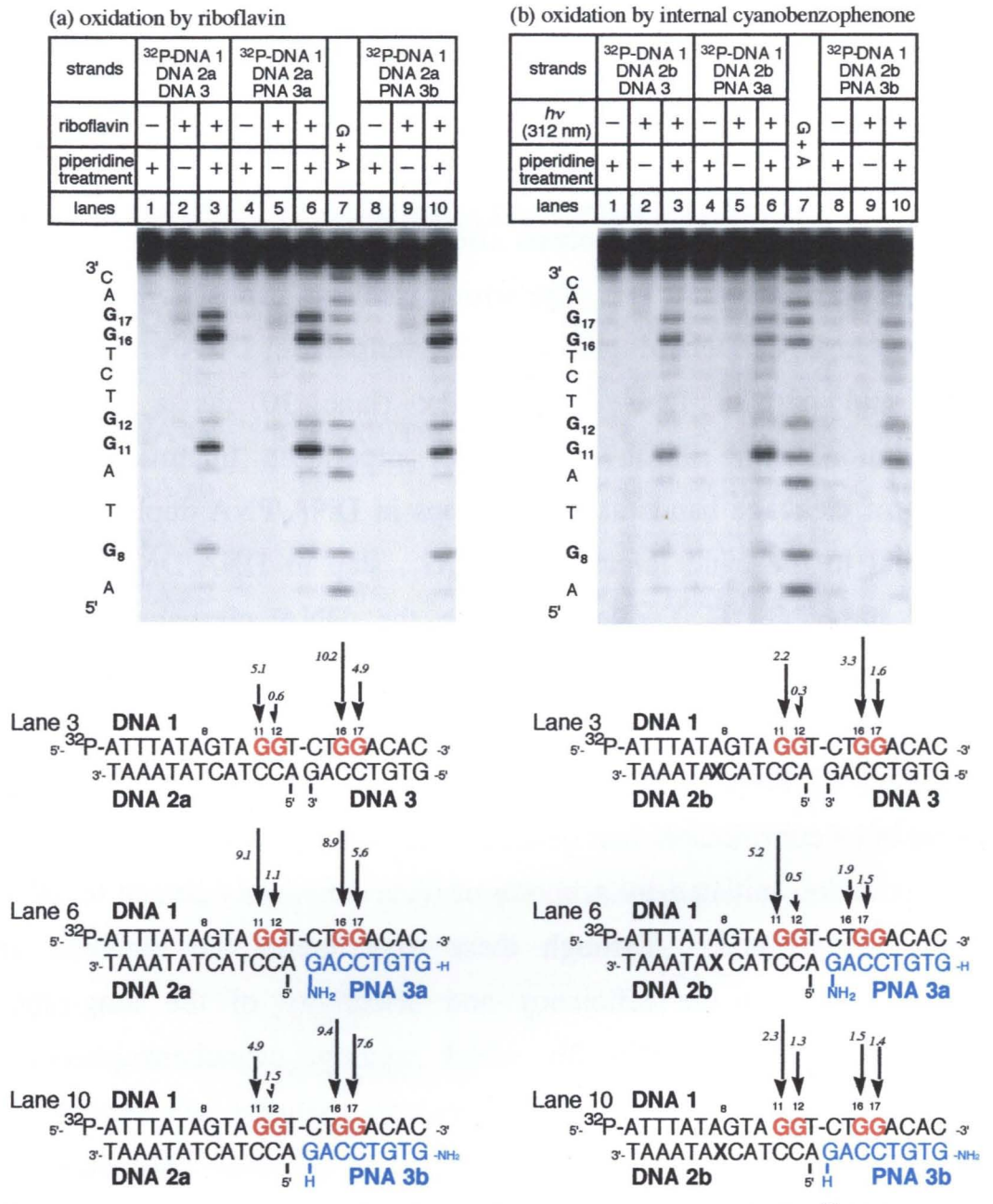

Figure 1. Autoradiograms of a denaturing gel electrophoresis for ^{32}P-5'-end labeled **DNA 1** after photooxidation of the duplexes. (a) 366 nm photoirradiation of duplexes in the presence and absence of riboflavin at 0 °C for 1 h followed by hot piperidine treatment (90 °C, 20 min). Lanes 1–3, **DNA 1/(DNA 2a+DNA 3)**; lanes4–6, **DNA 1/(DNA 2a+PNA 3a)**; lane 7, Maxam-Gilbert G+A sequencing lane; lanes 8–10, **DNA 1/(DNA 2a+PNA 3b)**. (b) 312 nm photoirradiation of duplexes containing cyanobenzophenone-substituted 2'-deoxyuridine incorporated into **DNA 2b** at 0 °C for 1 h followed by hot piperidine treatment (90 °C, 20 min). Lanes 1–3, **DNA 1/(DNA 2b+DNA 3)**; lanes 4–6, **DNA 1/(DNA 2b+PNA 3a)**; lane 7, Maxam-Gilbert G+A sequencing lane; lanes 8–10, **DNA 1/(DNA 2b+PNA 3b)**. The arrows and italic numbers represent relative intensities of cleavage bands obtained by densitometric analysis.

These results suggest that the hybridization of PNA to DNA decreased the efficiency of the remote oxidation at $\mathbf{G_{16}G_{17}}$ step. Furthermore, the 5'G ($\mathbf{G_{16}}$) selectivity of the DNA cleavage at $\mathbf{G_{16}G_{17}}$ in DNA/PNA duplex was completely lost.

In order to gain an insight into the efficiency and site-selectivity for the GG oxidation, molecular orbital calculation of GG step in DNA/PNA duplex was examined. We built 5'-GG-3'/H-CC-NH_2 duplex using parameters for antiparallel DNA/PNA duplex previously reported,[27] and obtained HOMO energy and HOMO distribution of this duplex by means of B3LYP/6-31G(d) calculation. The HOMO energy of 5'-GG-3'/H-CC-NH_2 duplex was –4.50 eV. This is slightly smaller than that of DNA/DNA duplex 5'-GG-3'/3'-CC-5' (–4.44 eV). The calculated HOMO energy suggests that like GG step of DNA/DNA duplex the GG step of DNA/PNA duplex is also oxidizable by one-electron oxidant with a similar high efficiency. The 5'G/3'G ratio of calculated HOMO distribution on GG step in DNA/PNA duplex was 100:57, which was smaller than that for DNA/DNA duplex (100:40) (Figure 2). These calculation data were consistent with the cleavage pattern actually obtained in the DNA oxidation with riboflavin, although the calculation data of small DNA/PNA model in a gas phase does not always correctly reflect the real photooxidation rate and selectivity in aqueous media.

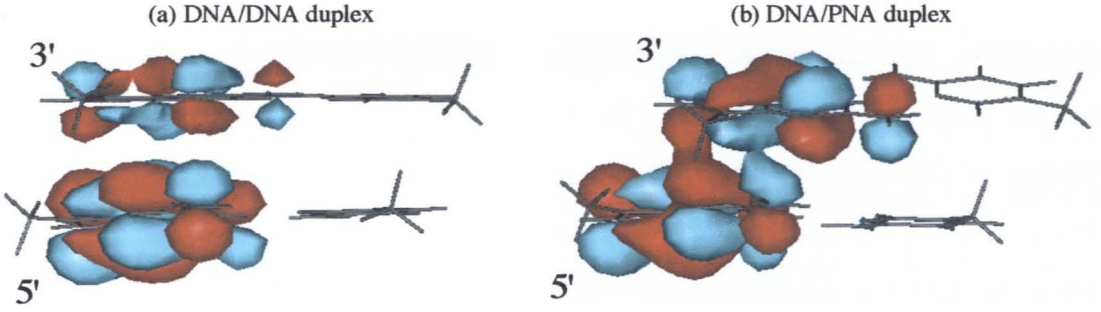

Figure 2. Orbital contour plots of the HOMOs of 5'-GG-3'/5'-CC-3' and 5'-GG-3'/H-CC-NH_2 obtained by B3LYP/6-31G(d) calculation. The sugar phosphate backbones and polypeptide backbone was replaced by methyl group.

The strong cleavage bands were observed at GG step in DNA/DNA duplex regardless of oxidation methods, whereas the GG cleavage in DNA/PNA duplex was considerably suppressed when the photooxidation was carried out with an internal cyanobenzophenone photosensitization in spite of the effective GG cleavage by riboflavin. This implies that the remote DNA oxidation through DNA/PNA duplex is less efficient than in DNA/DNA duplex. First of all, structural studies of DNA/PNA duplex indicate that the conformation is quite different from B-form DNA/DNA duplex.[27] In particular, the base stacking of DNA/PNA duplex is significantly different from B-form DNA duplex. In addition, the local structural changes could also occur not only in DNA/PNA duplex region but also at the DNA-PNA junction site as already observed at the DNA-RNA junction.[28] Thus, the change of the electronic overlap of the stacked bases in DNA/PNA hybrid as a result of structural alternations would cause the difference in the remote DNA oxidation efficiency.

In order to know the effect of triplex formation, we examined the photooxidation of DNA/$(PNA)_2$ triplex and compared the photooxidation efficiency with that of DNA triplex. The triplexes containing ^{32}P-5'-end labeled DNA, shown in Figure 3, were irradiated at 312 nm. While the cleavage bands at $\mathbf{G_{18}G_{19}}$ in the DNA triplex region were *ca.* 20% of $\mathbf{G_{11}G_{12}}$ in DNA duplex region (lane 3), the cleavage bands at $\mathbf{G_{18}G_{19}}$ in the DNA/$(PNA)_2$ triplex region (lane 6) were dramatically reduced and almost negligible, indicating that the triplex formation of DNA with two PNA strands completely suppressed the DNA cleavage as compared with DNA triplex. The extremely weak DNA cleavage in remote GG oxidation of DNA/$(PNA)_2$ triplex would also be due to the structural change caused by the hybridization of PNA to DNA as well as to the decrease of solvent accessibility by triplex formation.

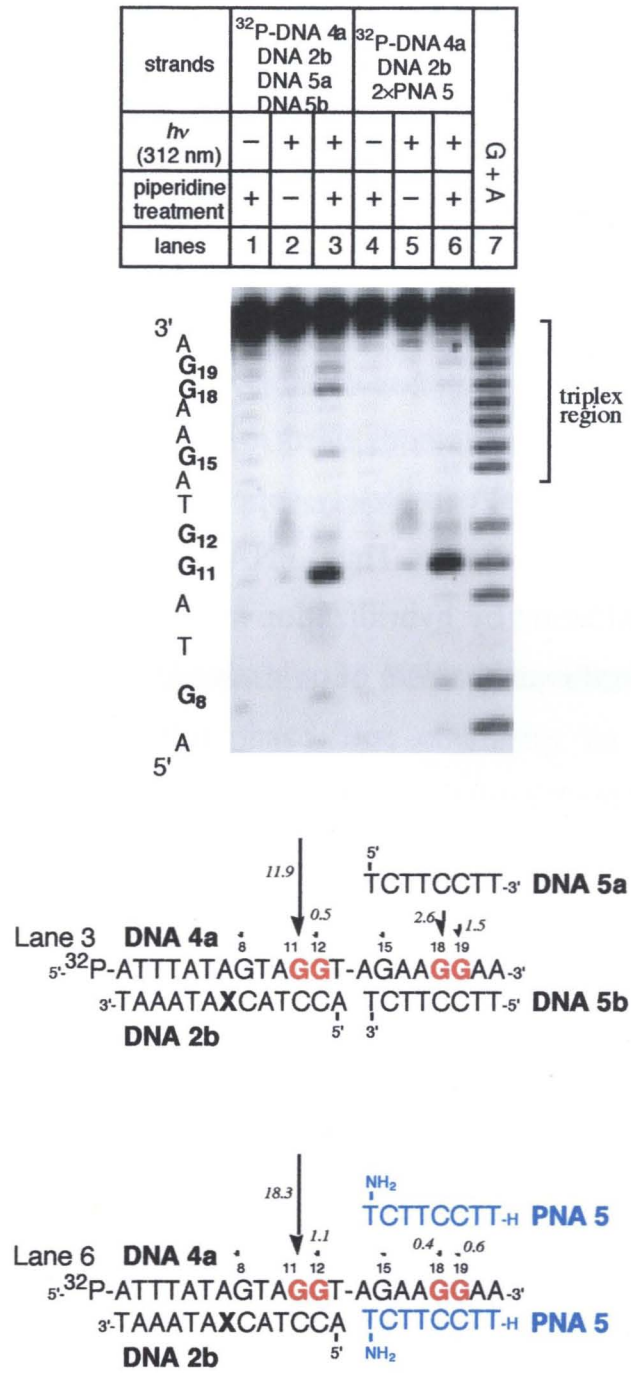

Figure 3. Autoradiograms of a denaturing gel electrophoresis for ^{32}P-5'-end labeled **DNA 4a** after photooxidation of triplexes. 312 nm photoirradiation of triplexws containing cyanobenzophenone-substituted 2'-deoxyuridine incorporated into **DNA 2b** at 0 °C for 1 h followed by hot piperidine treatment (90 °C, 20 min). Lanes 1–3, **DNA 4a**/(**DNA 2b**+**DNA 5a**+**DNA 5b**); lanes 4–6, **DNA 4a**/(**DNA 2b**+2×**PNA 5**); lane 7, Maxam-Gilbert sequencing lane. The arrows and italic number represent relative intensities of cleavage bands obtained by densitometric analysis.

Conclusion

In summary, DNA/PNA duplex was oxidized at GG step in the photooxidation with external riboflavin, whereas the efficiency of the remote GG oxidation was significantly lowered by the formation of DNA/PNA duplex. In addition, it was found that the hybridization of PNA to DNA resulted in a decrease of the 5'G selectivity of GG oxidation regardless of the oxidation methods used. Furthermore, the formation of DNA/$(PNA)_2$ triplex almost completely suppressed DNA cleavage derived from the remote GG oxidation. Thus, PNA acts as an effective inhibitor for remote DNA oxidation by hybridization to DNA and is used as a useful tool for the study on the mechanism of oxidative DNA lesion.

Experimental Section

General. Cyanobenzophenone-tethered oligodeoxynucleotides were synthesized as described elsewhere[24] on Applied Biosystems 392 DNA/RNA synthesizer. T4 kinase was purchased from NIPPON GENE (10 units/μL) and γ-[^{32}P]-ATP (10 mCi/mL) was from Amersham Pharmacia Biotech. Photoirradiation at 312 nm or 366 nm was carried out using a COSMO BIO CSF-20AF transilluminator. A GIBCO BRL Model S2 sequencing gel electrophoresis apparatus was used for polyacrylamide gel electrophoresis (PAGE).

Synthesis and Characterization of PNA Oligomers. PNA oligomers were synthesized by solid phase ^{t}Boc chemistry on a MBHA resin as described by Koch *et al.*[25] After the completion of PNA oligomer synthesis, the resin was treated with a solution of trifluoroacetic acid, trifluoromethanesulfonic acid, thioanisole, and *p*-cresol (6:2:1:1 v/v/v/v) for the cleavage of PNA oligomer from the resin and for the deprotection. The solution was filtered and precipitated in ethyl ether, centrifuged, and decanted. The residue was redissolved in trifluoroacetic acid, reprecipitated in ethyl ether, centrifuged, and then decanted to give the crude product. The crude oligomer was purified by reversed phase HPLC on a Wakosil II 5-C18-AR (20 × 150 mm) using a linear gradient of acetonitrile including 0.05% trifluoroacetic acid and aqueous 0.05% trifluoroacetic acid solvent system at a flow rate 4.0 mL/min and eluting products were detected by UV at 260 nm. Each PNA oligomer was characterized by MALDI-TOF MS; **PNA 3a** H-GTGTCCAG-NH_2, *m/z* 2202.82 (calcd for $[M+H]^+$ 2202.12); **PNA 3b** H-GACCTGTG-NH_2, *m/z* 2202.78 (calcd for $[M+H]^+$ 2202.12); **PNA 5** H-TTCCTTCT-NH_2, *m/z* 2103.26 (calcd for $[M+H]^+$ 2103.05).

T_m Measurement. A 2.5 μM solutions of the appropriate oligonucleotides and PNA oligomers in 10 mM phosphate buffer (pH 7.0 for duplex, pH 6.2 for triplex) were prepared. Melting curves were obtained by monitoring the absorbance at 260 nm as the temperature was ramped from 2 °C to 81 °C at a rate of 1 °C/min.

CD Measurement. The circular dichromism (CD) spectra were measured at 2 °C. In CD of antiparallel DNA/PNA duplex, a strong positive band at 261 nm and a weak negative band at 240 nm were observed. The CD spectrum was in good agreement with that of DNA/PNA duplex reported earlier.[26a] DNA triplex exhibited a CD spectrum with a positive band at 278 nm and a negative band at 246 nm, and DNA/$(PNA)_2$ triplex exhibited a positive CD band at 275 nm and a negative CD band at 247 nm, which was consistent with that reported previously.[26b]

Preparation of 5'-^{32}P-End-Labeled ODN. Oligonucleotides (ODNs, 400 pmol strand concentration) were labeled by phosphorylation with 4 μL of [γ-^{32}P]ATP and 4 μL of T_4 polynucleotide kinase using standard procedures.[29,30] The 5'-end-labeled oligonucleotides were recovered by ethanol precipitation and further purified by 15% nondenaturing gel electrophoresis and isolated by the crush and soak method.[31]

Cleavage of ^{32}P-5'-End-Labeled ODNs by Photoirradiation in the Presence of Riboflavin. Sample solutions were prepared by hybridizing a mixture of cold and radiolabeled oligonucleotides (**DNA 1**, 1 μM) with 1 μM of **DNA 2a** and 1 μM of **DNA 3**, **PNA 3a** or **PNA 3b** in sodium phosphate buffer (pH 7.0). Hybridization was achieved by heating the sample at 90 °C for 5 min and slowly cooling to room temperature. The

^{32}P-5'-end labeled ODN duplex (2.0×10^5 cpm) containing riboflavin was irradiated at 366 nm at 0 °C for 60 min. After irradiation, all reaction mixtures were precipitated with addition of 10 μL of *herring sperm* DNA (1 mg/mL), 10 μL of 3 M sodium acetate and 800 μL of ethanol. The precipitated DNA was washed with 100 μL of 80% cold ethanol and then dried *in vacuo*. The precipitated DNA was resolved in 50 μL of 10% piperidine (v/v), heated at 90 °C for 20 min and concentrated. The radioactivity of the samples was assayed using an Aloka 1000 liquid scintillation counter and the dried DNA pellets were resuspended in 80% formamide loading buffer (a solution of 80% formamide (v/v), 1 mM EDTA, 0.1% xylene cyanol and 0.1% bromophenol blue). All reactions, along with Maxam-Gilbert G+A sequencing reactions, were heat-denatured at 90 °C for 3 min and quickly chilled on ice. The samples (1–2 μL, 2–5 × 10^3 cpm) were loaded onto 15% of polyacrylamide/7 M urea sequencing gels and electrophoresed at 1900 V for 60 min and transferred to a cassette and stored at –80 °C with Fuji X-ray film (RX-U). The gels were analyzed by autoradiography with a densitometer and BIORAD Molecular Analyst software (version 2.1). The intensity of the spots resulting from piperidine treatment was determined by volume integration.

Cleavage of ^{32}P-5'-end-Labeled Oligonucleotides by Photoirradiation in the Presence of Cyanobenzophenone Tethered Oligodeoxynucleotides. Sample solutions were prepared by hybridizing a mixture of cold and radiolabeled oligonucleotides (**DNA 1**, 1 μM) with 1 μM of **DNA 2a** and 1 μM of **DNA 3**, **PNA 3a** or **PNA 3b** in sodium phosphate buffer (pH 7.0). Hybridization was achieved by heating the sample at 90 °C for 5 min and slowly cooling to room temperature. The ^{32}P-5'-end labeled ODN duplex (2.0×10^5 cpm) was irradiated at 312 nm at 0 °C for 60 min. The operation after irradiation was the same manner as

described for the DNA cleavage experiment using riboflavin.

Triplex samples were prepared by hybridizing a mixture of cold and radiolabeled oligonucleotides (**DNA 4a**, 1 μM) with 1 μM of **DNA 2b** and 1 μM of **DNA 5a** and **5b** or 2 μM of **PNA 5** in sodium phosphate buffer (pH 6.2).

HOMO Calculations. All calculations were performed at the B3LYP/6-31G(d) level using GAUSSIAN94. Geometries of stacked base pairs were constructed as follows.[32] The corresponding DNA duplex dimers were built up using the Insight II program (Version 97.0) with standard B-form helical parameters which have been optimized by X-ray crystallographic analysis of relevant monomers and X-ray diffraction data of polymers.[33] The corresponding PNA-DNA duplex dimers were built up using the Insight II program with helical parameters which have been optimized by NMR analysis data of polymers.[27] All the sugar backbones and peptide backbones of the duplex were replaced by methyl group at the N_1 (pyrimidine base) and N_9 (purine base). HOMO of the calculated dimers was displayed graphically using Gaussian I/F.

References and Notes

(1) Hall, D. B.; Holmlin, R. E.; Barton, J. K. *Nature* **1996**, *382*, 731–735.

(2) Burrows, C. J.; Muller, J. G. *Chem. Rev.* **1998**, *98*, 1109–1154.

(3) Grinstaff, M. W. *Angew. Chem. Int. Ed.* **1999**, *38*, 3629–3635.

(4) Núñez, M. E.; Barton, J. K. *Curr. Opin. Chem. Biol.* **2000**, *4*, 199–206.

(5) Schuster, G. B. *Acc. Chem. Res.* **2000**, *33*, 253–260.

(6) Giese, B. *Acc. Chem. Res.* **2000**, *33*, 631–636.

(7) Halliwell, B.; Gutteridge, J. M. C. *Free Radicals in Biology and Medicine*, Oxford University Press, Oxford, **1999**.

(8) Melvin, T.; Plumb, M. A.; Botchway, S. W.; O'Neill, P.; Parker, A. W. *Photochem. Photobiol.* **1995**, *61*, 584–591.

(9) Boon, P. J.; Cullis, P. M.; Symons, M. C. R.; Wren, B. W. *J. Chem. Soc. Perkin Trans. 2* **1984**, 1393–1399.

(10) Wolf, P. G.; Jones, D. D.; Candeias, L. P.; O'Neill, P. *Int. J. Rad. Biol.* **1993**, *64*, 7–18.

(11) Steenken, S.; Jovanovic, S. V. *J. Am. Chem. Soc.* **1997**, *119*, 617–618.

(12) Sugiyama, H.; Saito, I. *J. Am. Chem. Soc.* **1996**, *118*, 7063–7064.

(13) Saito, I.; Nakamura, T.; Nakatani, K.; Yoshioka, Y.; Yamaguchi, K.; Sugiyama, H. *J. Am. Chem. Soc.* **1998**, *120*, 12686–12687.

(14) Meggers, E.; Michel-Beyerle, M. E.; Giese, B. *J. Am. Chem. Soc.* **1998**, *120*, 12950–12955.

(15) Lewis, F. D.; Liu, X.; Liu, J.; Miller, S. E.; Hayes, R. T.; Waslelewski, M. R. *Science* **2000**, *406*, 51–53.

(16) Nakatani, K.; Dohno, C.; Saito, I. *J. Am. Chem. Soc.* **2000**, *122*, 5893–5894.

(17) Grozema, F. C.; Berlin, Y. A.; Siebbeles, L. D. A. *J. Am. Chem. Soc.* **2000**, *122*, 10903–10909.

(18) Núñez, M. E.; Noyes, K. T.; Gianolio, D. A.; McLaughlin, L. W.; Barton, J. K. *Biochemistry* **2000**, *39*, 6190–6199.

(19) Kan, Y.; Schuster, G. B. *J. Am. Chem. Soc.* **1999**, *121*, 11607–11614.

(20) Nielsen, P. E.; Egholm, M.; Buchardt, O. *Science*, **1991**, *254*, 1497–1500.

(21) Egholm, M.; Buchardt, O.; Christensen, L.; Behrens, C.; Freier, S. M.; Driver, D. A.; Berg, R. H.; Kim, S. K.; Nordén, B.; Nielsen, P. E. *Nature* **1993**, *365*, 566–568.

(22) Armitage, B.; Ly, D.; Koch, T.; Frydenlund, H.; Ørum, H.; Batz, H. G.; Schuster, G. B. *Proc. Natl. Acad. Sci. U.S.A.* **1997**, *94*, 12320–12325.

(23) Armitage, B.; Koch, T.; Frydenlund, H.; Ørum, H.; Batz, H. G.; Schuster, G. B. *Nucleic Acids Res.* **1997**, *25*, 4674–4678.

(24) Nakatani, K.; Dohno, C.; Saito, I.; *J. Org. Chem.* **1999**, *64*, 6901.

(25) Koch, T.; Hansen, H. F.; Andersen, P.; Larsen, T.; Batz, H. G.; Ottesen, K.; Ørum, H. *J. Peptide Res.* **1997**, *49*, 80.

(26) (a) Armitage, B.; Ly, D.; Koch, T.; Frydenlund, H.; Ørum, H.; Schuster, G. B. *Biochemistry* **1998**, *37*, 9417–9425. (b) Wittung, P.; Nielsen, P. E.; Nordén, B. *Biochemistry* **1997**, *36*, 7973–7979.

(27) Eriksson, M.; Nielsen, P. E. *Nat. Struct. Biol.* **1996**, *3*, 410–413.

(28) Selsing, E.; Wells, R. D.; Alden, C. J.; Arnott, S. *J. Biol. Chem.* **1979**, *254*, 5417–5422.

(29) Maxam, M.; Gilbert, W. *Proc. Natl. Acad. Sci. U.S.A.* **1977**, *74*, 560.

(30) Maniatis, T.; Fritsch, E. F.; Sambrook, J. *Molecular Cloning*, Cold Spring Harbor Laboratory Press, Plainview, New York, **1982**.

(31) Sambrook, J.; Fritsch, E. F.; Maniatis, T. *Molecular Cloning*, A Laboratory Manual, 2nd Ed., Cold Spring Harbor Laboratory Press, New York, **1989**.

(32) Yoshioka, Y.; Kitagawa, Y.; Takano, Y.; Yamaguchi, K.; Nakamura, T.; Saito, I. *J. Am. Chem. Soc.* **1999**, *121*, 8712–8719.

(33) (a) Arnott, S.; Hukins, D. W. L. *Biochem. Biophys. Res. Commun.* **1972**, *47*, 1504. (b) Arnott, S.; Selsing, E. *J. Mol. Biol.* **1974**, *88*, 509.

Chapter 3

Site-Specific Discrimination of Cytosine and 5-Methylcytosine in Duplex DNA by Peptide Nucleic Acids

Abstract

Cytosine methylation has long been recognized as an important factor in gene silencing. In clarifying the role of cytosine methylation, it is important to know the methylation status of cytosine nucleotides in genomic DNA. We employed peptide nucleic acids (PNA) and the fluorescence resonance energy transfer (FRET) for discrimination between cytosine and 5-methylcyotsine in DNA. We prepared PNA-DNA complex referred to as PD-loop containing fluorophore and quencher and examined the enzymatic digestion of the complex. Dramatic enhancement of fluorescence was observed for PD-loop containing cytosine in the target sequence, but not so dramatic for PD-loop containing 5-methylcytosine. Herein, we reported a simple discrimination between cytosine and 5-methylcytosine in double strand DNA by the use of fluorescence spectroscopy and fluorescence microscopy.

Introduction

5-Metylcytosine is involved in the regulation of gene expression and its presence in DNA is believed to be correlated with gene silencing.[1] Although 5-methylcytosine represents less than 1% of the bases in the mammalian genome, it is believed to cause *ca.* one third of all transition mutations responsible for human genetic diseases and cancer.[2] It has, thus, become important to know the methylation status in genomic DNA. There were several reports for mapping methylation patterns of genomic DNA, utilizing the Maxam and Gilbert chemical modification[3] or polymerase chain reaction (PCR) after sodium bisulfite-mediated conversion of cytosine to uracil.[4] However, these protocols for the detection of cytosine methylation require complicated and tedious procedures. In addition, the resulting data contain too much information on the cytosine methylation of whole DNA sequences for effective analysis of their functions. Therefore, the development of a simple and convenient method for the site-specific discrimination of cytosine methylation is imperative for genomic studies.

Peptide nucleic acids (PNA) is a nucleic acid analog possessing polypeptide backbone instead of sugar-phosphate backbone and is known to tightly bind to complementary DNA and RNA.[5] Remarkable properties of PNA are, i) the sequences within duplex DNA are recognized by strand invasion,[6] and ii) the displaced DNA strand allows binding with the probe oligomer (PO) to form PNA-DNA complex referred to as PD-loop (Figure 1). Presently, we report a simple method for the discrimination of cytosine and 5-methylcytosine in the double strand DNA by using PNA and fluorescence resonance energy transfer (FRET). We prepared PD-loop containing fluorescent donor and acceptor and examined enzymatic cleavage. Enzymatic cleavage of PD-loop resulted in a quite different

fluorescence emission intensity between PD-loop containing cytosine (C-PD-loop) and 5-methylcytosine (^{m}C-PD-loop) in the target sequence.

Results and Discussion

The outline for the discrimination system was described in Figure 1. We first incubated double strand DNA in the presence of two complementary PNAs to displace the DNA strand. Subsequently, the probe oligomer (PO) was added for hybridization with displaced strand. The resulting PD-loop was treated with restriction enzyme. The fluorophore fluorescein was attached to the 5'-end of PO, while the quencher dabsyl was attached to the 3'-end. Digestion of the PO was expected to be very small in the presence of 5-methylcytosine because the activity of restriction enzyme was lowered by the presence of 5-methylcytosine on its recognition site.[7] Consequently, in the enzymatic digestion of ^{m}C-PD-loop, the probe oligomer keeps fluorophore and quencher in close proxymity to each other, resulting in a fluorescence quenching by FRET. On the other hand, the fluorescence emission of fluorescein would be enhanced following enzymatic digestion of C-PD-loop as a result of concomitant release of the fluorescein-containing strand. DNA and PNA oligomers used in this study are summarized in Table 1.

Initially, we tested 80 mer DNA duplex (**DNA 1** or **DNA 2** / **DNA 3**) including a cytosine or a methylated cytosine in recognition site (5'-GXGC-3': X = cytosine or 5-methylcytosine) of *Hha* I. According to the protocol described above, we prepared PD-loop and monitored the increase of fluorescence emission resulting from enzymatic digestion of the PD-loop. Figure 2 shows a fluorescence spectra and a time course of the fluorescence increase of PD-loop treated with *Hha* I.

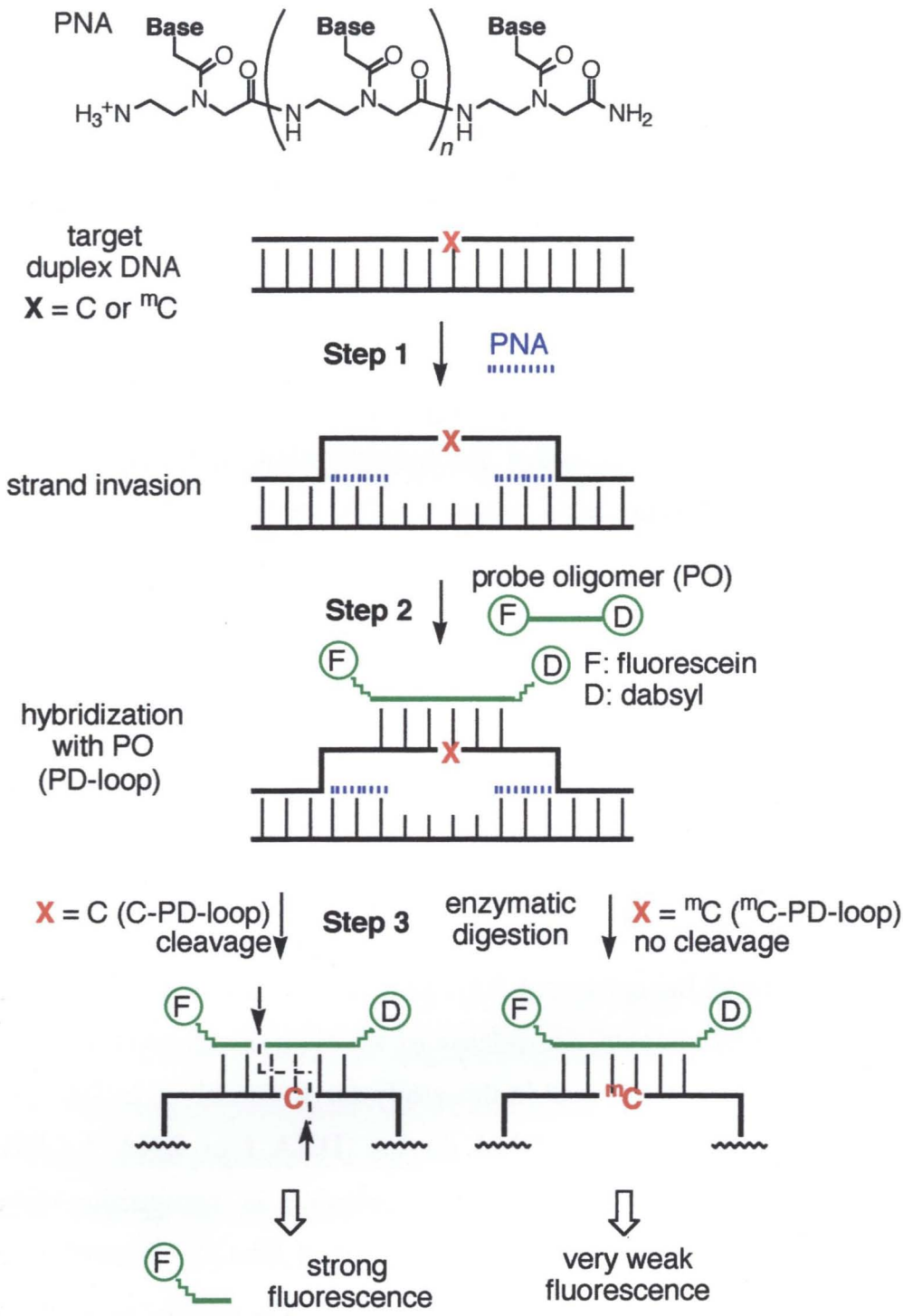

Figure 1. Schematic illustration of the protocol for the site-specific discrimination between cytosine (C) and 5-methylcytosine (^{m}C) in duplex DNA. Step 1: strand invasion with two PNA strand to target duplex DNA; step 2: hybridization of displaced DNA strand and probe oligomer (PO); step 3: specific cleavage of C-PD-loop by restriction enzyme.

Table 1. DNA and PNA oligomers used in this study.

Double strand DNA[a, b, c]

DNA **1**: X = C, DNA **2**: X = ^{m}C, DNA **3**: complement to DNA **1** and **2**
5'- · (24 mer) · *TTTTTTTTTT*GTCA**GXGC**ATGG*TTTTTTTTTT* · (24 mer) · -3'

DNA **4**: X = C, DNA **5**: X = ^{m}C, DNA **6**: complement to DNA **4** and **5**
5'- · (24 mer) · *TTTTTTTTTT*GTAC**CXGG**GATG*TTTTTTTTTT* · (24 mer) · -3'

DNA **7**: X = C, DNA **8**: X = ^{m}C, DNA **9**: complement to DNA **7** and **8**
5'- · (20 mer) · *CTCTTCCTCT*GT**GXGC**CG*GTCTCTCCCA* · (20 mer) · -3'

Probe oligomers[a, d]

PO **1**: 5'-FAAACCAT**GCGC**TGACAAAD-3'

PO **2**: 5'-FAAACATC**CGG**GTACAAAD-3'

PO **3**: 5'-FGACCG**GCGC**ACAGAD-3'

PNAs[e]

PNA **1**: H-TTTTTTTTTT-NH_2

PNA **2**: H-CTCTTCCTCT-NH_2

PNA **3**: H-GTCTCTCCCA-NH_2

[a]Recognition site of restriction enzyme are shown in bold type.
[b]PNA binding sites are shown in italic type.
[c]See experimental section for full DNA sequences.
[d]'F' signifies a fluorescein moiety and 'D' signifies dabsyl moiety.
[e]The PNAs are written from the amino to carboxy-terminal using normal peptide convensions: 'H' signifies a free amino group, while 'NH_2' signifies a terminal carboxamide.

As shown in Figure 2, fluorescence emission of C-PD-loop increased with increasing incubation time, resulting in a *ca.* 2.5-fold increase of fluorescence intensity. On the other hand, enhancement of fluorescence emission was suppressed for ^{m}C-PD-loop, with only 1.3-fold increase of fluorescence intensity. Thus, the results indicated that 5-methylcytosine in ^{m}C-PD-loop inhibited the activity of the restriction enzyme, and suggesting that it is possible to discriminate between cytosine and 5-methylcytosine in double-stranded DNA by monitoring of the

fluorescence emission of PD-loop containing fluorescein and dabsyl. In the absence of PNA, only small increase of emission was observed (Figure 2D), suggesting that PNA was indispensable for this system.

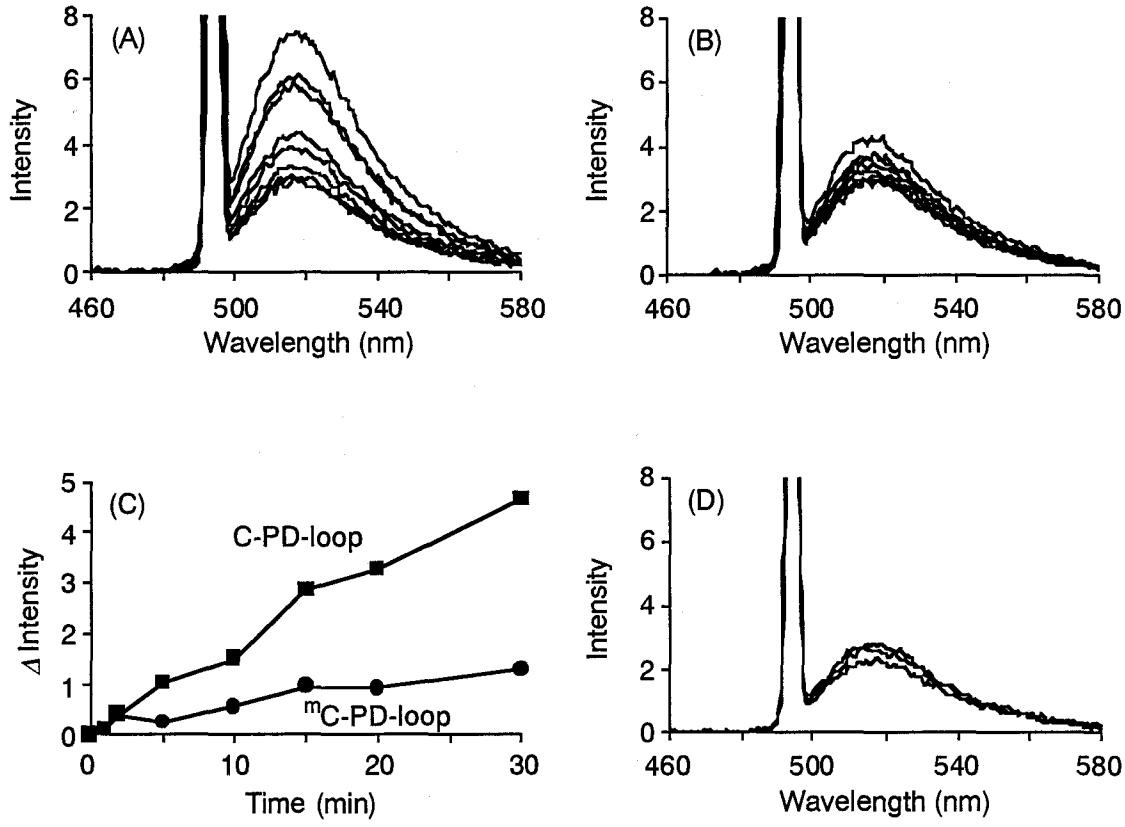

Figure 2. Fluorescence spectra and change of fluorescence intensity of PD-loop treated with restriction enzyme. The fluorescence spectra were measured at 495 nm excitation. (A) Fluorescent spectra given by *Hha* I digestion (0, 1, 2, 10, 15, 20, and 30 min from bottom to top) of C-PD-loop (**DNA 1/ DNA 3 / PNA 1 / PO 1**). (B) Fluorescent spectra given by *Hha* I digestion (0, 1, 2, 10, 15, 20, and 30 min from bottom to top) of ^{m}C-PD-loop (**DNA 2 / DNA 3 / PNA 1 / PO 1**). (C) Change of fluorescence intensity of PD-loop treated with *Hha* I at 518 nm. The fluorescence intensities are designated by (■) for C-PD-loop and by (●) for ^{m}C-PD-loop. (D) Fluorescent spectra after incubation with *Hha* I (0, 15, and 30 min from bottom to top) under the reaction condition in the absence of PNA 1 (**DNA 1 / DNA 2 / PO 1**).

We next examined the enzymatic digestion with another restriction enzyme in order to evaluate the generality of the system. *Hap* II restriction enzyme recognize 5'-CCGG-3' site and is also known that its activity is suppressed by the presence of 5-methylcytosine in the recognition site.[8] We tested our system on 80 mer double-stranded DNA containing CXGG (X = cytosine or 5-methylcyotsine) site. Enzymatic digestion of PD-loop by *Hap* II also exhibited a different emission intensity between C-PD-loop and ^{m}C-PD-loop (Figure 3A).

We next examined the enzymatic digestion of PD-loop formed by 72 mer double-stranded DNA (**DNA 7** or **DNA 8** / **DNA 9**), which is a partial sequence of exon 8 in human p53 gene containing recognition site of *Hha* I.[9] Since slightly acidic condition was required for the formation of PD-loop (**DNA 7** or **DNA 8** / **DNA 9** / **PNA 2** and **PNA 3** / **PO 3**), we carried out enzymatic digestion of PD-loop at pH 6.5. Even under acidic conditions, restriction enzyme *Hha* I exhibited cleavage activity, and enhancement of fluorescence intensity was observed with increasing the incubation time. As clearly seen in Figure 3B, enhancement of fluorescence intensity of C-PD-loop was dramatic, but that of ^{m}C-PD-loop was not so dramatic. Thus, the results strongly indicate that discrimination of cytosine and 5-methylcytosine in various DNA sequences was possible by monitoring the fluorescence increase of PD-loop after treatment with appropriate restriction enzymes.

The possibility of the visualization of the discrimination between cytosine and 5-methylcytosine in DNA by the use of PNA and FRET was examined by fluorescence microscopy. The analysis of the fluorescence microscopy was carried out on the agarose gel medium to avoid diffusion of the fluorescent products.[10] Figure 4 shows the fluorescence image of PD-loop (**DNA 7** or **DNA 8** / **DNA 9** / **PNA 2** / **PNA 3** / **PO 3**) treated with *Hha* I. The green fluorescence emission from C-PD-loop was brighter

than that from ^{m}C-PD-loop. Thus, the results suggest that it is possible to visualize the difference between cytosine and 5-methylcytosine in DNA by using this protocol.

As compared with current available methods for evaluating methylation status of DNA,[3,4] a major advantage of our method is that cytosine methylation can be detected optically without time-consuming procedure such as duplex denaturation and electrophoresis, although the general utility of our methods is limited by the sequences restrictions imposed on the target sequences and the well-described limitations for duplex invasion by PNA.[6]

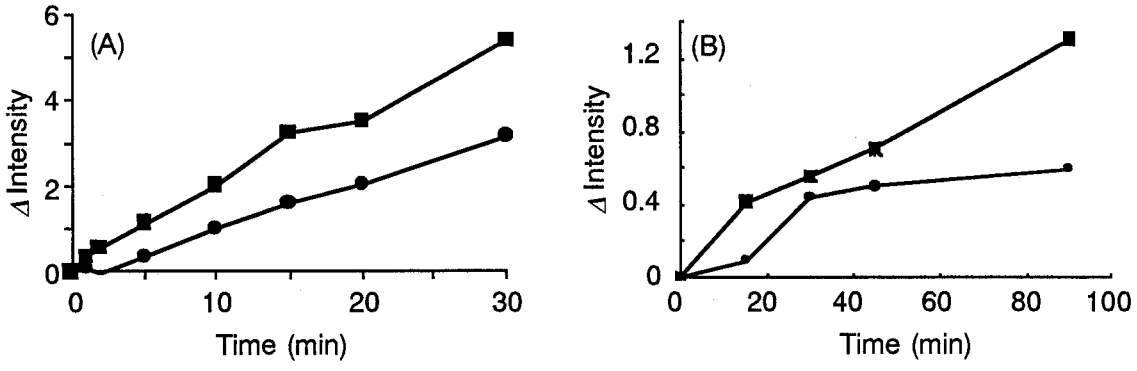

Figure 3. Change of fluorescence intensity of PD-loop treated with *Hha* I at 518 nm. The fluorescence spectra were measured at 495 nm excitation. The fluorescence intensities are designated by (■) for C-PD-loop and by (●) for ^{m}C-PD-loop. (A) Enzymatic digestion (*Hap* II) of PD-loop (**DNA 4** or **DNA 5** / **DNA 6** / **PNA 1** / **PO 2**). (B) Enzymatic digestion (*Hha* I) of PD-loop (duplex DNA coreesponding to codons 270–294 of p53 gene, exon 8: **DNA 7** or **DNA 8** / **DNA 9** / **PNA 2** / **PNA 3** / **PO 3**) at pH 6.5.

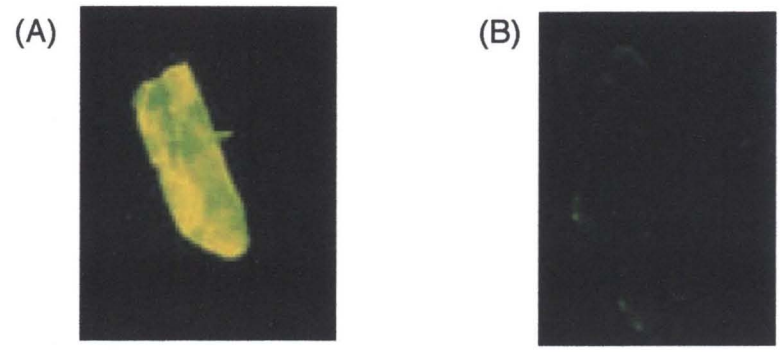

Figure 4. Fluorescence microscopy (60 min incubation) of PD-loop (**DNA 7** or **DNA 8 / DNA 9 / PNA 2 / PNA 3 / PO 3**) with *Hha* I. (A) C-PD-loop. (B) ^{m}C-PD-loop.

Conclusion

In summary, we have disclosed a simple method for site-specific discrimination between cytosine and 5-methylcytosine in double-stranded DNA by the use of enzymatic digestion of PD-loop containing fluorophore and quencher. Fluorescence intensity was considerably enhanced after the enzymatic digestion of C-PD-loop. On the other hand, ^{m}C-PD-loop showed only a weak fluorescence emission. Thus, the system described here would be useful for the detection of 5-methylcytosine in various genes.

Experimental Section

General. The reagents for DNA synthesizer were purchased from Glen Research. Other reagents were purchased at highest commercial quality and used without further purification unless otherwise stated. Calf intestine alkaline phophatase (AP) (1000 units/mL), snake venom phosphodiesterase (s.v. PDE) (1 mg / 0.5 mL), and Nuclease P1 (1 mg) were purchased from Boehringer Manheim. Fluorescent spectra were measured on SHIMADZU RF-5300PC spectrofluorophotometer.

DNA oligomers. Probe oligomers were synthesized on a Applied Biosystems Model 392 DNA/RNA synthesizer by using standard phosphoroamidite chemistries including fluorescein and 4-(4'-dimethylaminophenylazo)benzoic acid (dabsyl) modification. After automated synthesis, the probe oligomers were purified by reversed phase HPLC. The purity and concentration of the probe oligomers were determined by complete digestion with s.v. PDE, AP, and Nuclease P1 at 37 °C for 2 h. Identities of synthesized probe oligomers were confirmed MALDI TOF mass spectrometry. All other oligonucleotides were purchased from Pharmacia Biotech. The DNA used in this study were follows.; **DNA 1**: 5'-TCATCCTCGGCACCGTCACCCTGGTTTTTTT TTTGTCAGCGCATGGTTTTTTTTTTAGCCACTATCGACTATCATGG CGA-3', **DNA 4**: 5'-TCATCCTCGGCACCGTCACCCTGGTTTTTT TTTGTACCCGGGATGTTTTTTTTTTTAGCCACTATCGACTATCATGG CGA-3', **DNA 7**: 5'-TCCCCTTTCTTGCGGAGATTCTCTTCCTCT GTGCGCCGGTCTCTCCCAGGACACAAACACGCACCTCA-3'

PNA. PNAs were synthesized with a Boc strategy on a solid support synthesis as described.[11] The MBHA resin HCl salt was treated with 2M

DIPEA/NMP solution to activate for coupling. The Boc PNA monomer was then added with HBTU and DIPEA as a coupling activator. After coupling, the mixture was treated with acetic anhydride/pyridine/NMP (1/25/25 v/v/v). To remove the Boc group, the resulting mixture was treated with *m*-cresol/TFA (5/95), and then the next couplings were continued. Deprotection of Z group at A, C, and G nucleobases was done with p-cresol/thioanisole/trifluoromethansulfonic acid/TFA (1/1/2/6). The purification of the synthesized PNAs was performed on a WAKO sil II 5C18AR reverse-phase colunm by HPLC. Identity of synthesized PNA was confirmed MALDI TOF mass spectrometry. The PNAs used in this study were summarized in Table 1.

General procedure for the cleavage of PD-loop by restriction enzyme. All reactions were executed in a total volume of 22.2 μL with final concentrations of each species as indicated. 4 μL of 100 μM PNA was added to the solution of 135 nM DNA duplex, and mixture was incubated at 37 °C for 4 h. Subsequently, 2 μL of 10 μM probe oligomer was added, and mixture was incubated at 37 °C for 1 h. The resulting mixture (PD-loop) was incubated in 10 mM Tris-HCl (pH 7.5), 10 mM $MgCl_2$, 10 mM DTT and 50 mM NaCl with restriction enzyme (10 Units) at 37 °C. After enzymatic cleavage, reaction mixture was diluted with 477.8 μL of water. After dilution, fluorescent increase was monitored (ex. 495 nm).

Analysis by fluorescence microscopy. According to the protocol described above, PD-loop was prepared and the enzymatic digestion was carried out in total volume of 22.2 μL). After enzymatic digestion for 60 min, the sample was heated at 70 °C for 20 min. After heating, 7.8 μL of 1.7 % agarose gel solution was added to the sample, and then the combined mixture was maintained at room temperature for 8 h. The gel piece was

sandwiched between cover glasses and subjected to analysis by fluorescence microscopy. Fluorescence was detected with a WIB excitation method (excitation 460-490 nm,; BX51, Olympus Optical Co.). Photographs were taken on Fujichrome MS 100 / 1000 film.

References

(1) (a) Bird, A. *Cell* **1992**, *70*, 5–8. (b) Eden, S.; Cedar, H. *Curr. Opin. Genet. Dev.* **1994**, 4, 255–259. (c) Holliday, R.; Grigg, G. A. *Mutat. Res.* **1993**, *285*, 61–67. (d) Bird, A. P. *Nature* **1986**, 321, 209–213. (e) Li, E.; Beard, C.; Janenisch, R. *Nature* **1993**, *366*, 362–365. (f) Tremblay, K. D.; Saam, J. R.; Ingram, R. S.; Tilighman, S. M.; Bartolomei, M. S. *Nat. Genet.* **1995**, *9*, 407–413. (g) Pfeifer, G. P.; Steigerwald, S. D.; Mueller, P. R.; Wold, B.; Riggs, A. D. *Science* **1989**, *246*, 810–813. (h) Riggs, A. D.; Pfeifer, G. P. *Trends Genet.* **1992**, *8*, 169–174. (i) Antequera, F.; Boyes, J.; Bird, A. *Cell* **1990**, *62*, 503–514. (j) Herman, J. G.; Latif, F.; Weng, Y.; Lerman, M. I.; Zbar, B.; Liu, S.; Samid, D.; Duan, D. S.; Gnarra, J. R.; Linehan, W. M.; Baylin, S. B. *Proc. Natl. Acad. Sci. USA* **1994**, *91*, 9700–9704. (k) Merlo, A.; Herman, J. G.; Mao, L.; Lee, D. J.; Gabrielson, E.; Burger, P. C.; Baylin, S. B.; Sidransky, D. *Nat. Med.* **1995**, *1*, 686–692. (l) Herman, J. G.; Jen, J.; Merlo, A.; Baylin, S. B. *Cancer Res.* **1996**, *56*, 722–727. (m) Graff, J. R.; Herman, J. G.; Lapidus, R. G.; Chopra, H.; Xu, R.; Jarrard, D. F.; Isaacs, WB, Pitha, P. M.; Davidson, N. E.; Baylin, S. B. *Cancer Res.* **1995**, *55*, 5195–5199.

(2) (a) Spruck III, C. H.; Rideout III, W. M.; Jones, P. A. DNA *Methylation: Molecular Biology and Biological Significance.* Jost, JP and Saluz HP. (eds). Birkhäuser Verlag: Basel, **1993**, Switzerland, pp. 487–509. (b) Esteller, M; Garcia-Foncillas, J.; Andion, E.; Goodman, S. N.; Hidalgo, O. F.; Vanaclocha, V.; Baylin, S. B.; Herman, J. G. *N. Engl. J. Med.* **2000**, *343*, 1350–1354.

(3) Church, G. M.; Gilbert, W. *Proc. Natl. Acad. Sci. USA* **1984**, *81*, 1991–1995.

(4) (a) Frommer, M.; McDonald, L. E.; Millar, D. S.; Collis, C. M.; Watt,

F.; Grigg, G. W.; Molloy, P. L.; Paul, C. L. *Proc. Natl. Acad. Sci. USA* **1992**, *89*, 1827–1831. (b) Herman, H. G.; Graff, J. R.; Myöhänen, S.; Nelkin, B. D.; Baylin, S. B. *Proc. Natl. Acad. Sci. USA* **1996**, *93*, 9821–9826.

(5) Nielsen, P. E. *Acc. Chem. Res.* **1999**, *32*, 624–630.

(6) (a) Smulevitch, S. V.; Simmons, C. G.; Norton, J. C.; Corey, D. R. *Nat. Biotechnol.* **1996**, *14*, 566–568. (b) Bukanov, N. O.; Demidov, V. V.; Nielsen, P. E.; and Frank-Kamenetskii, M. D. *Proc. Natl. Acad. Sci. USA* **1998**, *95*, 5516–5520.

(7) (a) Ehrlich, M.; Wang, R. Y. –H. *Science* **1981**, *212*, 1350–1357. (b) Korch, C.; Hagblom, P. *Eur. J. Biochem.* **1986**, *161*, 519–524.

(8) Butkus, V.; Petrauskiene, L.; Maneliene, Z.; Klimasauskas, S.; Laucys, V.; Janulaitis, A. *Nucl. Acids Res.* **1987**, *15*, 7091–7102.

(9) Tornaletti, S.; Pfeifer, G. P. *Oncogene* **1995**, *10*, 1493–1499.

(10) Hashimoto, S.; Wang, B.; Hecht, S. M. *J. Am. Chem. Soc.* **2001**, *123*, 7437–7438.

(11) Egholm, M. E.; Buchardt, O.; Nielsen, P. E.; Berg, R. H. *J. Am. Chem. Soc.* **1992**, *114*, 1895–1897.

Chapter 4

Strand-Displacement Complex (P-loop) of Peptide Nucleic Acids and Duplex DNA as a Catalytic Template for Enzymatic Digestion

Abstract

Peptide nucleic acids (PNA) are known to bind to double-stranded DNA, resulting in the formation of strand-displacement complex (P-loop). This complex can be bind with its complementary single-stranded DNA, yielding PNA-DNA complex referred to as PD-loop. We report a quantitative analysis of enzymatic digestion of PD-loop. A single-stranded DNA (**SS DNA**), which was complement to a loop portion of P-loop, was cleaved by restriction enzyme in the presence of P-loop with high efficiency, and 6.7-fold amount of **SS DNA** over P-loop was cleaved. This result indicates that PD-loop can be a substrate of the restriction enzyme, and that P-loop acts as a catalytic template for enzymatic digestion of **SS DNA**. Further, the change of the structure of **SS DNA** from linear-type to dumbbell-type derived a drastic enhancement of the cleavage efficiency.

Introduction

Peptide nucleic acids (PNA) are known to tightly bind to double-stranded DNA yielding an extended strand-displacement complex (P-loop, Figure 1).[1] This complex is able to accommodate single-stranded DNA by a formation of PNA-DNA complex referred to as PD-loop.[2] By the use of this property of PNA, affinity capture[2a,3] and topological labeling[4] of double-stranded DNA and highly selective detection of specific sequences[5] within linear double-stranded DNA have become possible. Recently, we reported the discrimination between cytosine and 5-methylcytosine in double stranded DNA by the use of sequence selective formation of fluorescent labeled PD-loop and the cleavage of the complex by restriction enzymes.[6] A strong fluorescent emission was observed only in the case of enzymatic digestion of fluorescent labeled PD-loop, which did not have methylated cytosine.

Herein we report a quantitative analysis of enzymatic digestion of PD-loop. We prepared ^{32}P-5'-end labeled PD-loop and carried out enzymatic digestion. Cleavage experiment of PD-loop revealed that 6.7-fold amount of linear-type single-stranded DNA (**SS DNA**, Figure 1) over P-loop was cleaved by restriction enzyme. Furthermore, a structural change of the single-stranded DNA from linear-type (**SS DNA 1**) to dumbbell-type (**SS DNA 2**) derived a dramatic enhancement of the cleavage efficiency. On the other hand, enzymatic cleavage of DNA (**DNA 2**) which bound with PNA was suppressed in the increase of **SS DNA 1** concentration. These data strongly suggest that P-loop would act as a catalytic template for enzymatic digestion of **SS DNA**.

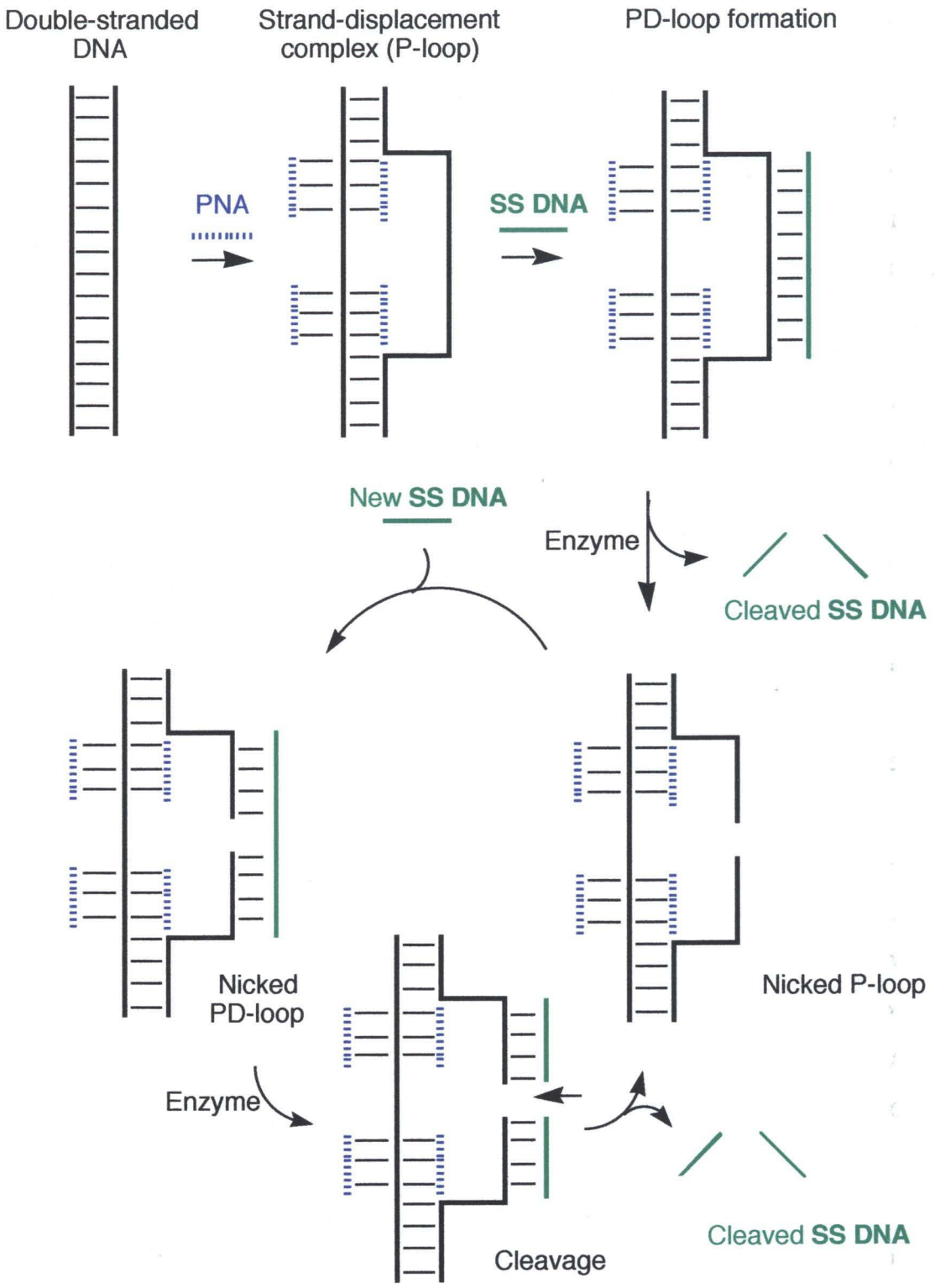

Figure 1. Schematic outline of the action of strand-displacement complex (P-loop) of PNA and double-stranded DNA as a catalytic template for enzymatic digestion of single-stranded DNA (**SS DNA**).

Results and Discussion

PNA oligomer was synthesized by standard solid phase *t*-BOC peptide chemistry,[7] purified by reversed phase HPLC and characterized by MALDI-TOF mass spectrometry. DNA and PNA oligomers used in this study were summarized in Table 1. PD-loop were prepared by the method described elsewhere.[2a]

Table 1. DNA and PNA oligomers used in this study.

Double strand DNA[a, b, c]

DNA 1: 5'-(24 mer)*TTTTTTTTTT*GTCA**GCGC**ATGG*TTTTTTTTTT*(24 mer)-3'
DNA 2: complement to DNA **1**

DNA 3: 5'-(24 mer)*TTTTTTTTTT***GCGC***TTTTTTTTTT*(24 mer)-3'
DNA 4: complement to DNA **3**

DNA 5: 5'-(24 mer)*TTTTTTTTTT*CA**GCGC**AC*TTTTTTTTTT*(24 mer)-3'
DNA 6: complement to DNA **5**

SS DNAs[a]

SS DNA 1: 5'-AAACCAT**GCGC**TGACAAA-3' (linear-type)

SS DNA 2: A^{A}CCAT**GCGC**TGAC^{A}A / A_{A}GGTAC GACTG$_{A}A$ (dumbbell-type)
5' 3'

SS DNA 3: 5'-AAA**GCGC**AAA-3'
SS DNA 4: 5'-AAAGT**GCGC**TGAAA-3'

PNA oligomer[d]

PNA 1: H-TTTTTTTTTT-NH_2

[a]Recognition site of restriction enzyme are shown in bold type.
[b]PNA binding sites are shown in italic type.
[c]See experimental section for full DNA sequences.
[d]The PNA is written from the amino to carboxy-terminal using normal peptide convensions: 'H' sigifies a free amino group, while 'NH_2' signifies a terminal carboxyamide.

Initially, we carried out enzymatic digestion of PD-loop containing 10 mer **PNA 1**, 18 mer linear-type **SS DNA 1** and 80 mer DNA duplex (**DNA 1 / DNA 2**) which had *Hha* I recognition site (5'-GCGC-3'). We prepared **PD-loop 1** (**DNA 1 / DNA 2 / PNA 1 / SS DNA 1**) including 10-fold amount of ^{32}P-5'-end labeled **SS DNA 1** over P-loop and monitored enzymatic digestion of **SS DNA 1** in **PD-loop 1** using restriction enzyme *Hha* I. Figure 2 shows the representative gel and the cleavage efficiency. As shown in Figure 2B, no cleavage was observed in the absence of **PNA 1** (lane 1), indicating that restriction enzyme could not recognize **SS DNA 1** as a substrate in the absence of P-loop. In contrast, cleavage efficiency of **SS DNA 1** in **PD-loop 1** increased with incubation time (lane 3 and 4). The velocity of product formation was calculated to be 0.17 nM / sec. It is noteworthy that 67% of **SS DNA 1** was cleaved through enzymatic digestion for 1 h (lane 4). That is, 6.7-fold amount of **SS DNA 1** over P-loop is digested by restriction enzyme. This result indicates that nicked P-loop produced after the enzymatic digestion of **PD-loop 1** would bind with new **SS DNA 1**, resulting in the formation of nicked PD-loop as a substrate of the restriction enzyme (Figure 1). In other words, nicked P-loop would act as a catalytic template for enzymatic digestion of **SS DNA**.

As a control experiment, we examined enzymatic cleavage of **SS DNA 1 / DNA 1** duplex. Also in this experiment, excess amount of **SS DNA 1** over **DNA 1** was cleaved by *Hha* I. However, the cleavage efficiency of DNA duplex was lower than that of **PD-loop 1** (Figure 2C). These results indicate that nicked P-loop acts as an efficient catalytic template for enzymatic digestion more than cleaved single-stranded DNA such as cleaved **DNA 1** in **SS DNA 1 / DNA 1** duplex.

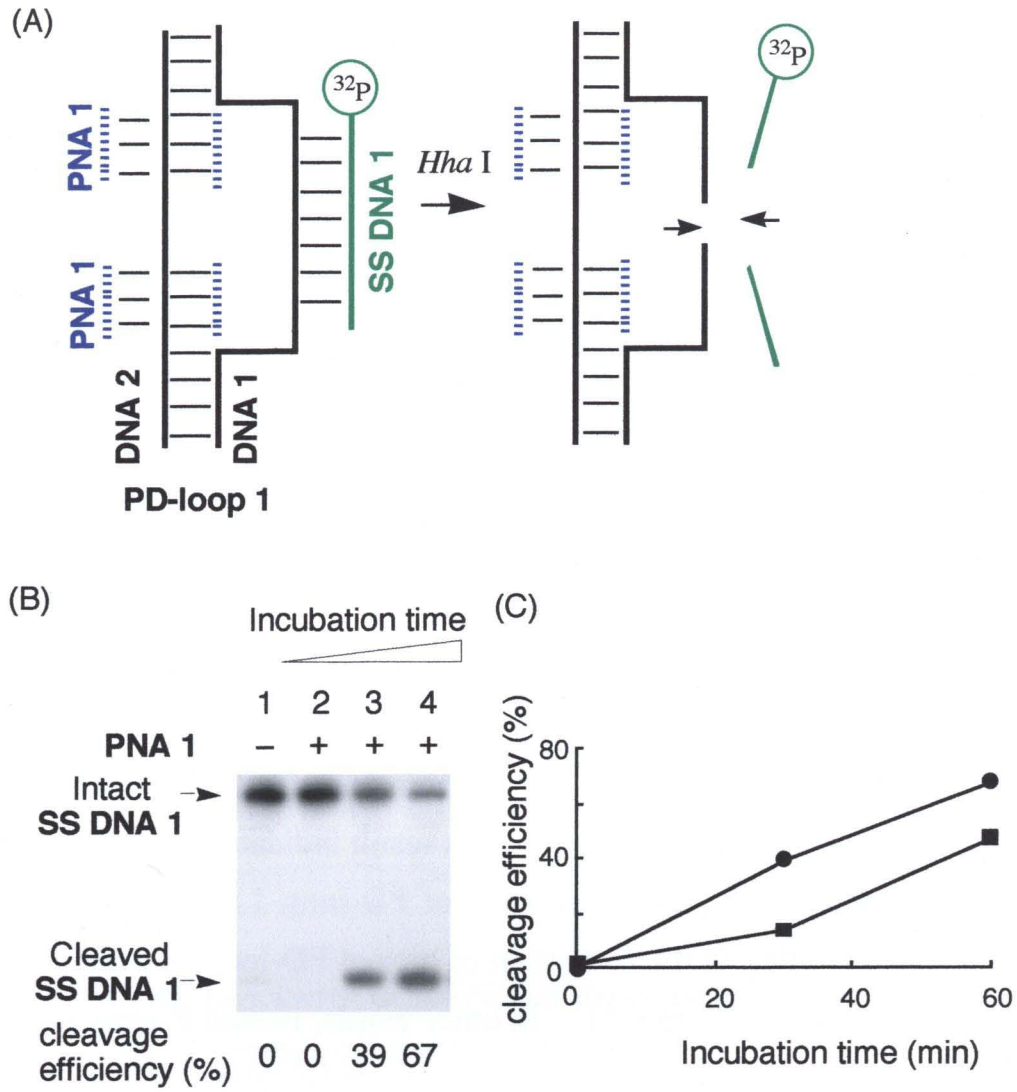

Figure 2. (A) Schematic outline for enzymatic digestion of **PD-loop 1**. The arrow indicate cleavage site of **PD-loop 1**. (B) An autoradiogram of a denaturing 15% polyacrylamide gel for the enzymatic digestion of 90 nM **PD-loop 1** (**DNA 1** / **DNA 2** / **PNA 1** / ^{32}P-5'-end labeled **SS DNA 1**) containing 900 nM **SS DNA 1**. Cleavage of **PD-loop 1** was conducted in the absence (lane 1) or the presence (lanes 2 to 4) of **PNA 1**. The presence of **PNA 1** is indicated by (+); absence is indicated by (-). The samples were incubated with restriction enzyme (*Hha* I, 10 units) for 0 (lane 2), 30 (lane 3), and 60 min (lanes 1 and 4). Cleavage efficiency of **SS DNA 1** was shown in figure. The arrows indicate intact and cleaved **SS DNA 1**. (C) Time course of the cleavage efficiency of enzymatic digestion. **PD-loop 1** are designated by (●). **DNA 1** / **SS DNA 1** duplex are designated by (■).

In order to gain further insight into this enzymatic cleavage of PD-loop, enzymatic cleavage experiments of **PD-loop 1** containing ^{32}P-5'-end labeled **DNA 2** were conducted. Figure 3 shows the result of this

experiment. While 61% of **DNA 2** was cleaved in the absence of **SS DNA 1** after incubation with *Hha* I for 1 h (lane 1), cleavage of **DNA 2** was suppressed by the presence of **SS DNA 1** (lane 2 and 3). These results indicate that **DNA 2** in **PD-loop 1** remains mainly intact under enzymatic cleavage condition. Since intact **DNA 2** would keep both cleaved ends of displaced strand (**DNA 1**) in close proximity to each other, **SS DNA 1** would bind to nicked displaced strand smoothly, resulting in the efficient cleavage of **SS DNA 1**.

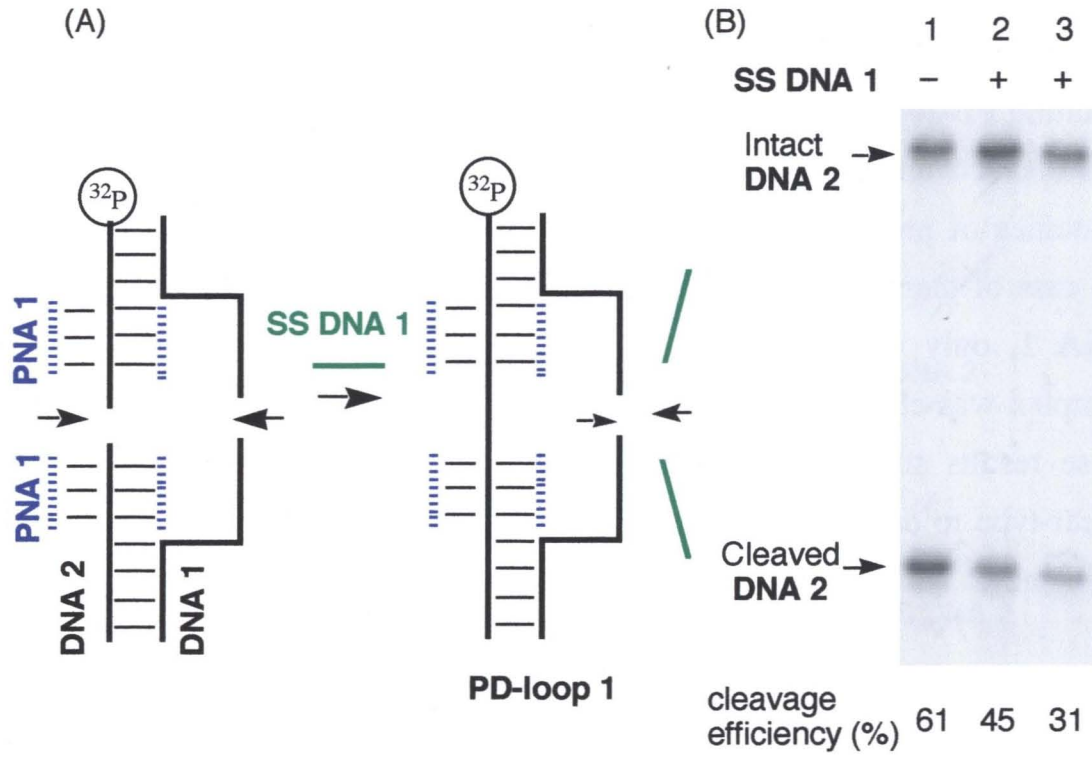

Figure 3. (A) Schematic outline for enzymatic digestion of **PD-loop 1** using ^{32}P-5'-end labeled **DNA 2**. The arrows indicate cleavage site of **PD-loop 1.** (B) An autoradiogram of a denaturing 15% polyacrylamide gel for the enzymatic digestion of **PD-loop 1**. 100 nM of **PD-loop 1** containing 0 (lane 1), 1 (lane 2), an 10 μM (lane 3) of **SS DNA 1** were incubated with restriction enzyme (*Hha* I, 10 units) for 1 h. The arrows indicate intact and cleaved **DNA 2**.

In order to improve the efficiency of enzymatic digestion of **SS DNA** in PD-loop, we next examined enzymatic digestion of **PD-loop 2 (DNA 1 / DNA 2 / PNA 1 / SS DNA 2)** which contained ^{32}P-5'-end labeled 30 mer dumbbell-type **SS DNA 2.** Since the product of enzymatic digestion of dumbbell-type **SS DNA 2** would form a hairpin-type structure, it is expected that binding of cleavage product (cleaved **SS DNA 2**) to P-loop would be suppressed (Figure 4A). We prepared **PD-loop 2** including 1, 10, 50, and 100-fold amount of dumbbell-type **SS DNA 2** over P-loop, and carried out enzymatic digestion of **PD-loop 2** using *Hha* I. The representative gel is summarized in Figure 4B. Analysis of cleavage of resulting **PD-loop 2** revealed that 47-fold amount of **SS DNA 2** over P-loop was cleaved under enzymatic digestion condition for 1 h (lane 4). The velocities of product formation were calculated to be 1.18 nM / sec. In the case of the enzymatic digestion of **PD-loop 1** including linear-type **SS DNA 1**, only 6.7-fold amount of **SS DNA 1** over strand-displacement complex was cleaved under enzymatic digestion condition for 1 h. Thus, these results suggest that the change of the structure of **SS DNA** from linear-type to dumbbell-type causes dramatic enhancement of the cleavage efficiency.

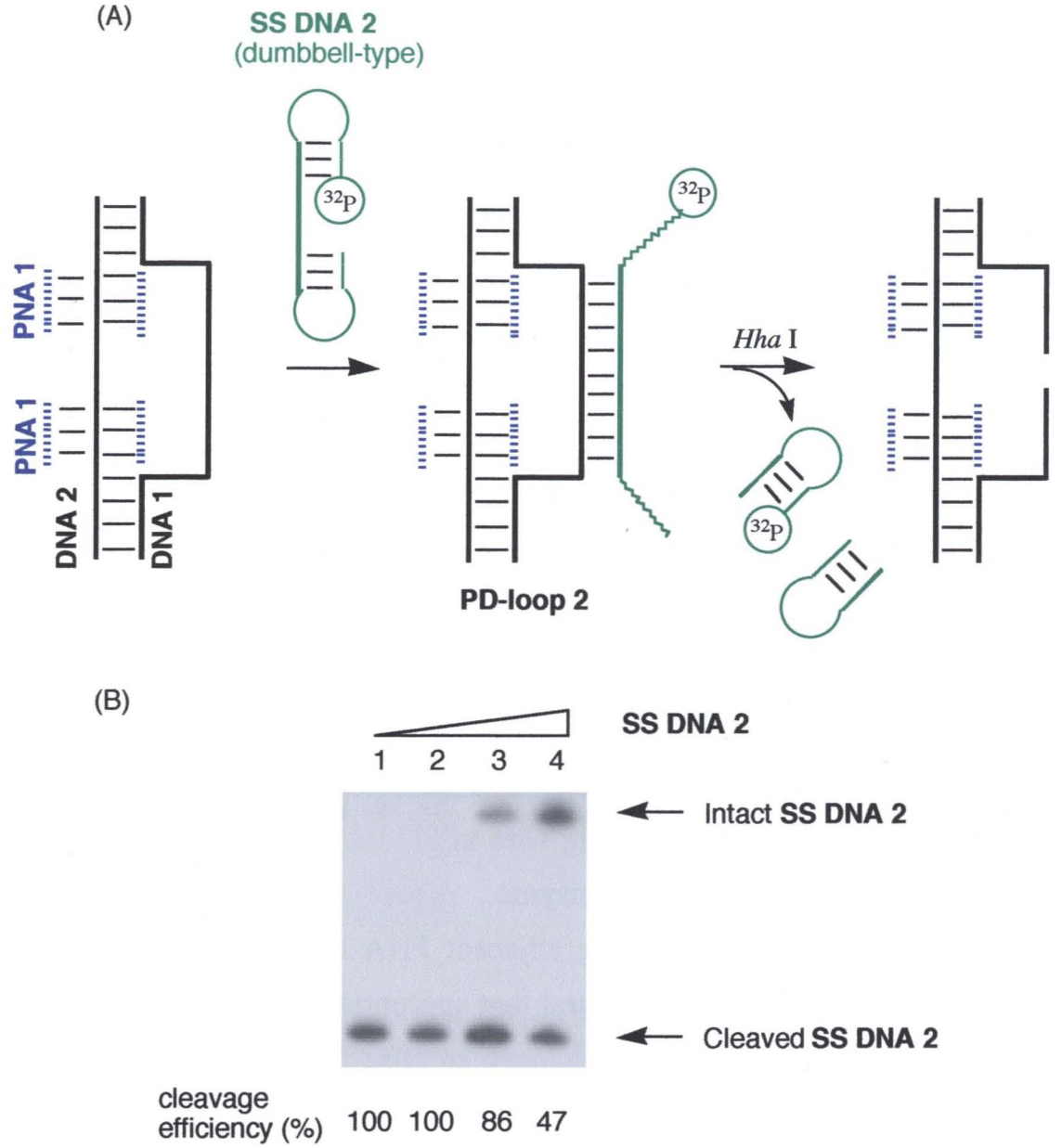

Figure 4. (A) Schematic outline for enzymatic digestion of **PD-loop 2** containing ^{32}P-5'-end labeled dumbbell-type **SS DNA 2.** Products of enzymatic digestion would form a hairpin-type structure. (B) An autoradiogram of a denaturing 15% polyacrylamide gel for the enzymatic digestion of **PD-loop 2** (**DNA 1** / **DNA 2** / **PNA 1** / ^{32}P-5'-end labeled **SS DNA 2**). 90 nM of **PD-loop 2** containing 0.09 (lane 1), 0.9 (lane 2), 4.5 (lane 3), and 9 μM (lane 4) of **SS DNA 2** were incubated with restriction enzyme (*Hha* I, 10 units) for 1 h. The arrows indicate intact and cleaved **SS DNA 2.**

It is reported that the formation of PNA-DNA double-duplex invasion complexes completely prevents the enzymatic digestion when the restriction site is a part of the PNA-binding site.[8] In order to investigate the effect of the distance between two PNA binding sites on this system, we next examined enzymatic cleavage of PD-loop which contained four or eight nucleotides separating adjacent PNA binding sites. We prepared **PD-loop 3** (**DNA 3** / **DNA 4** / **PNA 1** / **SS DNA 3**) and **PD-loop 4** (**DNA 5** / **DNA 6** / **PNA 1** / **SS DNA 4**) and carried out enzymatic digestion of PD-loop. Figure 5 shows the results of these experiments. Without PNA binding, no cleavage of **SS DNA** was observed (lane 1). In the presence of PNA, **SS DNA 4** in the **PD-loop 4**, which contained eight nucleotides separating PNA binding sites, was cleaved efficiently by the restriction enzyme (lane 2 and 3, Figure 5B). On the other hand, **SS DNA 3** in **PD-loop 3**, which contained four nucleotides separating two PNA binding sites remained totally intact (lane 2 and 3, Figure 5A), indicating that short distance between two PNA binding sites in PD-loop cause the inhibition of the activity of the restriction enzyme. These results suggest that the number of nucleotides separating adjacent PNA binding sites affects the enzymatic digestion of PD-loop, and that appropriate distance between two PNA binding sites is required to achieve an effective cleavage of **SS DNA** in PD-loop.

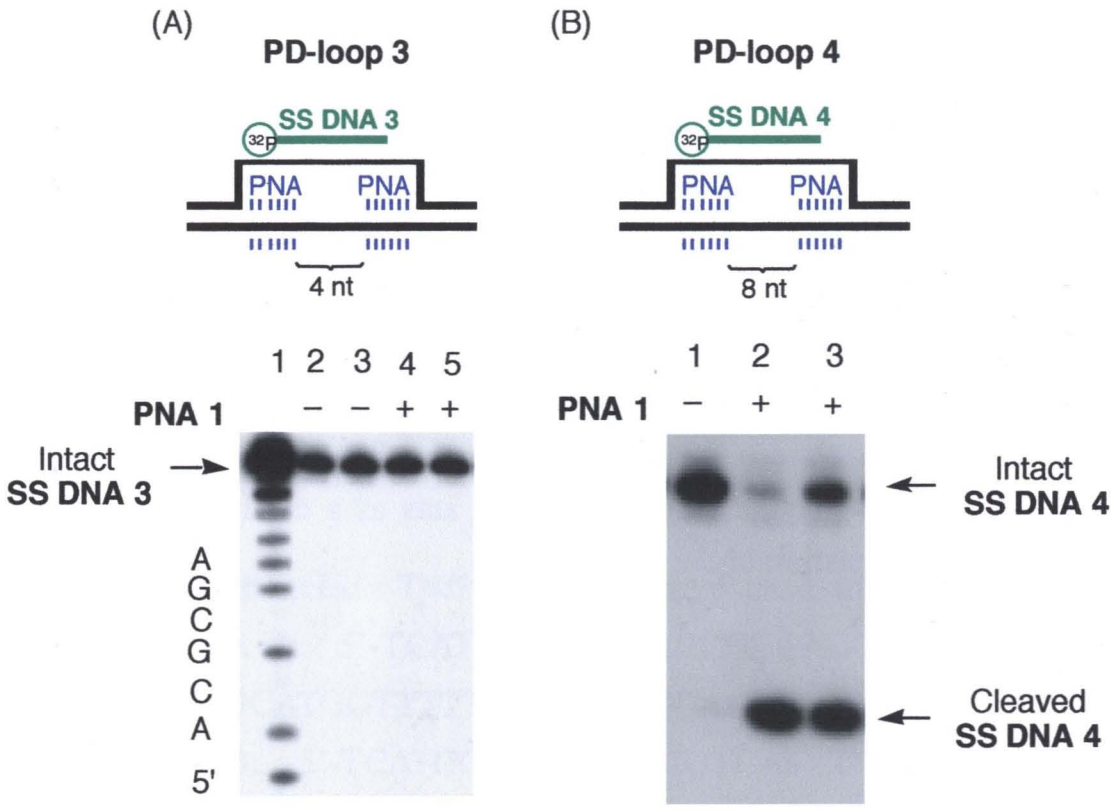

Figure 5. Effect of the distance between two PNA binding sites. **PD-loop 3** (**DNA 3 / DNA 4 / PNA 1 /** ^{32}P-5'-end labeled **SS DNA 3**) and **PD-loop 4** (**DNA 5 / DNA 6 / PNA 1 /** ^{32}P-5'-end labeled **SS DNA 4**) were incubated with restriction enzyme (*Hha* I, 10 units) for 1 h. The number of nucleotides separating between two PNA binding sites was four (**PD-loop 3**) and eight (**PD-loop 4**). (A) Enzymatic digestion of 100 nM **PD-loop 3** containing 100 (lane 2) and 500 nM (lane 3) of **SS DNA 3**. lane 1, Maxam-Gilbert A+G reaction; lane 2, digestion of single-stranded **SS DNA 3**; lane 3, digested without **PNA 1**; lane 4 and 5, digestion of **PD-loop 3**. (B) Enzymatic digestion of 100 nM **PD-loop 4** containing 100 (lane 2), and 500 nM (lane 3) of **SS DNA 4**. lane 1, digested without **PNA 1**; lane 2 and 3, digestion of **PD-loop 4**. The presence of **PNA 1** is indicated by (+); absence is indicated by (-). The arrows indicate intact and cleaved **SS DNAs**.

Conclusion

In the present study, we prepared PNA-DNA complex (strand-displacement complex / **SS DNA**) referred to as the PD-loop and carried out a quantitative analysis of the enzymatic digestion of PD-loop. Under the enzymatic digestion condition of PD-loop, excess amount of **SS DNA** over strand-displacement complex (P-loop) was digested. Furthermore, cleavage of dumbbell-type **SS DNA** in PD-loop proceeded *ca.* 7-fold more efficiently than that of linear-type **SS DNA**. Enzymatic cleavage experiment of PD-loop containing four or eight nucleotides separating adjacent PNA binding site revealed that appropriate distance between two PNA binding site was required to achieve the efficient enzymatic digestion of **SS DNA**. These results clearly indicate that PD-loop can be a substrate of the restriction enzyme, and that P-loop acts as a catalytic template for the enzymatic digestion of the **SS DNA**.

Experimental Section

General. Gel electrophoresis was carried out on a Gibco BRL Model S2 apparatus. All enzymes used in this study were from commercial sources. [γ-^{32}P]ATP (6000 Ci/mmol) was obtained from Amersham. All DNA oligomers were purchased from Pharmacia Biotech or QIAGEN. Boc PNA monomers and the 4-methylbenzhydrylamine resin (MBHA resin) HCl salt resin were purchased from PE Biosystems. Mass spectra of PNA were obtained on JEOL JMS-ELITE MALDI-TOF MASS SPECTROMETER. Centrifugal filer devices, Microcon®, was purchased from MILLIPORE. All aqueous solutions utilized purified water (MILLIPORE, Mili-Q sp UF).

Full DNA sequences. The DNA oligomers used in this study were follows.: **DNA 1**: 5'-TCATCCTCGGCACCGTCACCCTGGTTTTTTT TTTGTCAGCGCATGGTTTTTTTTTTAGCCACTATCGACTATCATGG CGA-3', **DNA 3**: 5'-TCATCCTCGGCACCGTCACCCTGGTTTTTTTT TTGCGCTTTTTTTTTTAGCCACTATCGACTATCATGGCGA-3', **DNA 5**: 5'-TCATCCTCGGCACCGTCACCCTGGTTTTTTT TTTCAGCGCAC TTTTTTTTTTAGCCACTATCGACTATCATGGCGA-3'.

PNA. PNA was synthesized with a Boc strategy on a solid support synthesis as described.[7] The MBHA resin HCl salt was treated with 2M DIPEA/NMP solution to activate for coupling. The Boc PNA monomer was then added with HBTU and DIPEA as a coupling activator. After coupling, the mixture was treated with acetic anhydride/pyridine/NMP (1/25/25 v/v/v). To remove the Boc group, the resulting mixture was treated with *m*-cresol/TFA (5/95), and then the next couplings were continued. Deprotection of Z group at A, C, and G nucleobases was done

with p-cresol/thioanisole/trifluoromethansulfonic acid/TFA (1/1/2/6). The purification of the synthesized PNA was performed on a WAKO sil II 5C18AR reverse-phase colunm by HPLC. Identity of synthesized PNA was confirmed MALDI TOF mass spectrometry.

Preparation of 5'-^{32}P-End Labeled DNA Oligomers. The DNA oligomers were 5'-end-labeled by phosphorylation with 4 μL of [γ-^{32}P]ATP and 4 μL of T4 polynucleotide kinase using standard procedures.[9] The 5'-end-labeled DNA oligomers were recovered by ethanol precipitation and futher purified by 15% preparative nondenaturing gel electrophoresis and isolated by the crush and soak method.[10]

General procedure of cleavage of PD-loop by restriction enzyme (*Hha* I) using ^{32}P-labeled SS DNA 1. Enzymatic digestion experiments were executed in a total volume of 20.0 μL or 22.2 μL with final concentrations of each species as indicated. Binding of PNA to 90 nM or 100 nM double-stranded DNA was carried out at 37 °C for 4 h with the corresponding PNA (200 eq. to DNA duplex). To avoid binding of PNA with the partially complementary **SS DNA**, free PNA were removed from samples by centrifugation with Microcon® (YM-30), centrifugal filter devices, at 0 °C. After centrifugation, binding of ^{32}P-5'-end-labeled **SS DNA** was carried out at 37 °C for 1 h. The resulting PD-loop was incubated in 10 mM Tris-HCl (pH 7.5), 10 mM $MgCl_2$, 10 mM DTT and 50 mM NaCl with *Hha* I (10 U) at 37 °C. The reaction was quenched by addition of 3 μL of solution containing SDS (1%), Glycerol (50%) and Bromophenol Blue (0.05%). After quenching, the reaction mixture was ethanol precipitated with 800 μL of ethanol. The precipitated DNA was washed with 100 μL of cold ethanol and then dried *in vacuo*. The radioactivity of the samples was then measured using an aloka 1000 liquid

scintillation counter and the dried DNA pellets were resuspended in 80% formamide loading buffer (a solution of 80% v/v formamide, 1 mM EDTA, 0.1% xylene cyanol and 0.1% bromophenol blue). All reactions were heat denatured at 90 °C for 3 min and quickly chilled on ice. The samples (1 mL, 10 × 10^3 cpm) were loaded onto 15% polyacrylamide and 7 M urea sequencing gel and electrophoresed at 1900 V for approximately 1 h.[11] The gel was dried and exposed to X-ray film with an intensifying sheet at –80 °C. The gels were analyzed by autoradiography with a densitometer and BIORAD Molecular Analyst software (version 2.1). The intensities of the spots were determined by volume integration.

Cleavage of double strand DNA (DNA 1 + ^{32}P-labeled SS DNA 1) by restriction enzyme (*Hha* I). Mixture of 90 nM **DNA 1** and 900 nM ^{32}P-labeled **SS DNA 1** was incubated in 10 mM Tris-HCl (pH 7.5), 10 mM $MgCl_2$, 10 mM DTT and 50 mM NaCl with *Hha* I (10 U) at 37 °C. The reaction was quenched by addition of 3 μL of solution containing SDS (1%), Glycerol (50%) and Bromophenol Blue (0.05%). After quenching, the reaction mixture was ethanol precipitated with 800 μL of ethanol. The precipitated DNA was washed with 100 μL of cold ethanol and then dried *in vacuo*. The polyacrylamide gel electrophoresis was carried out as the protocol described above.

Cleavage of PD-loop 1 contining ^{32}P-labeled DNA 2 by restriction enzyme (*Hha* I). Mixture of 100 nM **DNA 1** and 150 nM 5'-^{32}P-end-labeled **DNA 2** was heated to 90 °C for 5 min and slowly cooling to room templature. Binding of **PNA 1** (200 eq. to double stranded DNA) to resulting DNA duplex was carried out at 37 °C for 4 h. To avoid binding of PNA with the partially complementary **SS DNA 1**, free PNA were removed from samples by centrifugation with Microcon® (YM-30),

centrifugal filter devices, at 0 °C. After centrifugation, binding of **SS DNA 1** was carried out at 37 °C for 1 h. The resulting PD-loop was incubated in 10 mM Tris-HCl (pH 7.5), 10 mM $MgCl_2$, 10 mM DTT and 50 mM NaCl with *Hha* I (10 U) at 37 °C. The reaction was quenched by addition of 3 μL of solution containing SDS (1%), Glycerol (50%) and Bromophenol Blue (0.05%). After quenching, the reaction mixture was ethanol precipitated with 800 μL of ethanol. The precipitated DNA was washed with 100 μL of cold ethanol and then dried *in vacuo*. The polyacrylamide gel electrophoresis was carried out as the protocol described above.

References

(1) (a) Nielsen, P. E.; Egholm, M.; Berg, R. H.; Buchardt, O. *Science* **1991**, *254*, 1497–1500. (b) Nielsen, p. E. *Acc. Chem. Res.* **1999**, *32*, 624–630.

(2) (a) Bukanov, N. O.; Demidov, V. V.; Nielsen, P. E.; and Frank-Kamenetskii, M. D. *Proc. Natl. Acad. Sci. USA* **1998**, *95*, 5516–5520. (b) Demidov. V. V.; Frank-Kamenetskii, M. D. *In Peptide Nucleic Acids: Methods and Protocols*; Nielsen, P. E., Ed.; Humana Press: Totowa, NJ, 2002. (c) Demidov, V. V. *Exp. Rev. Mol. Diagnos.* **2001**, *1*, 343–351. (d) Smulevitch, S. V.; Simmons, C. G.; Norton, J. C.; Corey, D. R. *Nat. Biotechnol.* **1996**, *14*, 566–568.

(3) Demidov, V. V.; Bukanov, N. O.; Frank-Kamenetskii, M. D. *Curr. Issues Mol. Biol.* **2000**, *2*, 31–35.

(4) (a) Kuhn, H.; Demidov, V. V.; Frank-Kamenetskii, M. D. *Angew. Chem. Int. Ed. Engl.* **1999**, *38*, 1446–1449. (b) Kuhn, H.; Demidov, V. V.; Frank-Kamenetskii, M. D. *J. Biomol. Struct. Dyn.* **2000**, *Special Issue S2*, 221. (c) Demidov, V. V.; Kuhn, H.; Lavrentyeva-Smolina, I. V.; Frank-Kamenetskii, M. D. *Mehtods* **2001**, *23*, 123–131.

(5) (a) Broude, N. E.; Demidov, V. V.; Kuhn, H.; Gorenstein, J.; Pulyaeva, H.; Volkovitsky, P.; Drukier, A. K.; Frank-Kamenetskii, M. D. *J. Biomol. Struct. Dyn.* **1999**, *17*, 237–244. (b) Demidov, V. V.; Broude, N. E.; Lavrentyeva-Smolina, I. V.; Kuhn, H.; Frank-Kamenetskii, M. D. *ChemBioChem* **2001**, *2*, 133–139.

(6) Okamoto, A.; Tanabe, K.; Saito, I. *J. Am. Chem. Soc.* **2002**, *124*, 10262–10263.

(7) Egholm, M. E.; Buchardt, O.; Nielsen, P. E.; Berg, R. H. *J. Am. Chem. Soc.* **1992**, *114*, 1895–1897.

(8) Izvolsky, K. I.; Demidov, V. V.; Nielsen, P. E.; Frank-Kamenetskii, M. D. *Biochemistry*, **2000**, *39*, 10908–10913.

(9) Sambrook, J.; Fritsch, E. F.; Maniatis, T. *Molecular Cloning.* A Laboratory mannual, 2 nd ed.; Cold Spring Harbor Laboratories Press: Cold Spring Harbor, NY. **1989**.

(10) Maxam, A.; Gilbert, W.; *Methods in Enzymol.* **1980**, *65*, 499–560.

(11) (a) Rickwood, D.; Hames, B. D. *Gel Electrophoresis of Nucleic Acids: A Practical Approach*, 2nd Ed.; IRL Press: New York, 1990. (b) Brown, T. A. *DNA Sequencing*: The Basics; IRL Press: New York, 1994.

Chapter 5

Photo-Induced Drug Release from Functionalized Oligonucleotides Modulated by Molecular Beacon Strategy

Abstract

Photo-induced drug release system which required a recognition of DNA sequence was developed. The system is based on photo-induced release of drug from functionalized oligonucleotide and modulation of drug release by molecular beacon strategy. Phenacyl group was recognized as a general photoremovable protecting group for carboxylic acids, and it was known that photoreaction via triplet phenacyl esters were quenched by naphthalene derivatives. We have designed and synthesized a single-stranded oligodeoxynucleotide containing phenacyl ester of biotin and naphthalene derivative as a chromophore (**Chr**) for the release of biotin via triplet and a triplet quencher (**Que**), respectively. We investigated a release of biotin as a drug from oligonucleotide (**Chr-ODN-Que**) containing **Chr** and **Que** at each end of oligonucleotide. **Chr-ODN-Que** underwent a spontaneous conformational change when it hybridized to its complementary DNA, resulting in an extremely rapid release of biotin via triplet state of phenacyl group under photoirradiation condition. On the other hand, **Chr-ODN-Que** formed stem-and-loop structure in the absence of complementary DNA, resulting in a suppression of release of biotin as a result of triplet quenching by **Que**, which were kept in close proximity to **Chr**.

Introduction

Chemotherapeutic approaches to curing cancer depend on drugs that are selectively toxic to the disease-causing organism or the diseased cell.[1] There have been a number approaches to increase selectivity of anticancer agents through the use of immunoconjugates, antibody-, gene-, and bacterial-directed enzymatic activation of prodrugs and by capitalizing on elevated levels of certain enzymes and receptors within cancer cells.[2] Although all of these methods can in principle lead to more selective chemotherapeutic agents, they are by no means easy to implement.

The Moleculer Beacon (MB) is one of the most successive fluorescent probe for genetic analysis.[3] The MB is an oligodeoxynucleotide (ODN) which contains fluorephore and quencher at either end of ODN. Since the MB forms a stem-and-loop structure, the stem keeps the fluorophore and quencher in proximity each other, resulting in the quenching of fluorescence. When the MB hybridizes with complementary DNA, fluorophore and quencher are moved away from each other, leading to the restoration of fluorescence. Recent advance in these fluorescent probes and genomic sequencing make it possible to determine the genetic make up of diseases such as cancer.[4]

Herein we report a new chemotherapeutic approach that makes direct use of genetic information. This approach is based on a photo-induced drug release which is controlled by triplet energy transfer (TET) utilizing the MB strategy. The molecule is also a single-stranded ODN that possesses a stem-and-loop structure (Figure 1). Chromophore (**Chr**) for drug release via excited triplet is attached to the end of one arm and triplet quencher (**Que**) is attached to the end of the other arm. The stem keeps **Chr** and **Que** in close proximity to each other, causing the triplet energy of **Chr** to be quenched by TET. When the molecule encounters a

complementary DNA, it forms a hybrid that is longer and more stable than the hybrid formed by the stem sequences. Since **Chr** is no longer in close proximity to **Que**, photoreaction via excited triplet of **Chr** proceeds under photoirradiation conditions.

Phenacyl groups were known as a general photoremovable protective group for carboxylic acids.[5] Photoreaction of phenacyl ester involves the α-cleavage of the triplet state to form two radicals that abstract H-atoms from the reaction medium, resulting in the release of carboxylic acids. Additionally, it was known that photoreaction via triplet state of phenacyl groups were quenched by the presence of naphthalene derivatives.[6]

In this paper, we demonstrate a photo-induced release of biotin as a drug. We synthesized DNA oligomers containing a phenacyl ester of biotin and a naphthalene derivative as **Chr** and **Que**, respectively. Photoirradiation of DNA containing **Chr** and **Que** (**Chr-ODN-Que**) revealed extremely rapid release of biotin in the presence of complementary DNA. On the other hand, photo-induced release of biotin were suppressed in the absence of complementary DNA.

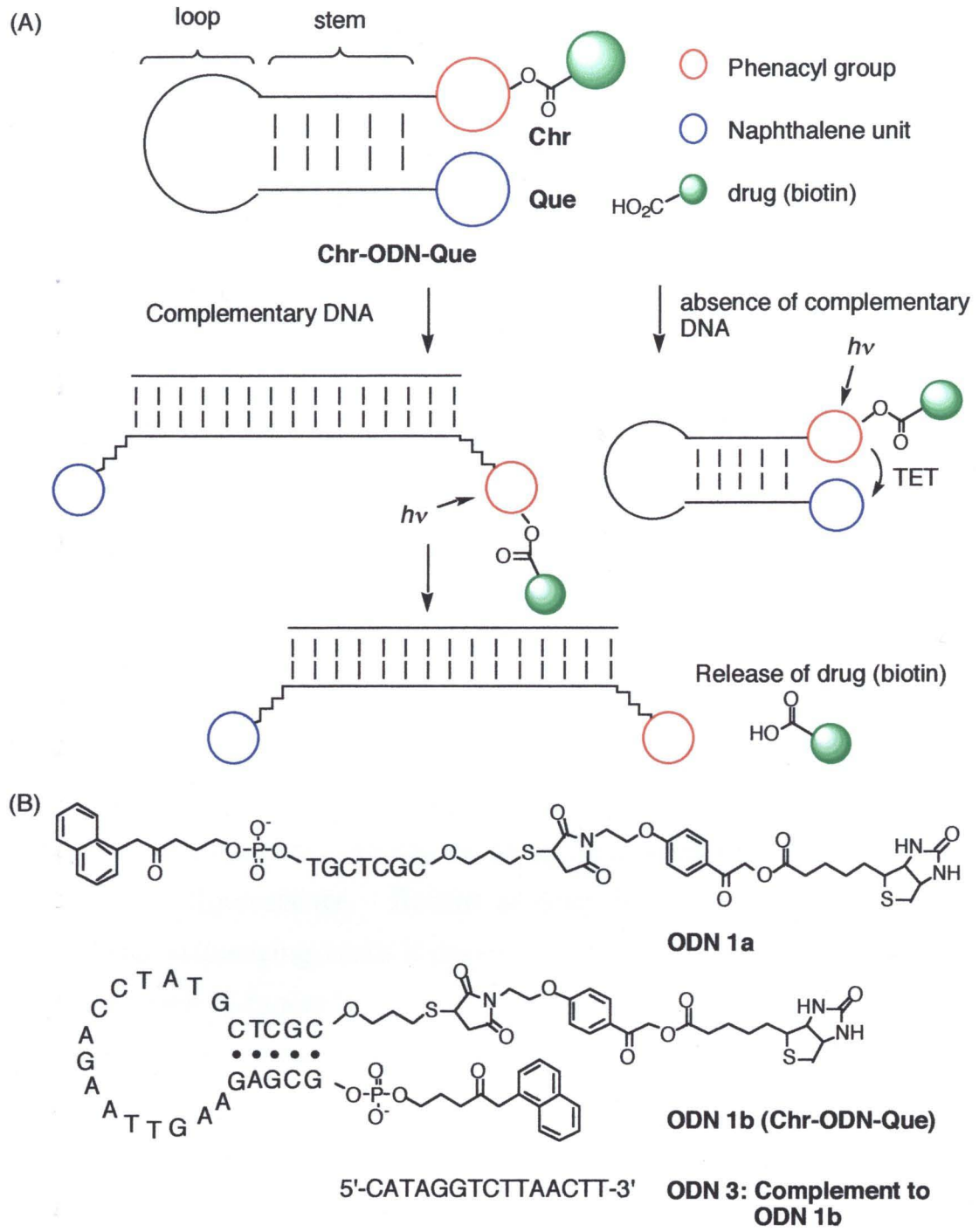

Figure 1. (A) Concept of drug release from functionalized oligonucleotides modulated by molecular beacon strategy. The oligonucleotide containing **Chr** and **Que** (**Chr-ODN-Que**) formed stem-and-loop structure in the absence of complementary DNA. On the other hand, the hairpin stem of **Chr-ODN-Que** cannot exist with the rigid double helix that is formed when **Chr-ODN-Que** hybridizes to its complementary DNA. Consequently, **Chr-ODN-Que** undergoes a conformational change that forces the arm sequence apart and causes **Chr** to move away from **Que**. Photoirradiation of **Chr-ODN-Que** / complementary DNA duplex results in the release of drug (biotin) whereas the release of drug (biotin) is suppressed by triplet quenching in the absence of complementary DNA. (B) DNA oligomers used in this study.

Results and Discussion

In order to introduce phenacyl ester and naphthalene units into oligodeoxynucleotide, we designed phenacyl ester containing maleimide moiety and naphthalene derivative containing phosphoroamidite moiety. Maleimide based reagents have been used extensively for crosslinking of peptide, proteins, and DNA through thiol groups.[7] On the other hand, phosphoroamidite chemistry was used for standard automated DNA synthesis.

The synthetic route to the phenacyl ester of biotin **6** is shown in Scheme 1. The hydroxy group of p-hydroxyacetophenone **1** was coupled with *N*-(2-bromoethyl)phthalimide to obtain **2**. Successive treatment of **2** with methylamine and maleic anhydride produced acetophenone derivative containing maleimide group **4**. α-Bromo acetophenone **5** was obtained by bromination of **4**. Coupling of bromide **5** with (+)-biotin furnished the synthesis of **6**.

The synthesis of naphthalene derivatives containing phosphoroamidite unit **10** is outlined in Scheme 2. Treatment of 1-naphthylacetic acid **7** with thionyl chloride and silylated ethanol amine produced **8**, which was desilylated to **9**. Phosphoroamidite **10** was obtained by a standard procedure from alcohol **9**.

Synthesis of ODN containing phenacyl ester and naphthalene unit are summarized in Scheme 3. Synthesis of 7 mer (**ODN 4a**), and 25 mer ODN (**ODN 4b**) containing naphthalene unit were carried out by automated DNA synthesis. Successive treatment of **ODN 4** with dithiothreitol (DTT) produced oligodeoxynucleotide containing thiol group (**ODN 5**). Treatment of **ODN 5** with phenacyl ester **6** furnished the synthesis of oligodeoxynucleotides containing phenacyl ester of biotin and naphthalene unit (**ODN 1**). The crude **ODN 1** were purified by reversed

phase HPLC. The incorporation of phenacyl ester and naphthalene unit into oligonucleotide was confirmed by enzymatic digestion and MALDI-TOF Mass (**ODN 1a**: calcd. 3018.29, found 3018.25, **ODN 1b**: calcd. 8394.60, found 8395.23).

Scheme 1[a]

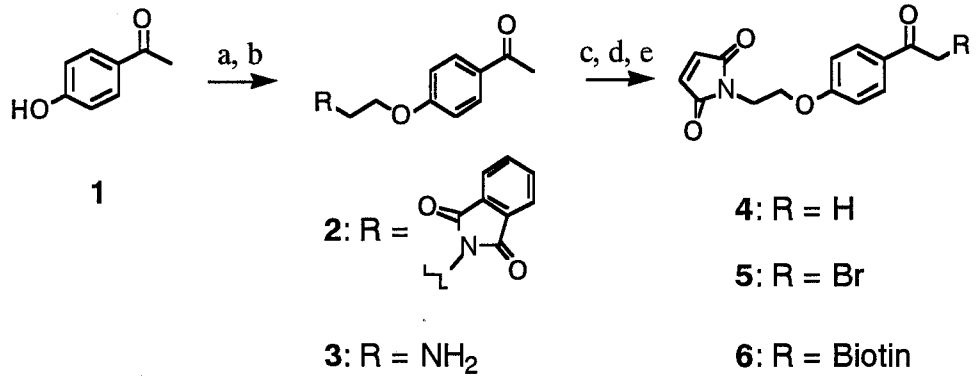

[a]Reagents: (a) K_2CO_3, *N*-(2-bromoethyl)phthalimide, reflux; (b) 40% $MeNH_2$; (c) maleic anhydride, reflux; (d)AcONa/AcOH, reflux; (e) biotin, Et_3N.

Scheme 2[a]

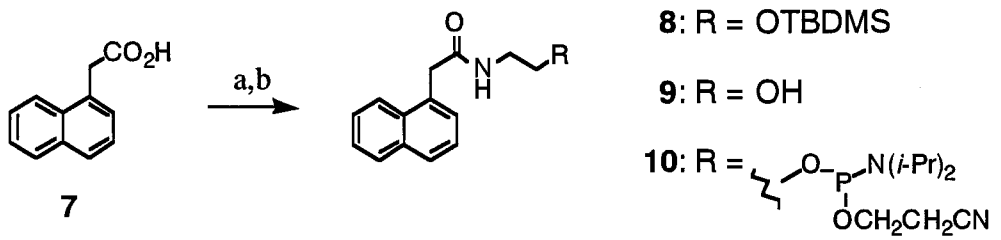

[a]Reagents: (a) $SOCl_2$, reflux; (b) $TBDMSOCH_2CH_2NH_2$, pyridine; (c) TBAF; (d) (i-Pr_2N)$POCH_2CH_2CN$, 1H-tetrazole.

Scheme 3[a]

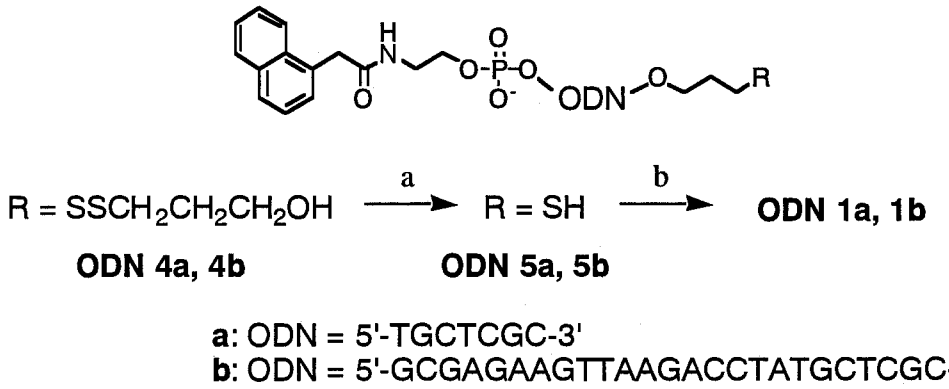

[a]Reagents: (a) 5 mM dithiothreitol, 25 mM sodium phosphate (pH 8.4), 23 °C, (b) 0.5 mM 6, 250 mM sodium phosphate (pH 7.0), 23 °C.

Initially, we examined photoirradiation of 7-mer single-stranded ODN (**ODN 1a**) in the presence of *i*-PrOH as a hydrogen donor in order to get photodegradation products, and analyzed the mass spectra of reaction products. In 5-min photoirradiation, **ODN 1a** completely decomposed and afforded the reaction product mixture. The molecular weight [$(M-H)^-$] for reaction products given by MALDI-TOF mass spectroscopy was 2775.49 indicating a formation of acetophenone **ODN 6** (calcd. 2775.99) as a result of concomitant release of biotin (Scheme 4). Although several peaks were detected in a HPLC for the reaction products of **ODN 1a**, it was confirmed with MALI-TOF mass spectroscopy that these all products had the same molecular weights. The reaction products likely involve the ODN containing pyrimidines dimerized by photosensitization of acetophenone unit generating in photocleavage of **ODN 1a**.[8]

Scheme 4[a]

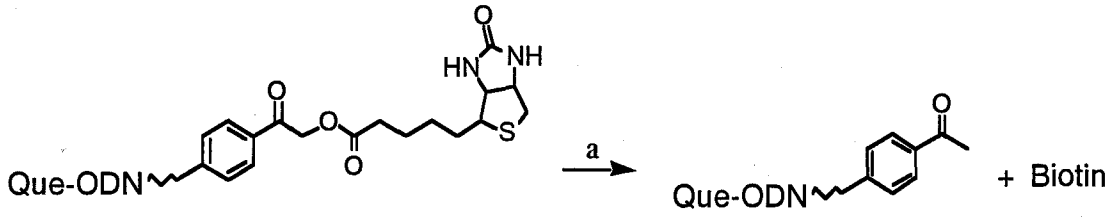

ODN 1a

ODN 6: MALDI-TOF [$(M-H)^-$]
calcd. 2775.99
found 2775.49

[a]Reagents: (a) $h\nu$ (312 nm), 15 mM sodium cacodylate (pH 7.0)–*i*-PrOH (2 :1).

In order to confirm the structure of 25 mer **ODN 1b** which would form stem-and-loop structure, measurement of the melting temperature (T_m) of **ODN 1b** in the absence of the complementary **ODN 3** was carried out. Even in the absence of the complementary **ODN 3**, T_m value of **ODN 1b** was 33.8 °C. This result suggests that **ODN 1b** possessing 5-base pair arm sequence can form stable stem hybrid.

We next examined the time profiles for the conversion of **ODN 1b** under photoirradiation condition in the presence of *i*-PrOH as a hydrogen donor. We carried out photoreaction of **ODN 1b** (irradiation at 312 nm) in the presence or absence of the complementary **ODN 3** at 0 °C and monitored a conversion of **ODN 1b** with time. The time profiles for **ODN 1b** conversion (Figure 2) revealed that extremely rapid conversion of **ODN 1b** proceeded in the presence of complementary **ODN 3**, and that **ODN 1b** was consumed > 50 % for 30 sec irradiation. On the other hand, conversion of **ODN 1b** was suppressed in the absence of **ODN 3**. These results clearly indicate that **ODN 1b** hybridizes spontaneously to its target strand at 0 °C and undergoes a conformational change that results in a rapid conversion of itself. On the other hand, in the absence of **ODN 3**, **ODN 1b** forms stem-and-loop structure, and triplet energy of phenacyl group transferred to naphthalene unit, resulting in the suppression of conversion of **ODN 1b**.

In order to quantify biotin released from **ODN 1b** by photocleavage of phenacyl ester, we next investigated replacement of 4-hydroxyazobenzene-2-carboxylic acid (HABA) binding to avidin by released biotin. It is known that the HABA binds to avidin to produce a complex that absorbs at 500 nm, and that biotin present in the solution of avidin-HABA complex will displace the HABA, causing the absorbance at 500 nm to decrease.[9] After the photoirradiation at 312 nm to a solution of **ODN 1b** (200 pmol) was carried out, the photoproduct filtered with centrifugal filter was mixed

to a solution of avidin–HABA complex, and then the absorbance at 500 nm (A_{500}) of the mixture was measured. Amount of biotin released from **ODN 1b** was determined by using a calibration curve of A_{500} given from control experiments (Figure 3). Photoirradiation of a stem-and loop type **ODN 1b** derived only a slight decrease of A_{500}, corresponding to 12% biotin release from **ODN 1b**. In contrast, a drastic decrease of A_{500} was observed in the presence of the complementary **ODN 3**, corresponding to 84% biotin release from **ODN 1b**. These results strongly suggest that efficient release of biotin from **ODN 1b** was occurred only in the presence of complementary **ODN 3**. Thus, the photo-induced release of drug from functionalized oligodeoxynucleotide which was modulated by MB strategy was achieved for the first time.

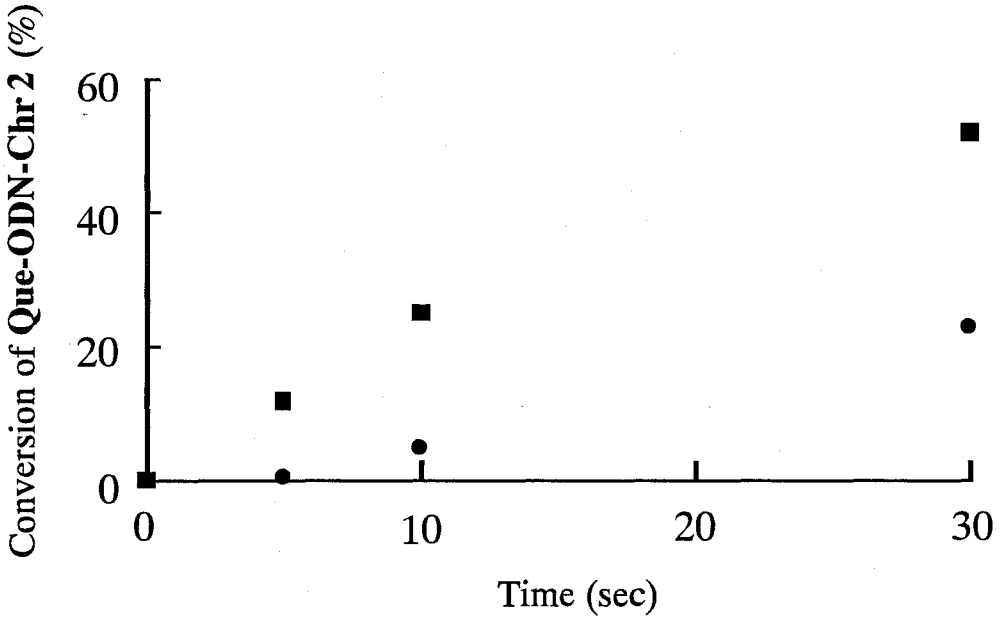

Figure 2. Conversion of **ODN 1b** during the photoirradiation in 10 mM sodium cacodylate (pH 7.0)–*i*-PrOH (2:1) at 0°C with 312 nm transilluminator (0, 5, 10, and 30 sec of irradiation time). Conversion of **ODN 1b** in the presence of complementary **ODN 3** is designated by (■) and conversion of **ODN 1b** in the absence of complementary DNA is designated by (●).

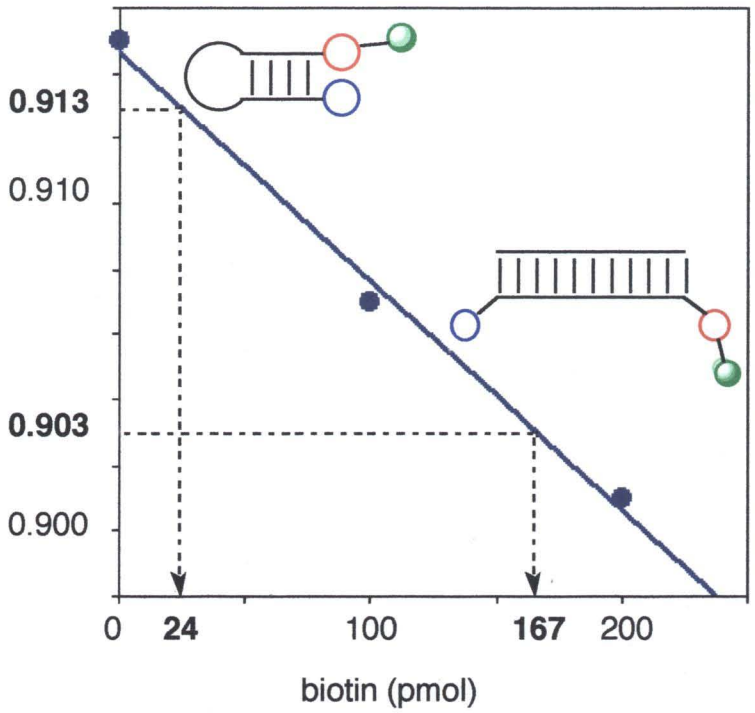

Stem-and-Loop: 24 pmol / 200 pmol ×100 = 12% biotin release
Duplex: 167 pmol / 200 pmol ×100 = 84% biotin release

Figure 3. Replacement of 2-(4'-hydroxyazobenzene)benzoic acid (HABA) binding to avidin by biotin released from **ODN 1b**. Photoirradiation at 312 nm to 200 pmol of **ODN 1b** in the presence or absence of the complementary **ODN 3** was carried out in 15 mM sodium cacodylate (pH 7.0)–iPrOH (2:1) at r.t. with a monochrometer (JASCO CRM-FD, 300 W Xe lamp, 40 counts; One count of photoirradiation approximately corresponds to a surface energy of 0.02 J/cm^2). After a filtration of photoproducts with Microcon® centrifugal filter (YM-3, 3000 NMWL), the filtrate was mixed to a solution of avidin–HABA complex (0.43 mg of ImmunoPure® Avidin, PIERCE and 62.5 mg of ImmunoPure® HABA, PIERCE) in 86 mM sodium phosphate (pH 7.2) and 130 mM sodium chloride, and then the absorbance at 500 nm (A_{500}) of the mixture was measured. Amount of released biotin was quantified by using the linear fit (a blue solid line, $y = 7.0 \times 10^{-5}\chi + 0.9147$; $R = 0.9966$) given based on A_{500} of an avidin–HABA solution in the presence of 0, 100 and 200 pmol of biotin.

Conclusion

In summary, we designed the oligodeoxynucleotides containing choromophore for drug release and quencher, and evaluated a release of drug from designed oligodeoxynucleotide under photoirradiation condition. We synthesized phenacyl ester of biotin containing maleimide moiety and naphthalene derivative as choromophore and quencher, and introduced these moieties into oligonucleotide (**Chr-ODN-Que, ODN 1b**). Photoreaction of **ODN 1b**, which formed stem-and-loop structure revealed that conformational change in the presence of complementary DNA resulted in extremely rapid release of biotin from **ODN 1b**. On the other hand, release of biotin was suppressed in the absence of complementary DNA as the result of triplet quenching. Thus, photo-induced drug release system which required the recognition of complementary DNA was developed for the first time.

Experimental Section

General methods and materials. Melting points were determined with Yanaco MP-500D micro melting point apparatus and uncorrected. ^{1}H NMR spectra was measured with Varian Mercury 400 (400 MHz) or JEOL JMN α-400 (400 MHz) spectrometer. ^{13}C NMR spectra was measured with JEOL JMN α-400 (100 MHz) or JEOL JMN α-500 (125 MHz) spectrometer. Coupling constant (J value) are reported in hertz. The chemical shifts are expressed in ppm downfield from tetramethylsilane, using residual chloroform (δ = 7.24 in ^{1}H NMR, δ = 77.0 in ^{13}C NMR) and dimethylsulfoxide (δ = 2.49 in ^{1}H NMR, δ = 39.5 in ^{13}C NMR) as internal standard. FAB Mass spectra was recorded on JEOL JMS HX-110 spectrometer. Wakogel C-200 was used for silica gel colum chromatography. Precoated TLC plates Merck silica gel 60 F_{254} was used for monitoring reactions. TLC spots were visualized with UV light or anisaldehyde (a solution of 9.0 mL p-anisaldehyde, 3.5 mL acetic acid and 10 mL sulfuric acid in 330 mL ehanol). Matrix-assisted laser desorption ionization time-of-flight (MALDI-TOF) mass spectrometry of oligonucleotides were obtained on JEOL JMS-ELITE MALDI-TOF MASS spectrometer with 2',3',4'-trihydroxyacetophenone as matrix. Calf intestine alkaline phosphotase (AP), snake venom phosphodiesterase (svPDE) and nuclease P1 (P1) were purchased from Boehringer Mannheim. The oligonucleotide was purchased from QIAGEN. The reagents for the DNA synthesizer such as A, G, T, C and 3'-Thiol-Modifier C3 S-S CPG support were purchased from Glen Research. The purity and concentration of all oligodeoxynucleotides were determined by complete digestion with svPDE, AP and P1 to 2'-deoxymononucleotides. Reversed phase HPLC was performed on a cosmosil 5C-18AR or CHEMCOBOND 5-ODS-H column (4.6×150 mm) with a Gilson Chromatography Model 305 using a UV detector Model 118 at 254 nm. Photoirradiation at 312 nm was

carried out using TFX-20.M. transilluminator and a Jasco CRM-FD monochromator. Centrifugal filer devices, Microcon (Y-3), was purchased from MILLIPORE. 4-hydroxyazobenzene-2-carboxylic acid (HABA) and avidine were purchased from PIERCE.

***N*-[2-(4-acetylphenoxy)ethyl]phthalimide (2).** To a solution of p-hydroxyacetophenone **1** (8.51 g, 62.5 mmol) and *N*-(2-bromoethyl) phthalimide (19.08 g, 75.1 mmol) in acetone (85 mL) was added potassium carbonate (44.88 g, 324 mmol), and the mixture was refluxed for 10.5 h. After removal of the solvent, the reaction mixture was extracted with EtOAc. The extract was washed with brine, dried over anhydrous $MgSO_4$, filtered, and concentrated in vacuo. The crude product was purified by silica gel column chromatography (25% EtOAc/hexane) to give **2** (4.5 g, 23 %) as a white solid: mp 162–163 °C; ^{1}H NMR ($CDCl_3$, 400 MHz) δ 7.89 (d, J = 9.0 Hz, 2H), 7.86 (dd, J = 3.1, 5.7 Hz, 2H), 7.73 (dd, J = 3.1, 5.7 Hz, 2H), 6.91 (d, J = 9.0 Hz, 2H), 4.28 (t, J = 5.7 Hz, 2H), 4.13 (t, J = 5.7 Hz, 2H), 2.53 (s, 3H); ^{13}C NMR ($CDCl_3$, 100 MHz) δ 196.7, 168.1, 162.1, 134.1, 132.0, 130.7, 130.6, 123.4, 114.3, 64.9, 37.1, 26.3; FABMS (NBA/$CHCl_3$) m/z 310 [$(M+H)^+$]; HRMS calcd. for $C_{18}H_{16}NO_4$ [$(M + H)^+$] 310.1079, found 310.1085.

***p*-(2-aminoethoxy)acetophenone (3).** To a solution of **2** (3.15 g, 10.18 mmol) in $CHCl_3$ (63 mL) and MeOH (32 mL) was added 40% aqueous methylamine (4.41 mL, 50.9 mmol), and the mixture was stirred at ambient temperature for 5 h. After concentration in vacuo, the resulting mixture was extracted with diluted HCl and washed with EtOAc. The water layer was then treated with sat. $NaHCO_3$ solution to pH = 10 and extracted with EtOAc. The extract was washed with brine, dried over anhydrous $MgSO_4$,

filtered and concentrated *in vacuo*. The crude product was purified by silica gel column chromatography (9% MeOH/$CHCl_3$) to give **3** (1.17 g, 64%) as a white solid: mp > 300 °C; ^{1}H NMR ($CDCl_3$, 400 MHz) δ 7.91 (d, J = 8.8 Hz, 2H), 6.92 (d, J = 8.8 Hz, 2H), 4.04 (t, J = 5.2 Hz, 2H), 3.10 (t, J = 5.2 Hz, 2H), 2.54 (s, 3H); MS, m/z (%) 179 (M^+) (46), 150 (94), 121 (100); HRMS calcd for $C_{10}H_{13}NO_2$ (M^+) 179.0946, found 179.0946.

***N*-[2-(4-acetylphenoxy)ethyl]maleimide (4).** To a solution of **5** (1.80 g, 10.04 mmol) in toluene (55 mL) was added maleic anhydride (1.00 g, 10.20 mmol), and the mixture was refluxed for 5 h. After removal of the solvent, the resulting mixture was dissolved in acetic anhydride. To the mixture was added sodium acetate (0.85 g, 10.13 mmol), and the mixture was refluxed for 1.5h. After the reaction was complete, the solvent was removed *in vacuo*. The resulting mixture was extracted with EtOAc. The extract was washed with sat. $NaHCO_3$, brine, dried over anhydrous $MgSO_4$, filtered and concentrated *in vacuo*. The crude product was purified by silica gel chromatography (25% EtOAc/hexane) to give **4** (1.34 g, 49%): mp 142–143 °C; ^{1}H NMR ($CDCl_3$, 400 MHz) δ 7.89 (d, J = 8.8 Hz, 2H), 6.87 (d, J = 8.8 Hz, 2H), 6.72 (s, 2H), 4.18 (t, J = 5.6 Hz, 2H), 3.95 (t, J = 5.6 Hz, 2H), 2.53 (s, 3H); ^{13}C NMR ($CDCl_3$, 100 MHz) δ 196.7, 170.4, 162.1, 134.3, 130.8, 130.6, 114.2, 64.8, 37.0, 26.4; FABMS (NBA/EtOAc), m/z 260 [$(M+H)^+$]; HRMS calcd for $C_{14}H_{14}NO_4$ [$(M+H)^+$] 260.0923, found 260.0924.

***N*-[2-(4-(2-bromo-1-oxo)ethyl)phenoxy]ethylmaleimide (5).** To a solution of **4** (215 mg, 0.829 mmol) in THF (5 mL) was added phenyltrimethylammonium tribromide (312 mg, 0.829 mmol), and the mixture was stirred at ambient temperature for 3 h. After the reaction, the mixture was extracted with EtOAc. The extract was washed with brine,

dried over anhydrous $MgSO_4$, filtered and concentrated *in vacuo*. The crude product was purified by silica gel chromatography (9% toluene/EtOAc) to give **5** (97.3 mg, 35%) as a white solid: mp 135–136 °C; ^{1}H NMR ($CDCl_3$, 400 MHz) δ 7.92 (d, J = 8.8 Hz, 2H), 6.90 (d, J = 8.8 Hz, 2H), 6.72 (s, 2H) 4.36 (s, 2H), 4.20 (t, J = 5.6 Hz, 2H), 3.95 (t, J = 5.6 Hz, 2H); ^{13}C NMR ($CDCl_3$, 100 MHz) δ 189.9, 170.4, 162.7, 134.3, 131.3, 127.4, 114.6, 64.8, 36.9, 30.6; FABMS (NBA/$CHCl_3$) m/z 338 [(M+H)$^+$]; HRMS calcd. for $C_{14}H_{13}NO_4Br$ [(M+H)$^+$] 338.0028, found 338.0031.

Phenacyl ester of biotin containing maleimide unit (6). To a solution of **5** (45.4 mg, 0.134 mmol) and (+)-biotin (33.0 mg, 0.134 mmol) in DMF (400 μL) was added triethylamine (20.4 mg, 0.201 mmol), and the reaction mixture was stirred at ambient temperature for 2 h. After the reaction the mixture was extracted with EtOAc. The extract was washed with brine, dried over anhydrous $MgSO_4$, filtered and concentrated *in vacuo*. The crude product was purified by silica gel chromatography (9% MeOH/$CHCl_3$) to give **6** (51 mg, 76%) as a white solid: mp 108–109 °C; ^{1}H NMR (DMSO-*d6*, 400 MHz) δ 7.90 (d, J = 9.0 Hz, 2H), 7.04 (s, 2H), 7.04 (s, 2H), 7.01 (d, J = 9.0 Hz, 2H), 6.43 (s, 1H), 6.36 (s, 1H), 5.39 (s, 2H), 4.30 (dd, J = 5.2, 7.6 Hz, 1H), 4.22 (t, J = 5.4 Hz, 2H), 4.16-4.15 (m, 1H), 3.80 (t, J = 5.4 Hz, 2H), 3.13-3.08 (m, 1H), 2.82 (dd, J = 5.2, 12.2 Hz, 1H), 2.57 (d, J = 12.2 Hz, 1H), 2.42 (t, J = 7.4 Hz, 2H), 1.68–1.31 (6H); ^{13}C NMR (DMSO-*d6*, 100 MHz) δ 191.1, 172.3, 170.7, 162.6, 162.3, 134.6, 130.0, 127.1, 114.5, 65.9, 64.9, 61.0, 59.1, 55.3, 39.8, 36.5, 33.0, 27.9, 27.8, 24.5; FABMS (NBA/DMSO) m/z 502 [(M+H)$^+$]; HRMS calcd. for $C_{24}H_{28}N_3O_7S$ [(M+H)$^+$] 502.1648, found 502.1650.

***N*-[2-(*tert*-butyl-dimethylsilanyloxy)ethyl]-1-naphthylacetamide (8).** A mixture of 1-naphthylacetic acid **7** (3.72 g, 20mmol) and thionyl chloride

(30 mL) was refluxed for 2 h. The solvent was removed *in vacuo*. The resulting crude 1-naphthylacetyl chloride was immediately used in next step.

To a solution of 2-aminoethanol (1.00 g, 16.37 mmol), *tert*-butyl-dimethylsilyl chloride (4.94 g, 32.74 mmol) and triethylamine (5.06 g, 50mmol) in THF (20 mL) was added 4-(dimethylamino)pyridine (367 mg, 3.0 mmol), and the mixture was stirred at ambient temperature for 3.5 h. Then 1-naphthylacetyl chloride in THF (10 mL) was added to the reaction mixture, which is stirred at ambient temperature for 12 h. After the reaction, the reaction mixture was extracted with EtOAc. The extract was washed with sat. $NaHCO_3$, sat. NH_4Cl then brine, dried over anhydrous $MgSO_4$, filtered and concentrated *in vacuo*. The crude product was purified by silica gel chromatography (17% EtOAc/hexane) to give **8** (2.40 g, 43%) as a pale orange solid: mp 90–93 °C; ^1H NMR ($CDCl_3$, 400 MHz) δ 7.94 (d, J = 8.4 Hz, 1H), 7.85 (d, J = 7.2 Hz, 1H), 7.79 (d, J = 8.0 Hz, 1H), 7.56-7.35 (4H), 5.68 (brs, 1H), 4.02 (s, 2H), 3.45 (t, J = 5.2 Hz, 2H), 3.25 (dt, J = 5.2, 5.2 Hz, 2H), 0.63 (s, 9H), -0.24 (s, 6H); ^{13}C NMR ($CDCl_3$, 125 MHz) δ 170.7, 134.0, 132.0, 131.0, 128.8, 128.5, 128.4, 126.8, 126.1, 125.6, 123.7, 61.4, 41.8, 41.5, 25.6, 17.9, -5.8; FABMS (NBA/$CHCl_3$), m/z 344 [$(M+H)^+$]; HRMS calcd for $C_{20}H_{30}NO_2Si$ [$(M+H)^+$] 344.2046, found 344.2044.

***N*-(2-hydroxyethyl)-1-naphthylacetamide (9).** To a solution of **8** (2.00 g, 5.82 mmol) in THF (20 mL) was added 1M tetrabutylammonium fluoride solution in THF (5.8 mL, 5.8 mmol), and the reaction mixture was stirred at ambient temperature for 3 h. The reaction mixture was diluted with H_2O. After the reaction, the mixture was extracted with EtOAc. The organic layer was washed with brine, dried over anhydrous $MgSO_4$, filtered and concentrated *in vacuo*. The crude product was purified by silica gel

chromatography (20% MeOH/$CHCl_3$) and then recrystalized from EtOAc to give **9** (1.09 mg, 82 %) as a colorless crystal: mp 110-111 °C; ^{1}H NMR (DMSO-d_6, 400 MHz) δ 8.13 (t, J = 5.6 Hz, 1H), 8.10-8.05 (m, 1H), 7.92-7.88 (m, 1H), 7.80 (dd, J = 2.0, 7.2 Hz, 1H), 7.55-7.39 (4H), 4.67 (t, J = 5.6 Hz, 1H), 3.89 (s, 2H), 3.40 (dt, J = 5.6, 5.6 Hz, 2H), 3.32 (s, 2H), 3.13 (dt, J = 5.6, 5.6 Hz, 2H); ^{13}C NMR (DMSO-d_6, 100 MHz) δ 170.1, 133.3, 132.8, 131.9, 128.3, 127.6, 127.6, 126.9, 125.8, 125.5, 125.4, 124.2, 59.8, 41.6, 39.9; FABMS (NBA/$CHCl_3$), m/e 230 [$(M+H)^+$]; HRMS calcd for $C_{14}H_{16}NO_2$ [$(M+H)^+$] 230.1181, found 230.1182.

***N*-[2-(*N*,*N*-diisopropylamino-2-cyanoethoxyphosphinyloxy)ethyl]-1-naphthylacetamide (10).** To the solution of **9** (50 mg, 0.23 mmol) and tetrazole (21 mg, 0.299 mmol) in dry CH_3CN was added 2-cyanoethyl *N,N,N',N'*-tetraisopropylphosphorodiamidite (69.3 mg, 0.23 mmol) and the mixture was stirred at ambient temperature for 1.5 h. After the reaction, the crude product **10** was used for automated DNA synthesizer without further purification.

General procedure for the synthesis of ODN 4. **ODN 4** were prepared by the β-cyanoethylphosphoramidite method on 3'-Thiol-Modifier C3 S-S controlled pore glass support (1 μmol) by using an Applied Biosystems Model 392 DNA/RNA synthesizer. After the automated synthesis, oligomers were cleaved from the support by conc. aqueous ammonia for 1 h, deprotected by heating the solutions at 55 °C for 12 h. The synthesized oligomers were purified by reversed phase HPLC, elution with a solvent mixture of 0.1 M triethylamine acetate (TEAA), pH 7.0, linear gradient over 60 min from 0 % to 60 % acetonitrile at a flow rate 3.0 mL/min. **ODN 4** were identified by MALDI-TOF mass.

General procedure for the synthesis of ODN 5. To a solution (total volume 420 μL) of **ODN 4** in 50 mM sodium phosphate buffer (pH 8.4) was added 10mM dithiothreitol (DTT) (400 μL), and incubated at 23 °C for 12 h. The reaction mixture was purified by reversed phase HPLC, elution with a solvent mixture of 0.1 M TEAA, pH 7.0, linear gradient over 60 min from 0% to 60% acetonitrile at a flow rate 3.0 mL/min. The obtained **ODN 5** were immediately used in next step.

General procedure for the synthesis of ODN 1. To a solution (total volume 120 μL) of **ODN 5** in 500 mM sodium phosphate buffer (pH 7.0) was added 1 mM aqueous **6** (100 μL), and incubated at 23 °C overnight. The reaction mixture were purified by reversed phase HPLC, elution with a solvent mixture of 0.1 M TEAA, pH 7.0, linear gradient over 60 min from 0 % to 60 % acetonitrile at a flow rate 3.0 mL/min, to give **ODN 1.** The incorporation of **6** into **ODN 1** was confirmed by enzymatic digestion and MALDI-TOF Mass (**ODN 1a**: calcd. 3018.29, found 3018.25, **ODN 1b**: calcd. 8394.60, found 8395.23).

Measurements of melting temperature of ODN 1b. Melting temperature of **ODN 1b** (4 μM) was measured eith SHIMADZU TMSPC-8 UV/VIS spectrometer in a buffer containing 10 mM sodium cacodylate and 33% 2-propanol. The absorbance of the sample was monitored at 260 nm from 2 °C to 70 °C with a heating rate of 0.5 °C /minute.

General procedure for the photoreactions of ODN 1. Photoreactions of single-stranded **ODN 1a** (20 μM), **ODN 1b** (6.7 μM), and **ODN 1b /ODN 3** duplex (6.7 μM duplex concentration) were carried out in a buffer containing 10 mM sodium cacodylate and 33% *i*-PrOH and 25 μM deoxyadenosine as internal standard. These solutions were irradiated with

transilluminator (312 nm) at 0 °C. After removal of 2-propanol *in vacuo*, the reaction mixtures were analyzed by reversed phase HPLC, elution with a solvent mixture of 0.1 M TEAA, pH 7.0, linear gradient over 60 min from 0 % to 60 % acetonitrile at a flow rate 1.0 mL/min.

Analysis of photoproduct (ODN 6). After the photoreaction of **ODN 1b** as described, the measurement of MALDI-TOF Mass of the resulting mixture was carried out (**ODN 6**: calcd. 2775.99, found 2775.49).

Procudure for the quantification of the released biotin from ODN 1b. Photoirradiation at 312 nm to 200 pmol of **ODN 1b** in the presence or absence of the complementary **ODN 3** was carried out in 15 mM sodium cacodylate (pH 7.0)–iPrOH (2:1) at r.t. with a monochrometer (JASCO CRM-FD, 300 W Xe lamp, 40 counts; One count of photoirradiation approximately corresponds to a surface energy of 0.02 J/cm^2). After a filtration of photoproducts with Microcon® centrifugal filter (YM-3, 3000 NMWL), the filtrate was mixed to a solution of avidin–HABA complex (0.43 mg of ImmunoPure® Avidin, PIERCE and 62.5 mg of ImmunoPure® HABA, PIERCE) in 86 mM sodium phosphate (pH 7.2) and 130 mM sodium chloride, and then the absorbance at 500 nm (A_{500}) of the mixture was measured. Amount of released biotin was quantified by using the linear fit (a blue solid line, $y = 7.0 \times 10^{-5}\chi + 0.9147$; $R = 0.9966$) given based on A_{500} of an avidin–HABA solution in the presence of 0, 100 and 200 pmol of biotin.

References

(1) (a) Albert, A. *Selective Toxicity: The Physico-chemical Basis of Therapy,* Chapman and Hall, London, **1979**. (b) Drews, J. *Science* **2000**, *287*, 1960–1964. (c) Sykes, R. *Int. J. Antimicrob. Agents* **2000**, *14*, 1–12.

(2) (a) Dubowchik G. M.; Walker M. A. *Pharmacol Ther.* **1999**, *83*, 67–123. (b) Duncan, R.; Connors, T. A.; Meada, H. *J. Drug. Target.* **1996**, *3*, 317–319.

(3) (a) Tyagi, S.; Kramer, F. R. *Nat. Biotechnol.* **1996**, *14*, 303–308. (b) Tyagi, S.; Btaru, D. P.; Kramer, F. R. *Nat. Biotechnol.* **1998**, *16*, 49–53. (c) Piatek, A. S.; Tyagi, S.; Pol, A. C.; Telenti, A.; Miller, L. P.; Kramer, F. R.; Alland, D. *Nat. Biotechnol.* **1998**, *16*, 359–363.

(4) (a) Golub, T. R.; slonim, D. K.; Tamayo, P.; Huard, C.; Gaasenbeek, M.; Mesirov, J. P.; Coller, H.; Loh, M.; Downing, J. R.; Caligiuri, M. A. *Science* **1999**, *286*, 531–537. (b) Gerhold, D.; Rushmore, T.; Caskey, C. T. *Trends Biochem. Sci.* **1999**, *24*, 168–173.

(5) (a) Sheehan, J. C.; Umezawa, K. *J. Org. Chem.* **1973**, *38*, 3771–3774. (b) Zhang, K.; Corrie, J. E. T.; Munasinghe, V. R. N.; Wan, P. *J. Am. Chem. Soc.* **1999**, *121*, 5625–5632. (c) Conrad II, P. G.; Givens, R. S.; Weber, J. F. W.; Kandler, K. *Org. Lett.* **2000**, *2*, 1545–1547.

(6) (a) Givens, R. S.; Jung, A.; Park, C. -H.; Weber, J.; Bartlett, W. *J. Am. Chem. Soc.* **1997**, *119*, 8369–8370. (b) Givens, R. S.; Weber, J. F. W.; Conrad II, P. G.; Orosz, G.; Donahue, S. L.; Thayer, S. A. *J. Am. Chem. Soc.* **2000**, *122*, 2687–2697.

(7) (a) Sharma, S. K.; Wu, A. D.; Chandramouli, N.; *Tetrahedron Lett.* **1996**, *37*, 5665–5668. (b) Partis, M. D.; Griffiths, D. G.; Roberts, G. C. *J. Prot. Chem.* **1983**, *2*, 263–277. (c) Haugaard, N.; Cutler, J.; Ruggieri, M. R. *Anal. Biochem.* **1981**, *116*, 341–343. (d) Papini, A.;

Rudolph, S.; Siglmuller, G.; Musiol, H. –J.; Gohring, W.; Moroder, L.; *Int. J. Peptide Protein Res.* **1992**, *39*, 348. (e) Ma, Z.; Taylor, J. –S. *Bioorg. Med. Chem.* **2001**, *9*, 2501–2510.

(8) (a) Chouini-Lalanne, N.; Defais, M; Paillous, N. *Biochem. Pharm.* **1998**, *55*, 441–446. (b) Charlier, M.; Helene, C. *Photochem. Photobiol.* **1968**, *15*, 527–536. (c) Wilucki, V.; Matthaeus, H.; Krauch, C. H. *Photochem. Photobiol.* **1967**, *6*, 497–500. (d) Epe, B.; Henzl, H.; Adam, W.; Saha-Möller, C. R. *Nucleic Acids Res.* **1993**, *21*, 863–869.

(9) (a) Green, N. M. Biochem. J. 1965, 94, 23c–24c. (b) Morpurgo, M.; Hofstetter, H.; Bayer, E. A.; Wilchek, M. *J. Am. Chem. Soc.* **1998**, *120*, 12734–12739.

Chapter 6

Novel Furan-Forming Photocyclization of 1,2-Diketones Conjugated with Ene-Yne

Abstract

We investigated photoinduced generation of (2-furyl)carbene and an efficient trap of the carbene. Upon photoirradiation at 365 nm 1,2-diketones conjugated with ene-yne undergo cyclization to furan derivatives with the formation of (2-furyl)carbene intermediates. In protic solvents the carbene was protonated to produce furan derivatives, whereas trapping the carbene in nonprotic solvents by adjacent 2-acetyl-1-cyclopentenyl system led to the formation of a novel 2,2'-bifuran derivative in a quantitative yield. Triplet quenching of 1,2-diketone and photoreaction of monoketones conjugated with ene-yne revealed that the lowest triplet excited state of 1,2-diketone was indispensable for the carbene generation.

Introduction

The structures of (2-furyl)carbenes and their extremely facile ring opening reactions have been the focus of considerable recent interest. Despite many attempts to generate (2-furyl)carbene **1** from diazoalkanes **2** by thermolysis and photolysis, they are formidably difficult to trap due to their high reactivity, which causes rapid rearrangement to ring-opening product **3**.[1,2] Previously, we have reported that photoirradiation of α-diazoketone in aqueous acetonitrile produced furan derivative **5**.[3] Additionally, it was reported that this photocyclization of α-diazoketone **4** proceeded via 1,2-diketone **6** as an intermediate.[3]

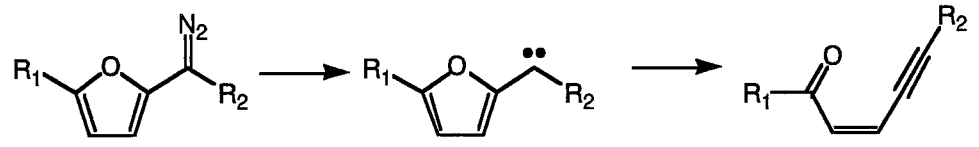

2 **1** **3**

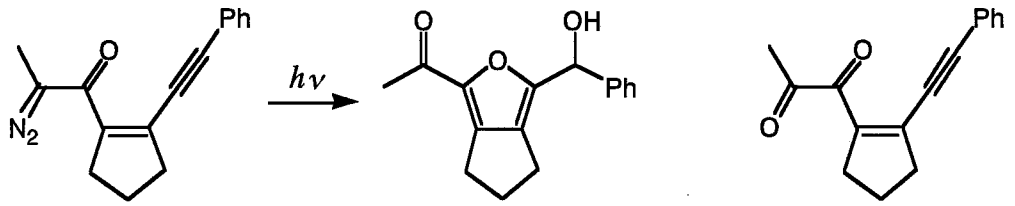

4 **5** **6**

Herein, we report the photoinduced generation of (2-furyl)carbene and an efficient trap of the carbene. 1,4-biradical **8** generated by photoexcitation of 1,2-diketone **7** underwent radical cyclization with a high quantum efficiency to produce (2-furyl)carbenes **9**. The resulting (2-furyl)carbene was intermoleculary trapped with water or alcohols efficiently. Further, this carbene was intramoleculary trapped by 2-acetyl-1-cyclopentenyl system resulting in formation of 2,2'-bifuran derivatives in quantitative yield.

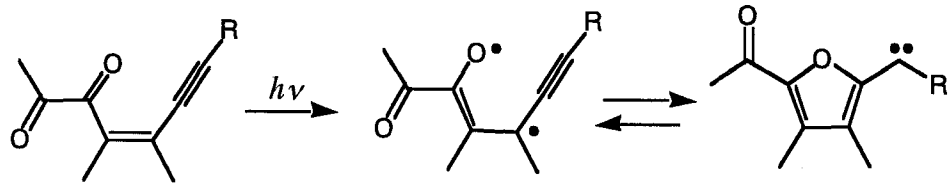

7 8 9

Results and Discussion

We first investigated a photoreaction of 1,2-diketone **6** in protic solvents. The photoirradiation of **6** in aqueous acetonitrile produced alcohol **10** in good yield. The photoreaction of **6** in acetonitrile-D_2O (1:1) (99.8 % atom D) produced alcohol **11**, in which the deuterium was incorporated exclusively into the benzylic position (>95% atom D). A similar incorporation of deuterium was observed with alcohol **12** when CD_3OD was used as a solvent. Since it is well established that a variety of electron rich carbenes react with alcohols by way of proton transfer,[4] it is highly likely that the photoreaction of **6** in protic solvents involves protonation of carbene at the benzylic position followed by addition of alcohol or water to the resulting cationic species (*e.g.*, **13**) (Scheme 1).

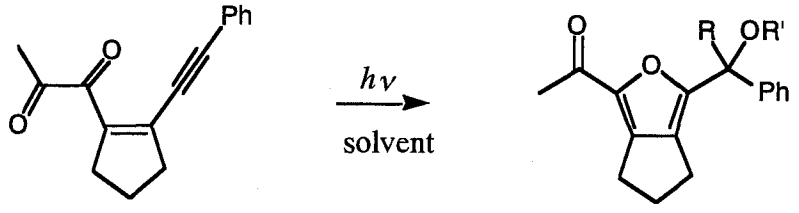

6

solvent	product	yield (%)
aq. CH_3CN	**10**: R = H, R' = H	73
CH_3CN-D_2O	**11**: R = D, R' = H	61
CD_3OD	**12**: R = D, R' = CD_3	36

Scheme 1

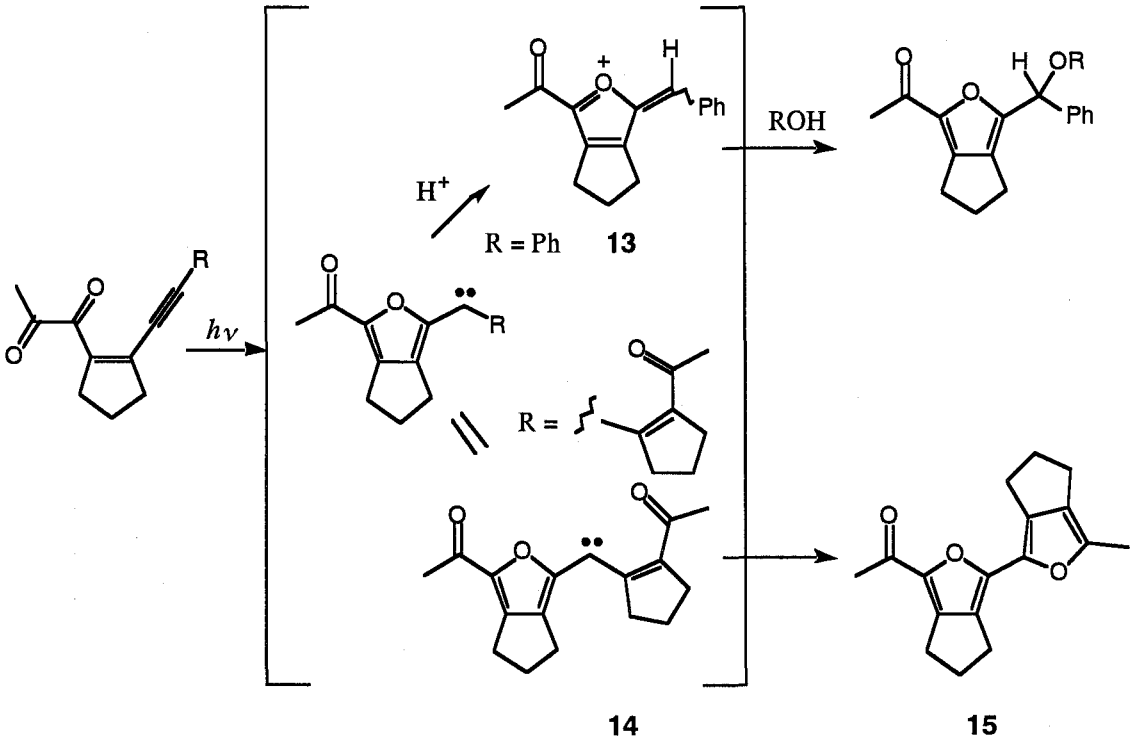

In order to confirm the carbene formation as an intermediate, the photoreaction of **6** was examined in nonprotic solvents. In spite of the efficient photocyclization of **6** to furan derivatives in protic solvents, the photoreaction in dry benzene or tetrahydrofuran was very sluggish. Attempts to trap the carbene with hydrogen donors such as tri-n-butyltin hydride and tris(trimethylsilyl)silane or with various alkenes were unsuccessful to result in a decomposition of the starting material **6**. These results seemed to suggest that the cyclization of 1,4-biradical to carbene (e.g., **8**→**9**) would be a reversible process.[1c] In order to trap carbene intermediated intramolecularly in nonprotic solvents, we have designed 1,2-diketone **22** with the expectation that the putative carbene would undergo simultaneous cyclization to result in a formation of the second furan ring (e.g.,**14**→**15** in Scheme 1).[5] Synthesis of **22** was accomplished by transformation of ester group of **20**, which was prepared by a coupling of alkyne **18** with 2-acetylcyclopent-1-enyltrifluoromethansulfonate **19**,

into 1,2-diketone functionality via α-diazoketone **21** (Scheme 2). Upon photoirradiation of **22** at 365 nm in benzene, 2,2'-bifuran **15** was obtained in a quantitative yield. The quantum yield for the disappearance of **22** was 0.19.

Scheme 2[a]

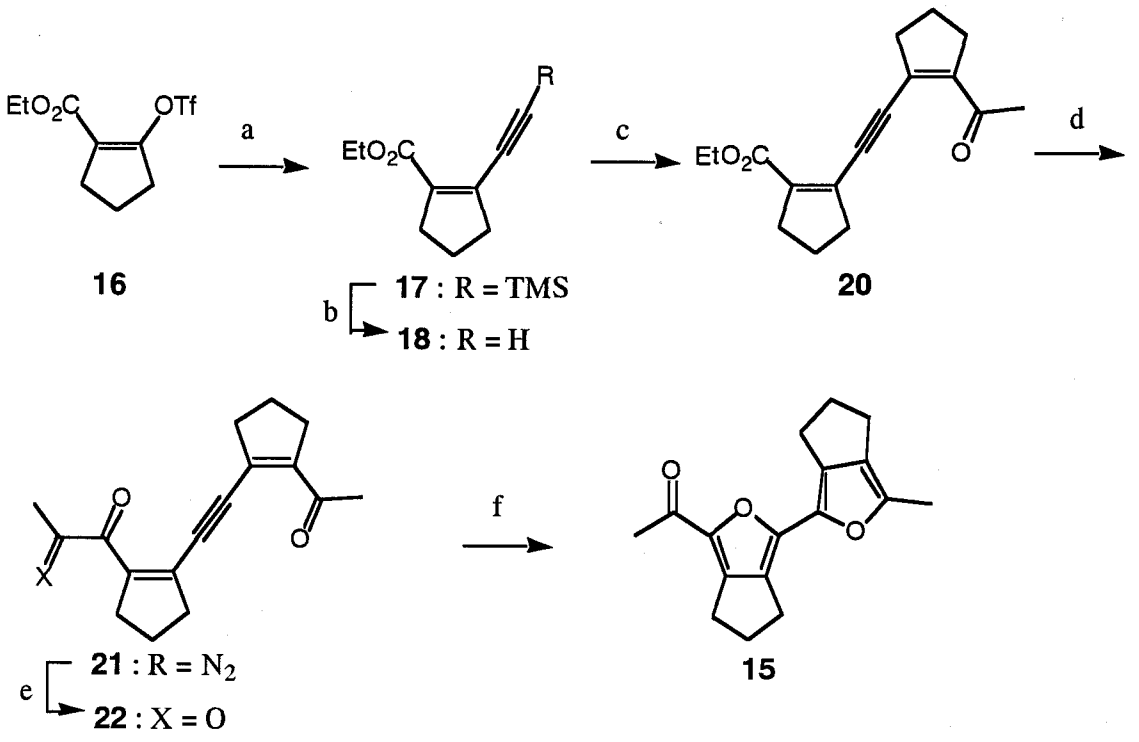

[a]Reagents and conditions: (a) trimethylsilylacetylene, $PdCl_2(PPh_3)$, 2,6-lutidine, CuI, DMF, 47%; (b) TBAF, AcOH THF, 82%; (c) 2-acetylcyclopent-1-enyltrifluoromethanesulfonate, $PdCl_2(PPh_3)$, 2,6-lutidine, CuI, DMF, 62%; (d) (1) NaOH, H2O, MeOH 45 °C; (2) $(COCl)_2$, benezene, then CH_3CHN_2, 33%; (e) PPh_3, ether then $NaNO_2$, 2N HCl, THF, 46%; (f) hn (365 nm), benzene, 95%.

In order to gain further insight into the mechanism of the photoreaction, we carried out photoreaction of monoketones **23** and symmetric diketone **26**. Synthesis of **23** and **26** was accomplished by a sequential coupling of enol triflate **19** with phenylacetylene or alkyne **25** (Scheme 3). Replacement of 1,2-diketone functionality in **6** by monoketone completely changed the course of the photoreaction. The photoreaction of

monoketone **23** in methanol produced mainly an intermolecular [2+2] photocycloadduct, whereas symmetric diketone **26** was stable under photoirradiation in benzene or aqueous acetonitrile. Additionally, we examined the triplet-sensitized photoreaction of symmetric diketone **26**, but no significant product was obtained. Thus, these results indicate that the 1,2-diketone chromophore is indispensable for the carbene generation.

Scheme 3[a]

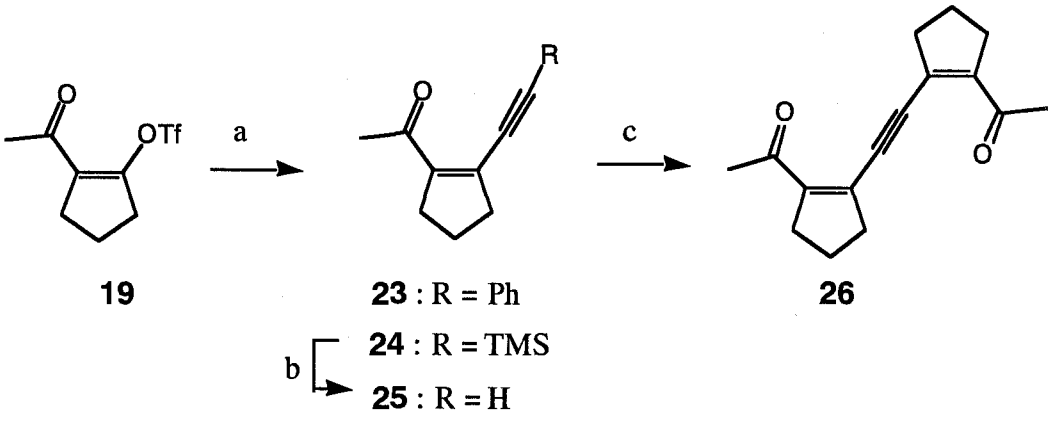

[a]Reagents and conditions: (a) phenylacetylene (for **23**), trimethylsilylacetylene (for **24**), $PdCl_2(PPh_3)$, 2,6-lutidine, CuI, DMF, 73% (for **23**), 93% (for **24**); (b) TBAF, AcOH THF, 73%; (c) 2-acetylcyclopent-1-enyltrifluoromethanesulfonate, $PdCl_2(PPh_3)$, 2,6-lutidine, CuI, DMF, 36%.

The photocyclization studied here are reminiscent of the cyclization of the propargyl 1,4-biradicals to produce the cycloalkenyl carbenes[5b,6,7] as well as of the related cyclization producing nitrenes as we reported earlier (Scheme 4).[8] It was rationalized that such cyclizations proceed via triplet biradicals.[6b] In order to clarify the mechanism for the carbene generating step in the photoreaction studied here, we next carried out triplet quenching of **6**. The disappearance of **6** under photoirradiation condition in the presence of varying amounts of pyrene (E_T = 202 kJ/mol)[9] as a triplet quencher showed a linear correlation between the relative quantum

efficiency and quencher concentrations with a Stern-Volmer slope of 18.6 x 10^3 M^{-1} (Figure 1). If we assume that the quenching by pyrene is diffusion controlled (~10^{10} M^{-1} S^{-1}), the lifetime of excited triplet **6** is 1.9 μs. This result and the fact that monoketone **23** and symmetric diketone **26** did not cyclize to produce furan derivatives under photoirradiation conditions indicate that the photocyclization of the 1,2-diketone conjugated with ene-yne proceeds from its lowest triplet excited state.

Scheme 4

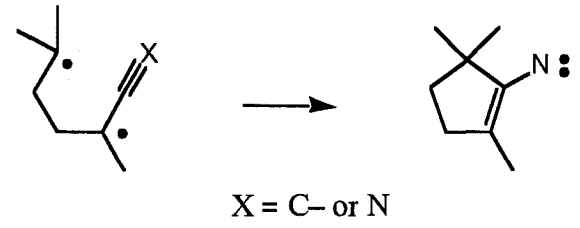

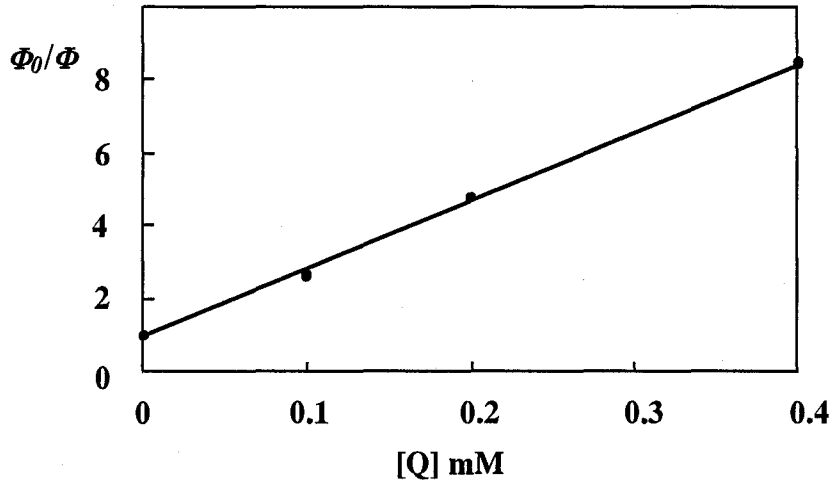

Figure 1. Stern-Volmer plot of relative quantum yields for the disappearance of **6** under photoirradiation condition in the presence of triplet quencher pyrene. The quantum yield measurements were carried out with **6** (1 mM) in the presence of the quencher (0, 0.1, 0.2, 0.4 mM) in aqueous acetonitrile at 350 nm. The relative quantum yield (Φ_0/Φ) was plotted against quencher concentration [Q].

Conclusion

In summary, we have disclosed a novel type of photoreaction of 1,2-diketones conjugated with ene-yne to produce (2-furyl)carbenes. Triplet quenching of 1,2-diketone and control photoreaction of monoketone revealed that triplet 1,2-diketone chromophore was indispensable for the generation of (2-furyl)carbene. (2-Furyl)carbenes could be efficiently trapped by protic solvents or adjacent carbonyl group to produce novel 2,2'-bifuran derivatives in one step. Thus, the system described here is useful for studying the generation and the efficient trap of the (2-furyl)carbenes.

Experimental Section

General methods and materials. ^{1}H NMR spectra were measured with Varian Gemini 200 (200 MHz), JEOL JNM α-400 (400 MHz) or JEOL α-500 (500 MHz) spectrometers. The chemical shifts are expressed in ppm downfield from residual chloroform (δ = 7.24) and benzene (δ = 7.15) as an internal standard. ^{13}C NMR spectra were measured with Varian Gemini 200 (50 MHz) and JEOL JNM α-400 (100 MHz) spectrometer. A Jasco V-550 UV/VIS spectrophotometer was used for the absorption spectra measurements. Mass spectra were recorded on a JEOL JMS SX-102A or a JEOL HX-100 spectrometer. A Funakoshi TEL-33 transilluminator and a Jasco CRM-FD monochromator was used for irradiation at 365 nm. A Wakogel C-200 was used for silica gel chromatography. Precoated TLC plates Merck silica gel 60 F_{254} was used for monitoring the reactions and also for preparative TLC. Tetrahydrofuran (THF) and ethyl ether (Et_2O) were distilled under N_2 from sodium/benzophenone ketyl prior to use. Dichloromethane (CH_2Cl_2), acetonitrile (CH_3CN), and benzene were distilled from CaH_2 at atmospheric pressure. 1,2-diketone **6** was synthesized according to literature procedure.[3] All other reagents and solvents were used as received.

Photoreaction of 6 in Aqueous Acetonitrile. 1-(3-(1-Hydroxy-1-Phenyl)methyl)-2,4,5,6-tetrahydro-2-oxapentalenyl)ethan-1-one (10). A solution of **6** (13.8 mg, 0.058 mmol) in acetonitrile (2.9 mL) and H_2O (2.9 mL) was irradiated with a transilluminator (365 nm) through a Pyrex filter at room temperature for 1 h. After concentration *in vacuo*, the resulting mixture was extracted with ethyl acetate, washed with brine, dried over anhydrous $MgSO_4$, filtered and concentrated *in vacuo*. The crude product was purified by silica gel chromatography (50% ethyl acetate/hexane) to give **10** (10.8 mg, 73%) as a white solid: ^{1}H NMR (400

MHz, C_6D_6) δ 1.69–2.00 (4 H), 2.09 (s, 3 H), 2.41 (t, 2 H, J = 7.2 Hz), 5.47–5.53 (1 H), 7.03–7.14 (3 H), 7.28–7.36 (2 H); ^{13}C NMR (100 MHz, C_6D_6) δ 23.8, 25.8, 26.2, 31.4, 70.0, 125.6, 126.8, 126.9, 127.9, 128.1, 128.6, 129.3, 132.4, 141.2, 143.1, 185.7; IR ($CHCl_3$) 3600, 3540–3320, 3022, 1660 cm^{-1}; MS *m/e* (%) 256 (M^+) (51), 238 (98), 213 [(M – $COCH_3$)$^+$] (100); HRMS calcd for $C_{16}H_{16}O_3$ (M^+) 256.1100, found 256.1146.

Photoreaction of 6 in deuterium oxide to give 11. A solution of **6** (9.8 mg, 0.04 mmol) in acetonitrile (2.1 mL) and deuterium oxide (2.1 mL) was irradiated with a transilluminator (365 nm) through a Pyrex filter at room temperature for 40 min. After concentration *in vacuo*, the resulting mixture was extracted with ethyl acetate, washed with brine, dried over anhydrous MgSO4, filtered and concentrated *in vacuo*. The crude product was purified by silica gel chromatography (20% ethyl acetate/hexane) to give **11** (6.4 mg, 61%) as a colorless oil: ^1H NMR (200 MHz, C_6D_6) δ 2.01–2.33 (4 H), 2.35 (s, 3 H), 2.78 (t, 3 H, J = 7.5 Hz), 7.27–7.45 (5 H); IR ($CHCl_3$) 3738–3334, 1663, 1656, 1221, 763, 736 cm^{-1}; MS *m/e* (%) 257 (M^+) (100), 240 [(M – OH)$^+$] (45), 214 [(M – $COCH_3$)$^+$] (80); HRMS calcd for $C_{16}H_{15}O_3D$ (M^+) 257.1160, found 257.1161.

Photoreaction of 6 in CD_3OD to give 12. A solution of **6** (6.8 mg, 0.03 mmol) in CD3OD (2.8 mL) was irradiated with a transilluminator (365 nm) through a Pyrex filter at room temperature for 1 h. After concentration *in vacuo*, the crude product was purified by silica gel chromatography (9% ethyl acetate/hexane) to give **12** (2.8 mg, 36%) as a colorless oil: ^1H NMR (200 MHz, C_6D_6) δ 1.68–2.18 (4 H), 2.10 (s, 3 H), 2.45 (t, 3 H, J = 7.5 Hz), 7.03–7.19 (3 H), 7.32–7.38 (2 H); IR ($CHCl_3$) 3314, 1683, 1663, 1559, 1220, 779 cm^{-1}; MS *m/e* (%) 274 (M^+) (20), 240 [(M – OCD_3)$^+$] (100), 231

[(M – $COCH_3$)$^+$] (55); HRMS calcd for $C_{17}H_{14}O_3D_4$ (M^+) 274.1502, found 274.1527.

Ethyl 2-(trimethylsilylethynyl)cyclopentenecarboxylate (17). To a mixture of enol triflate **16** (1.89 g 6.56 mmol), ethynyltrimethylsilane (773 mg, 7.9 mmol), bis(triphenylphosphine)palladium(II) chloride (138.0 mg, 0.2 mmol), and 2,6-lutidine (1.05 g, 9.8 mmol) in deaerated, anhydrous DMF (3 mL) was added cuprous iodide (75.0 mg, 0.39 mmol). The mixture was stirred at ambient temperature for 15 h under nitrogen. The resulting mixture was diluted with saturated NH_4Cl and extracted with ethyl acetate. The extract was washed with brine, dried over anhydrous $MgSO_4$, filtered, and concentrated *in vacuo*. The crude product was purified by silica gel chromatography (50% toluene/hexane) to give **17** (1.05 g, 47%) as a brown oil: ^{1}H NMR (400 MHz, $CDCl_3$) δ 0.21 (s, 9 H), 1.30 (t, 3 H, J = 7.2 Hz), 1.88 (m, 2 H), 2.60–2.71 (4 H), 4.22 (q, 2 H, J = 7.2 Hz); ^{13}C NMR (100 MHz, CDCl3) δ 0.00, 14.4, 22.3, 33.48, 39.6, 60.5, 100.5, 105.6, 133.5, 139.1, 164.3; IR (neat) 2960, 2141, 1720, 1260, 860 cm^{-1}; MS *m/e* (%) 236 (M^+) (15), 221 [(M – Me) $^+$] (20), 207 (25); HRMS calcd for $C_{13}H_{20}O_2Si$ (M^+) 236.1232, found 236.1224.

Ethyl 2-Ethynylcyclopent-1-enecarboxylate (18). To a solution of **17** (653 mg, 2.8 mmol) and acetic acid (829 mg, 13.8 mmol) in THF (6 mL)was added TBAF (4.1 mL, 1.0 M in THF, 4.1 mmol) at 0 °C, and the mixture was stirred at ambient temperature for 2 h. The resulting mixture was diluted with saturated $NaHCO_3$ and extract with ethylacetate. The extract was washed with brine, dried over anhydrous $MgSO_4$, filtered, and concentrated *in vacuo*. The crude product was purified by silica gel chromatography (3% ethyl acetate/hexane) to give **18** (370 mg, 82%) as a brown oil: ^{1}H NMR (400 MHz, $CDCl_3$) δ 1.29 (t, 3 H, J = 7.1 Hz), 1.91

(m, 2 H), 2.61–2.72 (4 H), 3.51 (s, 1 H), 4.21 (q, 2 H, J = 7.1 Hz); ^{13}C NMR (100 MHz, $CDCl_3$) δ 14.3, 22.2, 33.3, 39.1, 60.4, 79.4, 87.3, 133.1, 140.0, 164.0; IR (neat) 3270, 2970, 2100, 1710, 1610 cm^{-1}; MS *m/e* (%) 164 (M^+) (64), 136 (65), 119 (100); HRMS calcd for $C_{10}H_{12}O_2$ (M^+) 164.0837, found 164.0840.

Ethyl 2-(2-(2-Acetylcyclopent-1-enyl)ethynyl)cyclopent-1-enecarboxylate (20). To a mixture of 2-acetylcyclopent-1-enyl trifluoromethansulfonate (**19**) (1.22 g, 4.2 mmol), **18** (764 mg, 4.7 mmol), bis(triphenylphosphine)palladium(II) chloride (148 mg, 0.2 mmol), and 2,6-lutidine (680 mg, 6.4 mmol) in deaerated, anhydrous DMF (6 mL) was added cuprous iodide (80.6 mg, 0.4 mmol), and the mixture was stirred at ambient temperature for 6 h under nitrogen. The resulting mixture was diluted with saturated NH_4Cl and extracted with ethyl acetate. The extract was washed with brine, dried over anhydrous $MgSO_4$, filtered, and concentrated *in vacuo*. The crude product was purified by silica gel chromatography (67% toluene/hexane) to give **20** (711 mg, 62%) as a yellow solid: ^1H NMR (400 MHz, $CDCl_3$) δ 1.28 (t, 3 H, J = 7.1 Hz), 1.88 (quint, 2 H, J = 7.6 Hz), 1.96 (quint, 2 H, J = 7.7 Hz), 2.56 (s, 3H), 2.67–2.80 (8 H), 4.21 (q, 2 H, J = 7.1 Hz); ^{13}C NMR (50 MHz, $CDCl_3$) δ 14.3, 21.7, 22.2, 29.5, 33.0, 33.5, 38.8, 40.2, 60.4, 95.4, 97.4, 133.2, 133.4, 139.7, 148.1, 164.2, 196.6; IR ($CHCl_3$) 3011, 2361, 1697, 1651, 1376, 1247, 762 cm^{-1}; MS *m/e* (%) 272 (M^+) (10), 243 (100), 227 (10); HRMS calcd for $C_{17}H_{20}O_3$ (M^+) 272.1411, found 272.1391.

2-Diazo-1-(2-(2-(2-acetylcyclopent-1-enyl)ethynyl)cyclopent-1-enyl)propan-1-one (21). To a solution of **20** (654 mg, 2.4 mmol) in MeOH (15 mL) and H_2O (8 mL) was added NaOH (144 mg, 3.6 mmol), and the mixture was stirred at 45 °C for 3 h. After concentration in vacuo,

the resulting mixture was diluted with H_2O, washed with ethyl acetate, and acidified with 10% HCl. The mixture was extracted with ethyl acetate, washed with brine, dried over anhydrous $MgSO_4$, filtered, and concentrated in vacuo to give crude carboxylic acid (486 mg, 83 %), which was immediately used in the next step. Oxalyl chloride (251 mg, 2.0 mmol) was added to a solution of the crude carboxylic acid (161 mg, 0.7 mmol) in anhydrous benzene (5 mL), and the mixture was stirred for 4 h at room temperature. Benzene was removed under reduced pressure, and the crude acid chloride was dissolved in 50 mL of anhydrous ether. To a solution of diazoethane prepared from 696 mg of nitrosourea was added a solution of acid chloride at 0 °C, and the mixture was stirred for 3 h. Concentration of the resulting mixture under reduced pressure gave the crude diazo ketone, which was purified by silica gel chromatography (17% ethyl acetate/hexane) to give pure **21** (74 mg, 40%) as a yellow solid: ^{1}H NMR (400 MHz, $CDCl_3$) δ 1.88 (quint, 2 H, J = 7.6 Hz), 1.95 (quint, 2 H, J = 7.6 Hz), 2.02 (s, 3 H), 2.47 (s, 3H), 2.63–2.81 (8 H); ^{13}C NMR (100 MHz, $CDCl_3$) δ 9.0, 21.7, 22.4, 29.3, 33.2, 35.1, 38.1, 40.3, 94.1, 96.2, 126.1, 132.8, 147.6, 148.0, 196.2 (we could not observe two carbons); IR ($CHCl_3$) 3699, 3022, 3011, 2077, 1653, 1610, 1590, 1571, 1211, 761, 747 cm^{-1}; MS *m/e* (%) 254 [$(M - N_2)^+$] (100), 226 (20), 211 (35); HRMS calcd. for $C_{17}H_{18}O_2$ [$(M - N_2)^+$] 254.1306, found 254.1310.

1-(2-(2-(2-Acetylcyclopent-1-enyl)ethynyl)cyclopent-1-enyl)propane-1,2-dione (22). To a solution of **21** (56 mg, 0.2 mmol) in anhydrous ether (4 mL) was added triphenylphosphine (71 mg, 0.3 mmol), and the mixture was stirred at ambient temperature for 3 h. After concentration *in vacuo,* the resulting mixture was diluted with THF (4 mL). To the THF solution was added sodium nitrite (32 mg, 0.5 mmol) and cooled to 0 °C. To the mixture was added 2 N HCl (0.4 mL, 0.7 mmol), and the reaction mixture

was stirred at ambient temperature for 2.5 h. The resulting mixture was extracted with ethyl acetate, washed with brine, dried over anhydrous $MgSO_4$, filtered, and concentrated *in vacuo*. The crude product was purified by silica gel chromatography (17% ethyl acetate/hexane) to give **22** (25 mg, 46%) as a yellow oil: ^{1}H NMR (400 MHz, $CDCl_3$) δ 1.90 (quint, 2 H, J = 7.7 Hz), 2.00 (quint, 2 H, J = 7.7 Hz), 2.40 (s, 3 H), 2.48 (s, 3H), 2.68–2.81 (8 H); ^{13}C NMR (100 MHz, $CDCl_3$) δ 21.8, 22.1, 26.0, 29.4, 32.5, 33.3, 39.6, 39.7, 95.5, 98.3, 131.8, 138.6, 143.2, 149.4, 190.9, 197.0, 200.9; IR ($CHCl_3$) 3896, 2358, 1713, 1648, 1603, 746 cm^{-1}; MS *m/e* (%) 270 (M^+) (95), 227 (100), 199 (35); HRMS calcd. for $C_{17}H_{18}O_3$ (M^+) 270.1255, found 270.1243.

Photoreaction of 22 in benzene. 1-(3-(2,4,5,6-Tetrahydro-2-oxapentalenyl)-2,4,5,6-tetrahydro-2-oxapentalenyl)ethan-1-one (15). A solution of **6** (5.6 mg, 0.02 mmol) in anhydrous benzene (2.1 mL) was irradiated with a transilluminator (365 nm) through a Pyrex filter at room temperature for 1.5 h. The solvent was removed under reduced pressure, and the resulting mixture was purified by silica gel chromatography (10% ethyl acetate/hexane) to give **15** (5.3 mg, 95%) as yellow solids: ^{1}H NMR (400 MHz, $CDCl_3$) δ 2.24 (bs, 3 H), 2.39 (s, 3 H), 2.33–2.40 (2 H), 2.48–2.53 (2 H), 2.77–2.82 (4 H), 2.87 (t, 2 H, J = 7.4 Hz); ^{13}C NMR (50 MHz, $CDCl_3$) δ 12.9, 23.0, 24.3, 24.9, 26.2, 26.2, 31.5, 32.0, 129.4, 130.3, 133.8, 134.5, 141.2, 142.2, 143.2, 145.1, 197.7; IR ($CHCl_3$) 1640, 1627, 1209 cm^{-1}; MS *m/e* (%) 270 (M^+) (100), 227 [$(M - COCH_3)^+$] (65); HRMS calcd for $C_{17}H_{18}O_3$ (M^+) 270.1255, found 270.1220.

1-(2-(Phenylethynyl)cycopentenyl)-1-ethaneone (23). To a mixture of 2-acetylcyclopent-1-enyl trifluoromethansulfonate (**19**) (1.50 g, 5.2 mmol), phenylacetylene (580 mg, 5.7 mmol), bis(triphenylphosphine)palladium(II)

chloride (110 mg, 0.2 mmol), and 2,6-lutidine (830 mg, 7.8 mmol) in deaerated, anhydrous DMF (5 mL) was added cuprous iodide (60 mg, 0.3 mmol), and the mixture was stirred at ambient temperature for 13 h under nitrogen. The resulting mixture was diluted with saturated NH_4Cl and extracted with ethyl acetate. The extract was washed with brine, dried over anhydrous $MgSO_4$, filtered, and concentrated *in vacuo*. The crude product was purified by silica gel chromatography (50% toluene/hexane) to give **23** (792 mg, 73%) as a yellow solid: ^{1}H NMR (400 MHz, $CDCl_3$) δ 1.90 (quint, 2 H, J = 7.7 Hz), 2.63 (s, 3 H), 2.72 (tt, 2 H, J = 7.7, 2.3 Hz), 2.81 (tt, 2 H, J = 7.7, 2.3 Hz), 7.33–7.37 (3 H), 7.45–7.47 (2 H); ^{13}C NMR (100 MHz, $CDCl_3$) δ 21.8, 29.5, 33.0, 40.4, 86.4, 101.7, 122.5, 128.5, 129.2, 131.5, 133.9, 147.4, 196.5; MS *m/e* (%) 210 (M^+) (100), 195 [$(M - CH_3)^+$] (100), 167 [$(M - COCH_3)^+$] (25); HRMS calcd for $C_{15}H_{14}O$ (M^+) 210.1044, found 210.1059.

1-(2-(trimethylsilylethynyl)cyclopentenyl)ethan-1-one (24). To a mixture of 2-acetyl-1-cyclopent-1-enyl trifluoromethanesulfonate (**19**) (2.77 g, 9.63 mmol), bis(triphenylphosphine)palladium(II) chloride (203 mg, 0.3 mmol), and 2,6-lutidine (1.54 g, 14.5 mmol) in deaerated, anhydrous DMF (6 mL) were added ethynyltrimethylsilane (1.04 g, 10.6 mmol) and cuprous iodide (110 mg, 0.6 mmol), and the mixture was stirred at ambient temperature for 15 h under nitrogen. The resulting mixture was diluted with saturated NH_4Cl and extracted with ethyl acetate. The extract was washed with brine, dried over anhydrous $MgSO_4$, filtered, and concentrated *in vacuo*. The crude product was purified by silica gel chromatography (3% ethyl acetate/hexane) to give **24** (1.85 g, 93%) as a red oil: ^{1}H NMR (400 MHz, $CDCl_3$) δ 0.21 (s, 9 H), 1.83 (quint, 2 H, J = 7.7 Hz), 2.53 (s, 3 H), 2.63–2.72 (4 H); ^{13}C NMR (100 MHz, $CDCl_3$) δ –0.4, 21.7, 29.5, 32.9, 40.3, 101.6, 108.5, 133.6, 148.6, 196.7; IR ($CHCl_3$) 2905,

1651, 1585, 1374, 1252, 742 cm^{-1}; MS *m/e* (%) 206 (M^+) (80), 191 (100), 163 (20); HRMS calcd for $C_{12}H_{18}OSi$ (M^+) 206.1126, found 206.1133.

1-(2-Ethynylcyclopenyl)ethan-1-one (25). To a solution of **24** (907 mg, 4.4 mmol) and acetic acid (1.32 g, 22.0 mmol) in THF (7 mL) was added TBAF (6.6 mL, 1.0 M in THF, 6.6 mmol) at 0 °C, and the mixture was stirred at ambient temperature for 12 h under nitrogen. The resulting mixture was diluted with saturated $NaHCO_3$ and extracted with ethyl acetate. The extract was washed with brine, dried over anhydrous $MgSO_4$, filtered, and concentrated *in vacuo*. The crude product was purified by silica gel chromatography (2% ethyl acetate/hexane) to give **25** (432 mg, 73%) as a brown solid: ^1H NMR (400 MHz, $CDCl_3$) δ 1.86 (quint, 2 H, J = 7.7 Hz), 2.53 (s, 3 H), 2.65–2.75 (4 H), 3.64 (s, 1 H); ^{13}C NMR (100 MHz, $CDCl_3$) δ 21.5, 29.4, 32.9, 40.2, 80.2, 89.6, 132.4, 149.0, 196.5; IR ($CHCl_3$) 3302, 3017, 1657, 1589, 1265, 1215, 762, 743 cm^{-1}; MS *m/e* (%) 134 (M^+) (65), 119 (100), 91 (40); HRMS calcd for $C_9H_{10}O$ (M^+) 134.0731, found 134.0723.

1-(2-(2-(2-Acetylcyclopent-1-enyl)ethynyl)cyclopent-1-enyl)ethan-1-one (26). To a mixture of 2-acetylcyclopent-1-enyl trifluoromethansulfonate (**19**) (199 mg, 0.7 mmol), bis(triphenylphosphine)palladium(II) chloride (24.2 mg, 0.03 mmol), and 2,6-lutidine (111 mg, 1.0 mmol) in deaerated, anhydrous DMF (4 mL) were added **25** (102 mg, 0.8 mmol) and cuprous iodide (13.1 mg, 0.07 mmol). The mixture was stirred at ambient temperature overnight under nitrogen. The resulting mixture was diluted with saturated NH_4Cl and extracted with ethyl acetate. The extract was washed with brine, dried over anhydrous $MgSO_4$, filtered, and concentrated *in vacuo*. The crude product was purified by silica gel chromatography (2% ethyl acetate/toluene) to give **26** (66.2 mg, 36%) as a yellow oil: ^1H

NMR (400 MHz, $CDCl_3$) δ 1.91 (quint, 4 H, J = 7.5 Hz), 2.51 (s, 6 H), 2.70–2.79 (8 H); ^{13}C NMR (100 MHz, $CDCl_3$) δ 21.8, 29.4, 33.3, 39.9, 97.4, 132.5, 148.5, 196.0; IR (neat) 2921, 2842, 1651, 1605, 1418, 1251 cm^{-1}; MS *m/e* (%) 242 (M^+) (100), 227 (13), 199 (24); HRMS calcd for $C_{16}H_{18}O_2$ (M^+) 242.1307, found 242.1306.

Photoreaction of 23 to give intermolecular [2+2] photocycloadduct. A solution of **23** (20.7 mg, 0.10 mmol) in MeOH (17.9 mL) was irradiated with a transilluminator (365 nm) through a Pyrex filter at room temperature for 2.5 h. The solvent was removed under reduced pressure an the resulting mixture was purified by silica gel chromatography (20% ethyl acetate/hexane) to give [2+2] photocycloadduct (14.1 mg, 71%) as a yellow solid: ^1H NMR (400 MHz, $CDCl_3$) δ 1.66–2.12 (8 H), 2.34 (s, 3 H), 2.35 (s, 3 H), 2.81–2.86 (m, 2 H); ^{13}C NMR (100 MHz, $CDCl_3$) δ 22.1, 23.9, 26.9, 28.7, 29.2, 34.0, 34.3, 38.8, 55.2, 71.5, 85.7, 88.2, 122.8, 126.2, 128.2, 128.3, 128.8, 128.9, 131.6, 132.2, 136.1, 140.5, 142.5, 144.9, 198.0, 208.3; IR ($CHCl_3$) 3600, 3540–3320, 3022, 1660 cm^{-1}; MS *m/e* (%) 420 (M^+) (15), 405 [$(M - CH_3)^+$] (45), 377 [$(M - COCH_3)^+$] (100); HRMS calcd for $C_{30}H_{28}O_2$ (M^+) 420.2088, found 420.2082.

Photoreaction of 26. A solution of **26** (10.0 mg, 0.04 mmol) in benzene (4.1 mL) was irradiated with a transilluminator (365 nm) through a Pyrex filter at room temperature for 3 h. In another experiment, the same solution of **26** containing Michler's ketone (11.4 mg, 0.04 mmol) was photoirradiated for 1 h. A ^1H NMR spectrum of the crude photolysate obtained from both experiments showed complete recovery of **26**.

Quantum Yield Measurements. An acetonitrile solution (2 mL) of **22** (1

mM) in a Pyrex flask containing benzene as an internal standard was illuminated at 365 nm obtained from the monochromator for 25 counts by an integrator equipped with the monochromator. The monochromator was calibrated by the chemical actinometer of phenylglyoxylic acid (Φ = 0.72 at 365 nm)** under identical conditions. The quantum yields for the disappearance of **22** in benzene at 365 nm irradiation were measured as 0.19.

Triplet Quenching. Triplet quenching for the disappearance of **6** (1 mM) under photoirradiation condition was carried out in the presence of pyrene (0, 0.1, 0.2, and 0.4 mM) in acetonitrile and water (9 : 1) at 350 nm obtained from the monochromator. The disappearance of **6** was assayed by HPLC. Quantum yields for the disappearance of **6** were 0.042 (0.1 mM), 0.023 (0.2 mM), and 0.013 (0.4 mM). The Stern-Volmer slope was $18.6 \times 10^3\ M^{-1}$.

References

(1) (a) Hoffman, R. V.; Shechter, H. *J. Am. Chem. Soc.* **1971**, *93*, 5940–5941. (b) Hoffman, R. V.; Orphanides, G. G.; Shechter, H. *J. Am. Chem. Soc.* **1978**, *100*, 7927–7933. (c) Hoffman, R. V.; Shechter, H. *J. Am. Chem. Soc.* **1979**, *100*, 7934–7940. (d) Kirmse, W.; Lelgemann, R.; Friedrich, K. *Chem. Ber.* **1991**, *124*, 1853–1863. (e) Albers, R.; Sander, W. *Liebigs Ann.* **1997**, 897–905.

(2) Herges, R. *Angew. Chem. Int. Ed. Engl.* **1994**, *33*, 255–276.

(3) Nakatani, K.; Maekawa, S.; Tanabe, K.; Saito, I. *J. Am. Chem. Soc.* **1995**, *117*, 10635–10644.

(4) Kirmse, W. in *Advance Carbene Chemistry*; Brinker, U. H., Ed.; JAI Press; Greenwich, CT, 1994, Vol 1, pp. 1–57.

(5) (a) Tomer, K. B.; Harrit, N.; Rosenthal, I.; Buchardt, O.; Kumler, P. L.; Creed, D. *J. Am. Chem. Soc.* **1973**, *117*, 7402–7406. (b) Padwa, A.; Akiba, M.; Chou, C. S.; Cohenm, L. *J. Org. Chem.* **1982**, *47*, 183–191.

(6) (a) Mukherjee, A. K.; Margaretha, P.; Agosta, W. C. *J. Org. Chem.* **1996**, *61*, 3388–3391. (b) Agosta, W. C.; Margaretha, P. *Acc. Chem. Res.* **1996**, *29*, 179–182.

(7) (a) Hussain, S.; Agosta, W. C. *Tetrahedron* **1981**, *37*, 3301–3305. (b) Agosta, W. C.; Caldwell, R. A.; Jay, J.; Johnson, L. J.; Venepalli, B. R.; Scaiano, J. C.; Singh, M.; Wolff, S. *J. Am. Chem. Soc.* **1987**, *109*, 3050–3057. (c) Rathjen, H, -J.; Margaretha, P.; Wolff, S.; Agosta, W. C. *J. Am. Chem. Soc.* **1991**, *113*, 3904–3909. (d) Margaretha, P.; Reichow, S.; Agosta, W. C. *J. Org. Chem.* **1994**, *59*, 5393–5396. (e) Kisilowski, B.; Agosta, W. C.; Margaretha, P. *Chem. Comm.* **1996**, 2065.

(8) (a) Saito, I.; Kanehira, K.; Shimozono, K.; Matsuura, T. *Tetrahedron*

Lett. **1980**, *21*, 2737–2740. (b) Saito, I.; Shimozono, K.; Matsuura, T. *J. Am. Chem. Soc.* **1980**, *102*, 3948–3950. (c) Saito, I.; Shimozono, K.; Matsuura, T. *J. Org. Chem.* **1982**, *47*, 4356–4358. (d) Saito, I.; Shimozono, K.; Matsuura, T. *Tetrahedron Lett.* **1984**, *23*, 5439–5442.

(9) Murov, S. L.; Carmichael, I.; Hug, G. L. In *Handbook of Photochemistry*, 2 nd ed.; Marcel Dekker: New York, 1993.

List of Publications

Chapter 1 Synthesis and Properties of Peptide Nucleic Acids Containing a Psoralen Unit.
Okamoto, A.; Tanabe, K.; Saito, I.
Org. Lett. **2001**, *3*, 925–927.

Chapter 2 Modulation of Remote DNA Oxidation by Hybridization with Peptide Nucleic Acids (PNA).
Okamoto, A.; Tanabe, K.; Dohno, C.; Saito, I.
Bioorg. Med. Chem. **2002**, *10*, 713–718.

Control of Electron Transfer in DNA by Peptide Nucleic Acids.
Tanabe, K.; Yoshida, K.; Dohno, C.; Okamoto, A.; Saito, I
Nucleic Acids Symp. Ser. **2000**, *44*, 35–36.

Chapter 3 Site-Specific Discrimination of Cytosine and 5-Methylcytosine in Duplex DNA using Peptide Nucleic Acids.
Okamoto, A.; Tanabe, K.; Saito, I.
J. Am. Chem. Soc. **2002**, *124*, 10262–10263.

Chapter 4 Strand-Displacement Complex (P-loop) of Peptide Nucleic Acids and Duplex DNA as a Catalytic Template for the Enzymatic Digestion.
Tanabe, K.; Okamoto, A.; Saito, I.
To be submitted.

Chapter 5 Control of Photo-induced Drug Release by the Use of Conformational Change of DNA.
Tanabe, K.; Inasaki, T.; Okamoto, A.; Nishimoto, S. –I.; Saito, I.
Nucleic Acids Res. Suppl. in press.

Chapter 6 Novel Synthesis of Bifurans via Furan-Forming Photocyclization of α-Diketones Conjugated with Ene-Yne.
Nakatani, K.; Tanabe, K.; Saito, I.
Tetrahedron Lett. **1997**, *38*, 1207–1210.

Other Publications

1. α-Diazo Ketones as Photochemical DNA Cleavers: A Mimic for the Radical Generating System of Neocartinostatin Chromophore.
Nakatani, K.; Maekawa, S.; Tanabe, K.; Saito, I.
J. Am. Chem. Soc. **1995**, *117*, 10635–10644.

2. Chiral Amino Acid Recognition by a Porphirin-Based Artificial Receptor.
Kuroda, Y.; Kato, Y.; Higashioji, T.; Hasegawa, J.; Kawanami, S.; Takahashi, M.; Shiraishi, N.; Tanabe, K.; Ogoshi, H.
J. Am. Chem. Soc. **1995**, *117*, 10950–10958.

3. Tandem Cyclizations Involving Carbene as an Intermediate: Photochemical Reactions of Substituted 1,2-Diketones Conjugated with Ene-Yne.
Nakatani, K.; Adachi, K.; Tanabe, K.; Saito, I.
J. Am. Chem. Soc. **1999**, *121*, 8221–8228.

4. Site Selective Formation of Thymine Glycol-Containing Oligodeoxynucleotides by Oxidation with Osmium Tetroxide and Bipyridine-Tethered Oligonucleotide.

Nakatani, K.; Hagihara, S.; Sando, S.; Miyazaki, H.; Tanabe, K.; Saito, I

J. Am. Chem. Soc. **2000**, *122*, 6309–6310.

List of Presentations

1. "Novel Photocyclization of Diketone Conjugated with Ene-Yne System"
   K. Nakatani, K. Tanabe, I. Saito
   Symposium on Photochemistry, Fukuoka, Japan, October, 1995.

2. "Base Selective Cleavage of DNA by Diazoketone-Bipyridine Copper Complex"
   K. Nakatani, K. Tanabe, I. Saito
   70th Annual Meeting of Chemical Society of Japan, Tokyo, Japan, March, 1996.

3. "Novel Photocyclization and Reaction Mechanism of Diketone Conjugated with Ene-Yne System"
   K. Nakatani, K. Tanabe, Saito, I.
   70th Annual Meeting of Chemical Society of Japan, Tokyo, Japan, March, 1996.

4. "Novel Photocyclization of Diketone and Triketone Conjugated with Ene-Yne System"
   K. Nakatani, K. Tanabe, I. Saito.
   70th Symposium on Organic Synthesis, Tokyo, Japan, November, 1996.

5. "A Novel Furan-Forming Photocyclization of α-Diketone Conjugated with Ene-Yne"
   K. Nakatani, K. Tanabe, Y. Nomura, I. Saito.
   72th Annual Meeting of Chemical Society of Japan, Tokyo, Japan,

March, 1997.

6. "Design of Functionalized Peptide Nucleic Acids (3): Synthesis and Evaluation of Peptide Nucleic Acids Containing Psoralen Moiety"
K. Tanabe, A. Okamoto, I. Saito.
78th Annual Meeting of Chemical Society of Japan, Chiba, Japan, March, 2000.

7. "Control of Electron Transfer in DNA by Peptide Nucleic Acids (PNA)"
K. Tanabe, K. Yoshida, C. Dohno, A. Okamoto, I. Saito.
27th Symposium on Nucleic Acids Chemistry, Okayama, Japan, November, 2000.

8. "Design of Functionalized Peptide Nucleic Acids"
K. Tanabe, K. Yoshida, A. Okamoto, I. Saito.
4th International Chemical Congress of Pacific Basin Societies, Honolulu, USA, December, 2000.

9. "Reaction of Peptide Nucleic Acids Containing Psoralen Unit with DNA"
K. Tanabe, A. Okamoto, I. Saito.
79th Annual Meeting of Chemical Society of Japan, Kobe, Japan, March, 2001.

10. "DNA Manipulation by Peptide Nucleic Acids"
K. Tanabe, A. Okamoto, I. Saito.
16th Symposium on Biofunctional Chemistry, Chiba, Japan, September, 2001.

11. "PNA-Assisted Discrimination between Cytosine and 5-Methylcytosine (1): Utilization of Fluorescence Resonance Energy Transfer for Discrimination"
K. Tanabe, A. Okamoto, I. Saito.
81th Annual Meeting of Chemical Society of Japan, Tokyo, Japan, March, 2002.

12. "PNA-Assisted Discrimination between Cytosine and 5-Methylcytosine (2): Utilization of Hairpin-Type DNA Oligomers for Efficient DNA Cleavage"
K. Tanabe, A. Okamoto, I. Saito.
81th Annual Meeting of Chemical Society of Japan, Tokyo, Japan, March, 2002.

13. "Discrimination between Cytosine and 5-Methylcytosine in DNA by Peptide Nucleic Acids (PNA)"
K. Tanabe, A. Okamoto, S. –I. Nishimoto, I. Saito.
24th Annual Meeting of the Japanese Society for Photomedicine and Photobiology, Hamamatsu, Japan, July, 2002.